LIQUID BONDED LIGHT WATER REACTOR FUEL: ENHANCED LIGHT WATER REACTOR SAFETY AND PERFORMANCE

By

RICHARD FREDERICK WRIGHT

A DISSERTATION PRESENTED TO THE GRADUATE SCHOOL
OF THE UNIVERSITY OF FLORIDA IN PARTIAL FULFILLMENT
OF THE REQUIREMENTS FOR THE DEGREE OF
DOCTOR OF PHILOSOPHY

UNIVERSITY OF FLORIDA

1994

ACKNOWLEDGEMENTS

The author wishes to express his gratitude to Professor James S. Tulenko for his vision, patience, guidance, enthusiasm, and breadth of knowledge of nuclear fuel design. Without his support, this work would not have been possible.

I am also indebted to Dr. Richard G. Connell, Professor Emeritus Glen J. Schoessow, Thad M. Adams, and Mark Dubecky whose work on this project parallels my own, and who have provided contributions to this work. I would like to thank my committee members; Drs. D.E. Hintenlang, E.T. Dugan, G.R. Dalton, and F.E. Dunnam for their help and guidance. Also Kathy Phillips for all her help.

I would like to acknowledge Dr. Odelli Osser of EPRI and Dennis O'Shay of Florida Power Corp. for their help in obtaining the ESCORE computer program, and the U.S. Department of Energy for funding this research.

I would also like to thank Dr. Frederick J. Moody, Dr. J. Edward Schmidt, and Robert A. Markley for being friends and mentors, and for helping me to put my education, career and life into the proper perspective.

I would like to give special thanks to my wife, Denise, and my children, Laura and Rick, and Jim and Betty Hart for their love and support. Most of all I would like to thank my parents, especially my father, who was my inspiration.

TABLE OF CONTENTS

LIST OF TABLES

LIST OF FIGURES

Abstract of Dissertation Presented to the Graduate School
of the University of Florida in Partial Fulfillment of the
Requirements for the Degree of Doctor of Philosophy

LIQUID BONDED LIGHT WATER REACTOR FUEL:
ENHANCED LIGHT WATER REACTOR SAFETY AND PERFORMANCE

By

Richard Frederick Wright

December 1994

Chairman: James S. Tulenko
Major Department: Nuclear Engineering Sciences

Light water reactor (LWR) fuel performance is limited by thermal and mechanical constraints associated with the design, fabrication, and operation of fuel in a nuclear reactor. These limits define the lifetime of the fuel, the maximum power at which the fuel can be operated, the probability of fuel structural failure during the fuel lifetime, and the transient performance of the fuel during an accident. The purpose of this study is to explore one technique for extending these limits; liquid metal bonding of LWR fuel. Current LWR fuel rod designs consist of enriched uranium oxide (UO_2) fuel pellets enclosed in a zirconium alloy cladding. The space between the pellets and the cladding is filled at beginning-of-life by an inert gas (typically helium). This gas space allows for the thermal expansion and swelling of the fuel, fission gas release, as well as the creepdown

of the clad; additionally, the gap allows the fuel pellets to be inserted into the fuel rod during the fabrication process. Due to the low thermal conductivity of the gas, the gas space thermally insulates the fuel pellets from the reactor coolant outside the fuel rod, elevating the fuel temperatures.

Filling the gas space with a high conductivity liquid thermally "bonds" the fuel to the cladding and eliminates the large temperature change across the gap. The resultant lower fuel temperatures directly impact fuel performance limits and transient performance. Liquid bonding of liquid metal reactor (LMR) fuel has been used in several research reactors, as liquid sodium is used as the bonding liquid to limit the peak temperatures during normal operation, and to reduce the stored energy in the fuel pellets.

The application of liquid metal bonding techniques developed for the LMR metal fuel program to LWR fuel are explored for the purposes of increasing LWR fuel performance and safety. An assessment of the technical feasibility of this concept is presented, including the results of research into materials compatibility testing and the predicted lifetime performance of Liquid Bonded LWR fuel. A fuel performance analysis computer program, based on the ESCORE light water reactor fuel performance code, has been developed and is used to determine the benefits of liquid metal bonding for light water fuel.

The results of these studies show that the liquid metal bond is compatible with the cladding and fuel pellets, and could decrease the likelihood of clad failure over the lifetime of the fuel when compared to conventional gas-bonded fuel rods. Further studies with the fuel performance code show that the benefits of lower fuel

temperatures over the lifetime of the fuel indicate that this fuel design is safer than conventional fuel designs, and enhances light water reactor safety and performance.

CHAPTER 1
BACKGROUND

In an effort to enhance the safety and performance of water reactors, the development of various innovative fuel designs was explored. Since many of the safety concerns associated with nuclear reactor fuel deal with high fuel temperatures, a new fuel rod design that operates at lower temperatures, for a given power level, would be inherently safer.

Light Water Reactor Fuel Temperatures and Limits

Current light water reactor (LWR) fuel rod operational limitations include thermal/mechanical limits such as cladding stress and strain, fuel rod internal pressure, and maximum fuel temperature. These limits result largely from thermal characteristics of the fuel operated at high linear power levels (kW/ft), large temperature differences resulting from the poor thermal conductivity of oxide fuel, and the large temperature drop across the pellet/clad gas gap. The limits define such factors as the maximum permitted power at normal operation and fuel temperature margin to melting during anticipated reactor transients.

Due to these high operating temperatures, high energy stored in conventionally designed light water reactor fuel rods significantly increases the likelihood of fuel damage during loss of coolant events.

The thermal resistance for heat transfer from the fuel pellet to the coolant for a typical LWR fuel rod at the beginning-of-life is made up of 1) thermal conductivity through the fuel pellet (53%), 2) thermal conductivity through the gas gap (35%), 3) thermal conductivity through the cladding (4.7%), and 4) the film drop between the clad surface and the coolant (7.3%). The ability to transfer heat out of the fuel rod can be influenced most by modifying the fuel pellet design, or reducing the thermal resistance across the gas gap. The heat transfer through the fuel pellet can be enhanced by either increasing the fuel thermal conductivity (i.e. changing from UO_2 to another fuel type), or by decreasing the pellet diameter. Since neither of these alternatives were deemed acceptable without fundamentally changing the fuel design, reducing the large thermal resistance associated with the pellet/cladding gap by replacing the gas between the pellets and cladding with a liquid metal was explored.

In addition, the benefits of lower fuel temperatures, integrated over the life of the fuel rod, result in significantly lower fission gas release and fuel swelling. Both of these factors positively impact the fuel performance at the end-of-life, and could be useful for extending the fuel to higher burnup levels than those achieved by conventional fuel.

Sodium Bonded Metal Fuel Technology

Fuel for liquid metal reactors (LMRs) is similar to LWR fuel for most operating plants. The rods contain fuel pellets made of uranium or plutonium oxide encased in a stainless steel cladding. An inert gas, typically helium, fills the interstitial spaces between the pellets and the cladding. In order to develop an inherently safer reactor design, some LMRs such as the Experimental Breeder Reactor (EBR-II) in Idaho Falls [1], use a metallic fuel consisting of uranium-plutonium-zirconium alloy which is formed into pellets and encased in stainless steel cladding. The metallic fuel has a much lower melting temperature (2000°F) compared to the oxide fuel (4500°F), and a much higher thermal conductivity (20 Btu/hr-ft-°F) compared to the oxide fuel (4 Btu/hr-ft-°F). Thus, the centerline temperature of the metallic fuel is far lower than the oxide fuel for comparable power and fuel dimensions.

To operate the fuel at acceptable power levels while maintaining margin to the fuel melting temperature, it was determined that the high thermal resistance between the pellet and the cladding across the gas gap must be significantly reduced. To accomplish this, liquid sodium was introduced into the gap, effectively eliminating the gap resistance [1]. The resulting fuel design was found to operate safely at high power levels, and to maintain fuel temperature safety margins. In the event of a fuel rod failure, the liquid sodium inside the rod would mix with the

liquid sodium coolant, and with the exception of the loss of fission product retention, the rod would maintain its operational integrity.

Disadvantages to using this fuel design are mainly due to fuel manufacturing and handling, and the lower fission gas retention capability of the metallic fuel. Extreme care must be taken to isolate the liquid metal from the environment outside the reactor as sodium reacts violently with air or water.

Liquid Bonding in LWR Fuel

The use of a liquid metal bond in a light water reactor fuel rod would enhance the heat transfer between the fuel and the reactor coolant, resulting in significantly lower operating temperature, and a safer fuel design. For this reason, it is proposed that liquid bonding techniques be investigated for possible use in LWR fuel design. Several advantages and disadvantages for the proposed design can be cited.

Potential Benefits

The safety benefits resulting from lower fuel operating temperatures that influenced the development of liquid bonded LMR fuel can be applied to LWR fuel design. In order to achieve the high power levels and long fuel life needed in power reactors, fuel temperature considerations become the principal design

limitation. As was previously stated, a large percentage of the thermal resistance to removing heat from the fuel occurs in the gas gap between the fuel pellets and the cladding. By replacing the gas with a liquid, the resistance is dramatically reduced, and the fuel temperature is significantly lower for the same power level. The lower radial temperature profile leads to significantly lower stored energy in the fuel pellet, which is of primary concern during reactor transients. Additionally the lower temperature reduces the thermal expansion of the pellet and reduces the fission gas release both of which enhance fuel performance. Both the steady-state and transient thermal performance of liquid bonded LWR fuel is discussed in greater detail in Chapter 5.

Disadvantages

Most of the disadvantages associated with using liquid bonding techniques in LWR fuel design stem from lack of developed technology, especially in the field of materials research. As will be shown, the bonding liquid (liquid metal) must be chemically compatible with reactor materials including fuel (UO_2), cladding (Zircaloy), coolant (water), as well as fission products, shims, etc.

In addition, for the commercial viability of any new fuel design, it must be able to replace and coexist with existing LWR fuel. Factors such as nuclear interactions, performance during reactor transients, propensity to fuel rod failure, behavior after failure, fission gas release and resultant rod pressure,

manufacturability, and the effect of the liquid bond material on fuel assembly parameters must be assessed.

The purpose of this study is to

1. Determine the technical feasibility of liquid bonded light water reactor fuel through a qualitative discussion of candidate bonding liquids, fuel thermal mechanical limits, fuel reliability, fuel response to postulated severe accidents, and manufacturing techniques. Through this assessment, candidate liquid metal(s) will be identified, and a plan implemented for laboratory testing of the constituent materials, and the development of analytical tools to determine the performance characteristics of the proposed fuel design.
2. Demonstrate the material compatibility between the liquid metal bond material and the Zircaloy-4 cladding through comprehensive testing of candidate liquid metals at typical reactor operating temperatures, and anticipated transient temperatures.
3. Demonstrate the performance of liquid bonded LWR fuel by developing an analytical tool to determine the thermal-mechanical performance under irradiation conditions.
4. Identify new fuel designs which take full advantage of the temperature reduction benefits of the liquid metal bond.

The following chapters provide the results of research into each of these aspects of liquid bonded light water reactor fuel. Based on this research, recommendations are made concerning the applicability of this advanced fuel design in enhancing the safety and performance of commercial light water reactors.

CHAPTER 2
TECHNICAL FEASIBILITY

The potential benefits of liquid bonded LWR (LBLWR) fuel can be realized if the fuel can be shown to be technically and operationally feasible. This technical feasibility depends on a number of factors. First, the choice of liquid must be compatible with materials found in a light water reactor environment. Secondly, the liquid must remain thermally stable; without experiencing chemical breakdown, or changing phase over the anticipated temperature range and radiation environment. In addition, interaction between the liquid and the neutron population must be minimal. Also, the fuel must demonstrate a clear advantage over current LWR fuel design, especially in the areas of fuel lifetime extension and safety. Finally, the liquid bonded LWR fuel must be easy to manufacture and must be able to replace and coexist with current LWR fuel in a reactor environment.

Choice of Bonding Liquid

Several criteria define the choice of a liquid for use in a LWR liquid bonded fuel design. The most important of these is the ability of the liquid to maintain its heat transfer characteristics over the anticipated steady-state operating temperature

range, as well as the expected transient temperature range. The liquid must not experience chemical breakdown and must remain in the liquid phase over wide ranges of temperature. In addition, the liquid must expand in a minimal fashion upon freezing to prevent clad failure when the fuel is at low temperatures.

The selected liquid must coexist with other fuel materials, as well as the reactor coolant, water. Chemical reaction with these materials over the defined temperature range must be minimal. In addition, the liquid must have a minimal impact on the nuclear environment in the reactor. Finally, the fission gases released from the liquid bonded fuel must be accommodated so that the fuel rod internal pressure is less than the reactor coolant system pressure at operating conditions.

Temperature Range Criteria

Typical LWR fuel operating temperatures range from the coolant temperature (typically 600°F) to the fuel centerline temperature (typically 2500°F to 3000°F). This large temperature range is due to the low thermal conductivity of the UO_2 fuel and the significant temperature gradient across the gas gap. The fuel power rating is limited, in part, by the fuel centerline temperature, which cannot exceed the melting point of UO_2, 4700°F [2]. A major consideration for choosing a bonding liquid is the temperature range over which the liquid remains in the liquid phase. The material must be liquid at reactor operating conditions, before power is

produced in the fuel; i.e. the material, if solid at low temperatures, must liquefy in the hot, no power expected temperature conditions of the reactor coolant.

The candidate liquid must have a relatively high boiling point and a low vapor pressure to assure that it remains in the liquid phase at the highest expected steady-state or transient fuel centerline temperature. This temperature range extends from approximately 500°F to 3500°F. Many candidate liquids such as water, organics, and molten salts cannot operate effectively over this large temperature range. It is clear upon considering these limitations that the only acceptable choices available are the liquid metals. Table 2-1 summarizes the best choices from among the low melting point liquid metals [2]. Each of these metals is adequate at the low temperature limit, as the melting points are near or below 600°F. However, mercury, sodium, and potassium all boil at temperatures below the high end of the temperature range and are therefore considered unacceptable. Gallium, lead, bismuth, tin, lead-bismuth eutectic, lead-bismuth-tin ternary alloy, and lithium are all acceptable choices based on the temperature range criteria.

Nuclear Interaction

Aside from the temperature criteria, it is also important that the bonding liquid interact as little as possible with the neutron flux. In addition, the activation products resulting from interaction between the neutron flux and the bonding liquid must be evaluated to determine the extent to which they affect the fuel performance and spent fuel handling. It is expected that the increased radiation

Table 2-1: Melting and Boiling Temperatures for Candidate Liquids		
Liquid	Melting Point (°F)	Boiling Point (°F)
Mercury	-38	674
Gallium	85	4171
Lead	621	3181
Bismuth	520	3020
Tin	449	4711
Lead-Bismuth	257	3038
Lead-Bismuth-Tin	355	3311
Sodium	207	1623
Potassium	145	1399
Lithium	335	2447

from radioactive isotopes resulting from this interaction would be small when compared to the activity of the fission products in the spent fuel.

Organic liquids such as Dowtherm are composed of complex molecules which chemically disassociate in a radiation environment. Liquid metals have been shown to remain chemically stable in high neutron fluxes which is witnessed by their use both as reactor coolants and thermal bonding for fuel rods in LMRs.

Table 2-2 shows the thermal neutron cross section for each of the liquid metals chosen on the basis of temperature [2]. Except for lithium, all of the remaining candidate liquid metals exhibit very low absorption cross sections and would not significantly affect the reactor neutron economy. Lithium's relatively high cross section is due in large part to the presence of ^{6}Li in natural lithium. If this relatively scarce isotope (7.4 percent by weight) is removed, the lithium absorption cross section is reduced to 0.370 barn. If desired, the ^{6}Li in natural lithium could be used as a burnable poison control mechanism to provide a more uniform power distribution over the life of the fuel. For example, for a fuel rod containing 0.012 lbm of natural lithium at beginning of life, the inventory of ^{6}Li is reduced by approximately one-third after one cycle (15,000 MWd/MT). Lithium-6 undergoes an n-α reaction producing helium and tritium, both of which contribute to the internal gas pressure.

The neutron absorption effects of lead, bismuth, tin and lithium-7 have been found to be negligible, and account for fewer absorptions than the Zircaloy-4

Table 2-2

Average Thermal Neutron Absorption Cross Sections for Liquid Metals

Liquid Metal	Number Density ($x10^{-24}$)	Micro Cross Section (barn)	Macro Cross Section (cm^{-1})
Mercury	.0407	380.00	15.500
Gallium	.0511	2.80	0.143
Lead	.0330	0.170	0.006
Bismuth	.0281	0.034	0.001
Tin	.0330	0.625	0.021
Lead-Bismuth	.0303	0.094	0.003
Pb-Bi-Sn	.0312	0.271	0.008
Sodium	.0254	0.525	0.013
Potassium	.0134	2.07	0.028
Lithium (natural)	.0463	71.0	3.29
Lithium-7	.0460	8.04	0.370

cladding. After absorbing a neutron, bismuth transforms to polonium-210, a highly radioactive isotope, but the increase in the activity due to the small amount of polonium is not expected to be significant compared to the fission product activity.

The reduced fuel temperature effect of the liquid bonded fuel has a significant positive safety effect from a reactivity standpoint. Lower temperature operation causes a reduction in neutron absorption by uranium-238, as Doppler broadening of the resonance absorption peaks is lessened. Also, as is shown in Figure 2-1, the Doppler coefficient for a typical PWR rod in a thermal reactor is a strong function of temperature [3]. Thus, for a PWR liquid bonded fuel at 9 kW/ft, the Doppler coefficient is -1.2×10^{-5} $\Delta\rho/°F$ compared to a value of -0.95×10^{-5} $\Delta\rho/°F$ for gas bonded fuel. This difference (26% increase in the absolute value) means that from a safety standpoint, the Doppler coefficient of the liquid bonded fuel will respond more negatively per degree temperature increase. Since the Doppler coefficient is one of the fuel's fastest acting safety mechanisms, an accidental insertion of reactivity will be mitigated faster and more safely by the liquid bonded fuel. In addition, the lower absorption of thermal neutrons by uranium-238 at normal operating conditions improves the overall neutron economy.

The power defect contribution from the Doppler coefficient (hot/no power to hot/power, 9 kW/ft) is much smaller for the liquid bonded fuel (.0005 $\Delta\rho$) than for the gas bonded fuel (.0013 $\Delta\rho$), because of the smaller fuel temperature change. Over fuel lifetime, the helium gas bonded fuel has greater production of fissile plutonium due to the U-238 absorptions resulting from the temperature Doppler

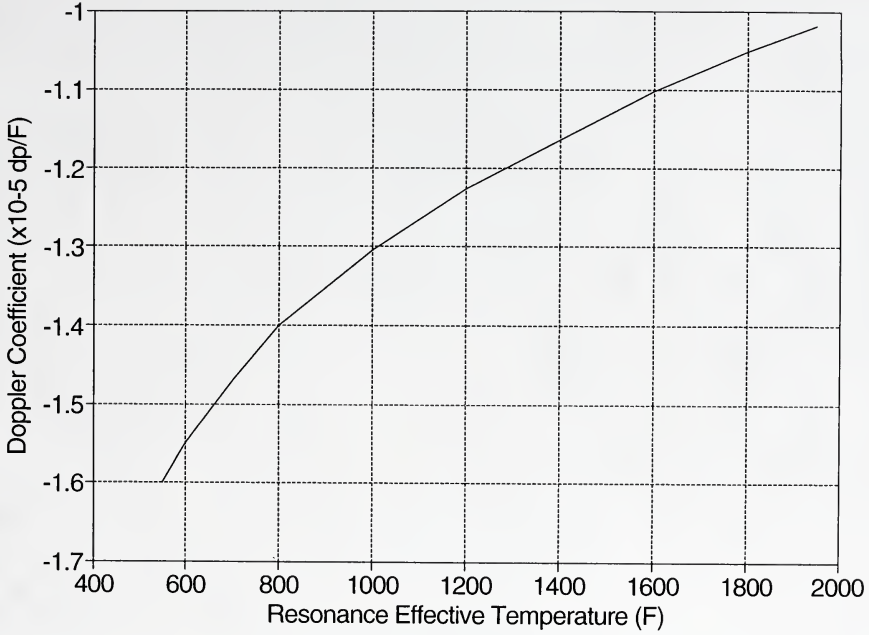

Figure 2-1: Doppler Coefficient vs. Effective Fuel Temperature at BOL [3]

broadening effect. This results in the reactivity curve being slightly less negative for burnup of conventional, gas-bonded fuel than for the lower operating temperature liquid bonded fuel. Thus, it is expected that a slightly higher beginning of life boron concentration is required for the liquid bonded fuel to achieve the same discharge burnup as the gas bonded fuel. Detailed calculations have been performed to determine the exact neutronic (fuel management) effect of the reactivity curve and indicate that the LBLWR fuel can operate within the current control rod patterns and boron concentration ranges.

Material Compatibility

Of critical concern for the use of liquid metal in light water reactor fuel is the compatibility of the bonding liquid with other LWR core materials. The materials of importance include the coolant/moderator (light water), zirconium cladding, UO_2 fuel, and fission products. The chemical reaction between the liquid and each of these materials must be minimal over the expected temperature range. Compatibility with the fuel and cladding is an obvious concern since the bonding liquid wets both materials. Also important is the liquid bond reaction with the light water coolant. In the event of a breach of the fuel cladding, violent reaction between the bonding liquid and water would be unacceptable from a safety standpoint. Further, the bonding liquid's final disposition and potential effect on the primary coolant loops is important.

Some of the candidate liquid metals such as potassium and sodium react violently with water at any temperature. The available literature [4,5] suggests that lead, bismuth, lead-bismuth eutectic, and tin do not react vigorously with water in the expected temperature range, and that lithium reacts moderately compared with other alkaline metals. Gallium is expected to behave corrosively with zirconium at the expected temperature range and it has been shown that zirconium is soluble to some degree in lead, bismuth, and tin [6]. Figures 2-2, 2-3 and 2-4 show the phase diagrams for zirconium/bismuth, zirconium/lead, and zirconium/tin, respectively. Tests run at 932°F by Hodge, Turner and Platten [6], showed little zirconium dissolution in the lead-bismuth eutectic under conditions similar to those expected in an operating fuel rod. There is no indication that significant chemical reactions occur between the other liquid metals (lead, bismuth, tin, and lithium) and UO_2, zirconium, and fission products.

Material compatibility tests were conducted by Thad M. Adams and Mark Dubecky under the direction of Dr. Richard G. Connell, Jr., of the Materials Sciences and Engineering Department and Dr. Glen J.Schoessow of the Nuclear Engineering Sciences Department of the University of Florida to determine the high temperature reaction characteristics of the liquid metal(s) chosen with the fuel rod materials [7,8]. The tests were conducted with donated UO_2 fuel and Zircaloy cladding from the Babcox & Wilcox Fuel Company and SIMFUEL, a simulated spent fuel, from Atomic Energy of Canada, Ltd. These tests are described in greater detail in Chapter 3.

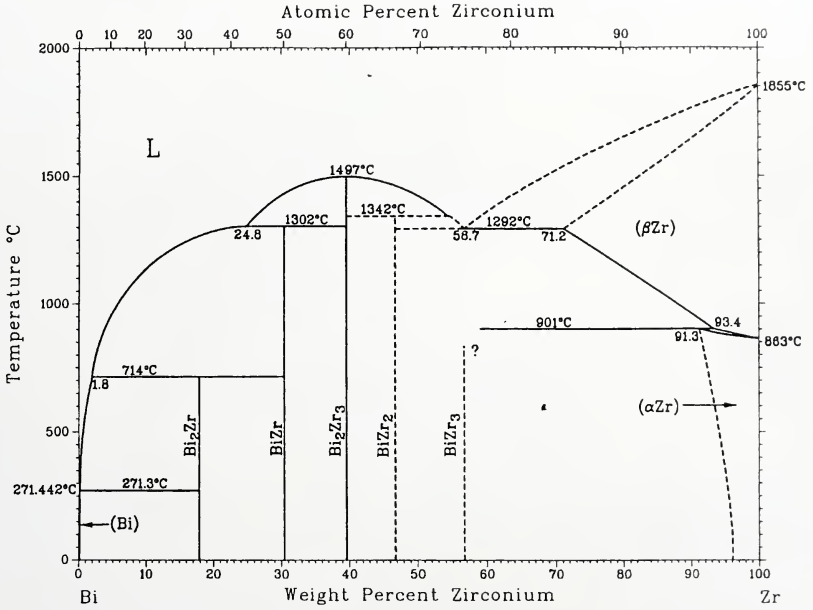

Figure 2-2: Binary Alloy Phase Diagram for Zirconium-Bismuth [6]

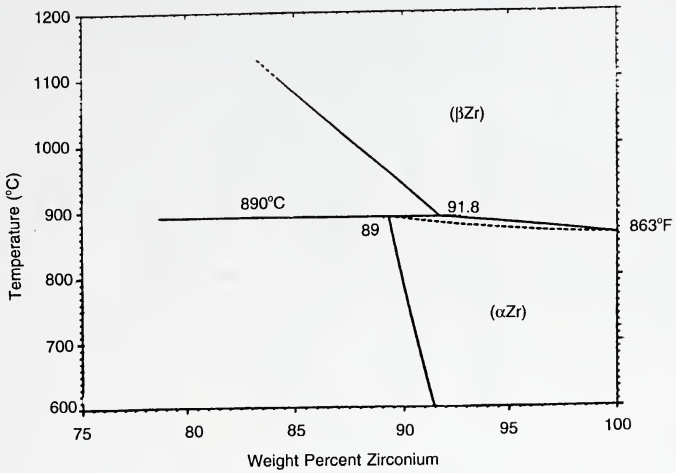

Figure 2-3: Binary Alloy Phase Diagram for Zirconium-Lead [6]

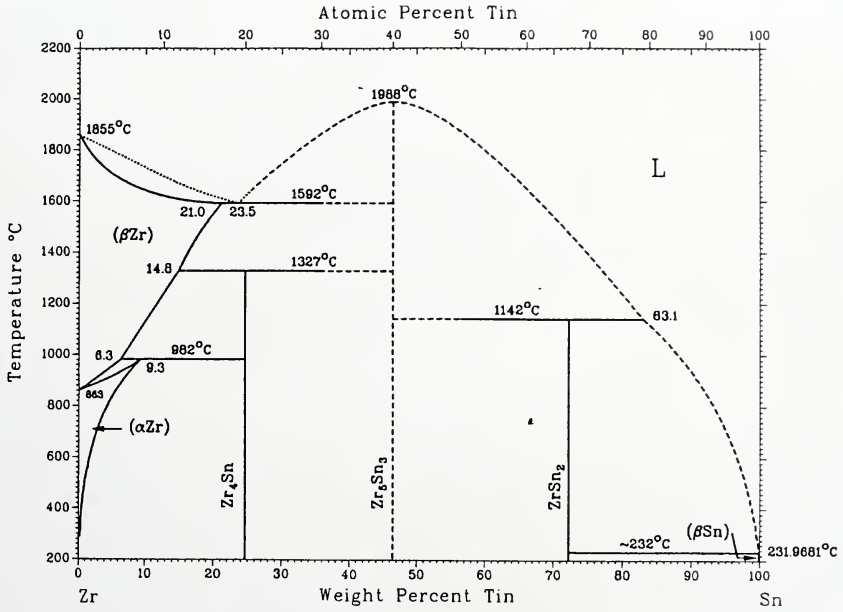

Figure 2-4: Binary Alloy Phase Diagram for Zirconium-Tin [6]

Fuel Rod Characteristics

It is important that any new LWR fuel design be able to replace and coexist with existing LWR fuel. For this reason, liquid bonded LWR fuel rods for existing reactors must be the same size as current LWR fuel, perform at or above current fuel burnup limits, and, when formed into fuel assemblies, exhibit acceptable handling characteristics during transportation and refueling.

For comparison purposes, PWR 15 x 15, PWR 17x17, and BWR 8x8 fuel rods are evaluated as liquid bonded fuel rod reference designs. The pellet and cladding dimensions, shown in Table 2-3, were chosen to be the same as the current helium filled fuel rod. For this evaluation, the gas gap volume was assumed to be filled with liquid metal. The size of this gap currently used in conventional gas-bonded fuel designs is selected based on manufacturing considerations that allow for pellet insertion, themal considerations which minimize the temperature rise across the gap during reactor operation, and other considerations including the accommodation of fission gas. Liquid bonded fuel pellets operate with no significant temperature drop across the gap; thus, the gap size is not an important consideration. The use of a liquid metal bond allows the gap size to be increased to any value desired for ease of manufacturing without concern for the effect on fuel temperature. As is shown in Chapter 6, however, other factors such as rod weight and fission gas plenum requirements will influence the gap size and liquid inventory.

Table 2-3: Fuel Rod Parameters for PWR and BWR Fuel			
Parameter	Westinghouse 15x15	Westinghouse 17x17	General Electric 8x8
Pellet OD	.3659 in	.3225 in	0.41 in
Pellet Length	0.6 in	0.6 in	0.41 in
Cladding ID	.3734 in	.3290 in	.419 in
Cladding OD	.422 in	.374 in	.483 in
Fuel Length	144 in	144 in	150 in
Rod Length	150.45 in	150.45 in	159.6 in
Pre-pressure	545 psia	545 psia	45 psia
Theo. Density	94%	94%	96%
Pellet Volume	.00876 ft^3	.00681 ft^3	.0115 ft^3
Pellet Mass	5.959 lbm	4.614 lbm	7.868 lbm
Clad Volume	.00253 ft^3	.00207 ft^3	.00419 ft^3
Clad Mass	1.03 lbm	0.84 lbm	1.706 lbm
Gap Volume	.000412 ft^3	.000338 ft^3	.000509 ft^3
Liquid Bond Mass:			
Lithium	.0123 lbm	.010 lbm	.0283 lbm
Pb-Bi	.263 lbm	.216 lbm	.585 lbm
Pb-Bi-Sn	.235 lbm	.192 lbm	.521 lbm
Total Assembly Weight			
Helium	1429 lbm	1367 lbm	657.8 lbm
Lithium	1432 lbm	1370 lbm	659.5 lbm
Pb-Bi	1484 lbm	1424 lbm	694.1 lbm
Pb-Bi-Sn	1478 lbm	1418 lbm	690.1 lbm

Reduced fuel temperatures affect the fuel nuclear performance and material properties. For example, as shown in Figure 2-5, the thermal conductivity of UO_2 decreases with increasing temperatures over the temperature range of interest [9]. Thus, the liquid metal bonded fuel will operate in a more favorable UO_2 thermal conductivity range and will experience lower radial thermal gradients. The combination of lower fuel temperatures and lower thermal gradients results in lower thermal expansion and significantly lower thermal swelling. Cracking of the UO_2 pellets is also expected to be significantly lower due to the lower operating temperatures and temperature gradients thus improving fuel performance. Irradiation testing illustrating these performance enhancements has been performed on liquid sodium bonded fast reactor fuels using uranium metal, uranium nitride, and uranium carbide [10]. Chemical reactions between UO_2 and sodium has precluded irradiation testing of liquid sodium bonded oxide fuel.

The total fission gas release rate is a function of the fuel burnup and the temperature history of the fuel. Fuel maintained at a lower temperature has a reduced gas release rate, and thus less gas is released over an equivalent fuel lifetime. Since liquid bonding dramatically reduces the fuel temperature, less gas is released, requiring less gas plenum volume to accommodate the fission gas. However, the displacement of the liquid bond material as the cladding creeps down during operation decreases the available fission gas volume. The gas volume behavior is discussed in greater detail in Chapter 6.

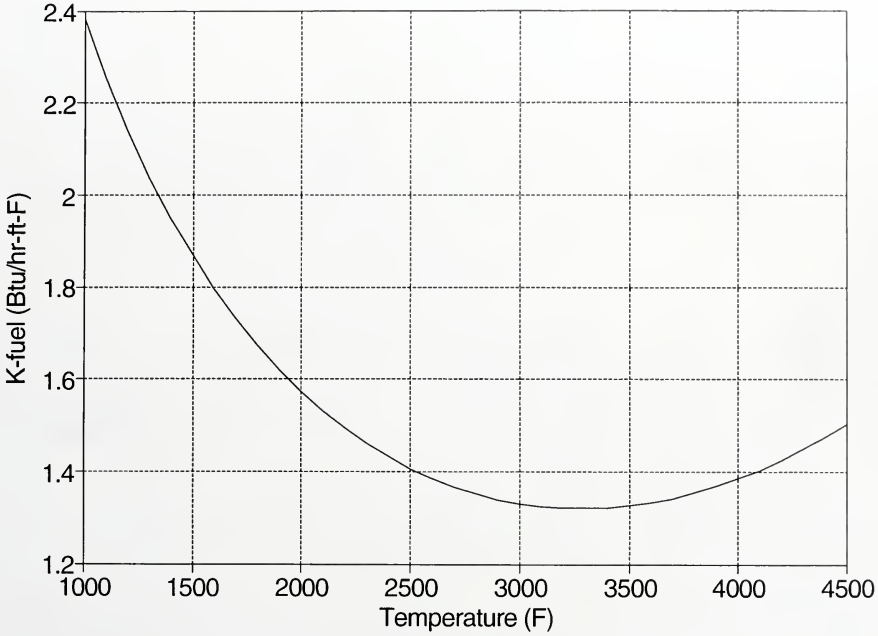

Figure 2-5: Uranium Dioxide Thermal Conductivity vs. Temperature [9]

It is important to maintain a path for the fission gas from the surface of the fuel pellet to the gas plenum to avoid local "hot spots" caused by gas blanketing. Experimental and analytical studies into gas blanketing are shown in Chapter 4.

A liquid bonded fuel rod will be heavier than a conventional LWR fuel rod, by an amount equal to the weight of the bonding liquid. As is shown in Table 2-3, the liquid bond increases the fuel rod weight by 0.012 lbm for lithium, 0.235 lbm for lead-bismuth-tin, and 0.263 lbm for lead-bismuth. The weight of the fuel assembly is increased by 0.18% for lithium, 3.4% for lead-bismuth-tin, and 3.8% for lead-bismuth. This increase would not significantly affect fuel handling capabilities.

As is shown in Table 2-3, assembly weight increases in a similar fashion for the 17x17 PWR fuel, and for the 8x8 BWR fuel.

Best Candidates

Based on expected operating temperature range, nuclear interaction, material compatibility, and fuel rod characteristics, the choice of the bonding liquid comes down to three candidate liquid metals; lead-bismuth eutectic, lead-bismuth-tin, and lithium. Each candidate exhibits a low melting temperature to assure liquid behavior during reactor start-up and operating conditions. Each exhibits a high boiling point temperature and low vapor pressure to assure liquid behavior at operating conditions and expected transients. Each does not significantly affect the core neutron economy, and each has been singled out as having a high degree of chemical compatibility with other reactor materials at elevated

temperatures. Lithium exhibits a moderate reaction with the light water coolant. Based on these criteria, the lead-bismuth-tin ternary alloy and the lead-bismuth eutectic are considered the best candidates, and lithium is considered a backup candidate.

Thermal Considerations

As has been shown, the key advantages of liquid bonded fuel is the lower fuel temperatures associated with the reduced thermal resistance across the gap between the fuel pellet and the cladding. The reduced thermal resistance has three important consequences:

1. Steady-state operating temperatures are significantly lower when compared with conventional fuel with low gap conductance.
2. Stored energy in the fuel is significantly lower. This condition leads to a far lower peak cladding temperature in the event of a loss of coolant accident.
3. Lower fuel temperatures over the fuel lifetime result in lower fuel pellet cracking due to lower thermal stress, reduced fission gas release, reduced thermal expansion, and safer nuclear characteristics. In addition, the fuel swelling is reduced and the plastic strain in the cladding is lower allowing for higher fuel burnup.

An initial scoping thermal/hydraulic analysis of the liquid bonded LWR fuel was performed, prior to detailed fuel performance calculations, to determine the steady-state and transient characteristics of the fuel, and the advantages compared with conventional LWR fuel. A qualitative discussion of the LBLWR fuel temperature characteristics is presented below, while the details of this analysis are presented in Chapters 5 and 6.

Steady-State Fuel Temperatures

The gas gap thermal resistance results in the high average fuel temperatures and high thermal gradients observed in conventional LWR fuel. The thermal gradients are due to the low thermal conductivity of the UO_2 resulting from the high operating temperatures as is shown in Figure 2-5. The temperature drop across the gap is a strong function of the gap conductance which comprises three components; conduction through gas, conduction at contact points between the cladding and the fuel pellet, and radiation heat transfer from the fuel surface to the inside surface of the cladding. A significant amount of research has been performed to characterize the gap conductance [11,12,13], which varies as a function of the fuel burnup. Typically, for PWR fuel, the gap conductance ranges from 500 Btu/hr-ft^2-°F to 3000 Btu/hr-ft^2-°F [9] and is a strong function of the gap size.

For liquid bonded fuel, the sole path for radial heat transfer in the fuel gap region is conduction through the liquid metal bond. For lead-bismuth with a

thermal conductivity of 8 Btu/hr-ft-°F, the gap conductance is 30,000 Btu/hr-ft^2-°F. Thus the temperature drop across the gap, which ranges from 300°F to 1000°F for a peak power conventional fuel rod over a typical range of gap conductance, is negligible for the liquid bonded case.

The advantages of lower fuel temperatures during steady-state operation are many. For a given power level, the margin to fuel centerline melting is substantially increased. In addition, parameters such as fuel thermal expansion, pellet stress and strain, and fission gas release, which are functions of the fuel temperature, are all reduced. Most importantly, the fuel rod stored energy is significantly lower, which greatly enhances the fuel transient performance.

Details of steady-state thermal analysis of the fuel rod are presented in Chapters 5 and 6.

Transient Performance

The lower temperatures expected for LBLWR fuel are important for mitigating the effects of reactor transients. Specifically, the lower stored energy in the LBLWR fuel rod reduces the rod heatup associated with loss of coolant and loss of flow transients. In addition, the large margin between operating fuel temperatures and the fuel melting point makes it more likely that the rod will survive power excursions resulting from local reactivity insertion accidents without undergoing a center melt condition.

The transient performance of LBLWR fuel is assessed in Chapter 5.

Thermal/Mechanical Limits and Design Criteria

Several criteria have been identified [9] with regard to fuel rod thermal/mechanical design, and fuel performance limits are determined by these criteria. A qualitative discussion of these criteria, and how they are affected by the use of liquid bonding follows:

1. Rod Internal Pressure Criterion. "The internal pressure of the highest power rod in the reactor will be limited to a value below that which could cause the diametral gap to increase due to outward cladding creep during steady-state operation and extensive departure from nucleate boiling (DNB) propagation to occur" [9:66]. The basis for this criterion is to assure that the diametral gap will not increase causing a decrease in the cooling water flow area between adjacent rods which will decrease the local heat transfer coefficient causing an approach to DNB conditions. Though the DNB condition resulting from flow blockage is still a concern for LBLWR fuel, the gas pressure in the fuel rod can be maintained at levels similar to current fuel designs. It is important to note that clad creep-down during the beginning of life can displace the liquid metal into the gas plenum, decreasing the volume needed for fission gas accumulation. Design features such as larger plena, optimized liquid bond loading, and lower rod pre-pressurization are necessary to accommodate the gas pressure. In addition, the effects of the liquid metal on the cladding will either decrease

or increase the resistance to creep. This effects are evaluated in Chapter 3.

2. Clad Strain Criterion. "For steady-state operation the total tensile creep strain is less than 1 percent from the unirradiated condition. For each transient event the circumferrential, elastic plus plastic strain shall not exceed a tensile strain range of 1 percent from the existing steady-state condition" [9:66]. Provided that liquid metal does not react with and alter the properties of the cladding, there will be no difference between the performance limits due to clad strain for conventional and liquid bonded fuel. In addition, lower fuel temperatures will reduce fuel thermal expansion which, in turn, reduces the pellet-cladding interaction. These effects are evaluated in Chapter 3.
3. Clad Stress Criterion. "The volume average effective clad stress shall not exceed the tensile yield strength of the clad material. This criterion arises from local pellet-cladding interaction due to thermal expansion of the fuel" [9:67]. Because liquid bonded fuel operates at significantly lower temperatures, the thermal expansion is reduced, and fuel performance limits due to clad stress are significantly improved.
4. Clad Temperature Criterion. "The clad surface temperature (oxide-to-metal interface) shall not exceed 750°F for steady-state operation, and 800°F for short-term transient operation" [9:67] As clad surface temperatures are a function of the rod power, clad surface area, and the bulk fluid conditions,

fuel performance limits due to clad temperature are the same for liquid bonded and conventional fuel.

5. Fuel Temperature Criterion. "The maximum fuel temperature shall be less than the melting temperature of the fuel" [9:68]. As is shown by the thermal analysis in Chapter 5, the peak operating temperature of the liquid bonded fuel is significantly lower than conventional fuel, and provides much more margin to fuel melting. Fuel performance parameters which are strong functions of fuel temperature such as fission gas release, pellet thermal expansion, fuel cracking, and pellet/cladding interaction are also dramatically improved.

Other criteria deal with clad fatigue, plenum spring support, clad flattening due to axial gaps, and axial rod growth. Fuel performance limits associated with these criteria are not significantly affected by the presence of a liquid metal bond.

The results of this qualitative discussion of thermal/mechanical fuel performance limits indicate that the potential for significant improvement exists from liquid bonded fuel, especially in the areas of maximum fuel temperature and pellet-clad interaction.

Fuel Rod Failure

To be considered a viable design option, the failure probability of liquid bonded fuel must be less than or equal to that of conventional fuel. In addition, the

consequences of failure and the effect a liquid bonded fuel rod failure on the core integrity and the reactor primary coolant system must be shown to be minimal.

As was discussed previously, cladding failure due to thermal/mechanical considerations is mitigated by the lower operating temperatures in the liquid bonded fuel rod, which reduce the onset of hard pellet-clad interaction. The interaction between the liquid metal bond and the cladding must be assessed to determine whether cladding integrity can be reliably maintained over the fuel lifetime. Chapter 3 discusses the results of material compatibility tests performed to characterize the liquid metal interaction with the clad material.

In the event of a failure of a liquid bonded fuel rod during reactor operation, high temperature water at 2200 psia for PWRs, and 1050 psia for BWRs will contact the liquid metal. The metal water reaction is of the form

$$M + xH_2O \longrightarrow MO_x + xH_2 + Q_{react} \qquad (2\text{-}1)$$

The heat of reaction, Q_{react}, varies for each liquid metal. Alkaline metals such as lithium, sodium, potassium, and cesium, exhibit the most vigorous reaction, ranging from moderate for lithium, to explosive for cesium. By comparison, lead bismuth, and tin react in a relatively benign manner, and have been singled out for use as reactor coolants [14].

Severe Accident Analysis

As discussed previously, liquid bonded fuel is less likely to experience a loss of fuel rod integrity in the event of a severe accident. This better performance is primarily due to the lower fuel operating temperatures and the correspondingly lower stored energy in the fuel rod. However, a severe accident in a reactor core consisting of both liquid bonded fuel and conventional fuel could expose the liquid bonded fuel to temperatures above the zirconium metal/water reaction threshold (1700°F), and cause a loss of fuel integrity. What effect the presence of the liquid bonded fuel has on the accident progression and overall severity must be determined. A qualitative discussion of the behavior of liquid bonded fuel in a severe accident is presented.

A Class IX accident in a LWR is defined as an event which falls beyond the plant design basis. This event involves, in general terms, loss of core cooling, and loss of active accident mitigation systems (emergency feedwater, core sprays, etc.). This results in core uncovery, and subsequent core degradation. Factors such as the speed at which the core uncovers (size of a primary system break), total stored energy in the fuel assemblies at the time of uncovery, decay heat levels, and the availability of engineering safeguard features (emergency core cooling system and residual heat removal), determine the severity of the accident.

For a large break loss of coolant accident (LOCA), core uncovery occurs while the fuel is essentially at operating temperature. During this phase, the liquid

bonded fuel, which operates at a lower temperature, would retard the overall heat up of the core. Conventional fuel rods with high stored energy would experience zirconium-water reaction due to cladding surface temperatures in excess of 1700°F. As a result of the exothermic nature of this reaction, large amounts of heat are generated and concentrated in the vicinity of the fuel pellets, causing fuel melting and relocation, and the evolution of hydrogen gas.

In a mixed core, as the conventional fuel rods heat up, the adjacent liquid bonded assemblies will experience an increase in cladding surface temperature due to radiation heat transfer from the hot neighboring assemblies. In addition, molten cladding and fuel relocating from disassociated conventional fuel rods could contact adjacent liquid bonded fuel rods and induce failure. After the LBLWR fuel cladding is breached, the bonding liquid metal is expelled and is added to the disassociated core material. The bonding metal could experience a metal-water reaction, as discussed previously, generating heat and additional hydrogen gas. Compared to the energetic reaction between steam and zirconium, the oxidation of the liquid metal bond is not expected to add significantly to the heat and hydrogen generated.

After the core material is relocated to the bottom of the reactor vessel, the reactor pressure vessel wall is thermally attacked and fails. The core material is deposited in the reactor containment, along with the non-condensible gases (hydrogen) generated during the accident. The hydrogen gas could ignite (in non-inerted containments) or explode causing pressure spikes inside the

containment. The buildup of hydrogen along with other non-condensible gases generated by the core material attacking containment structures could overpressurize and fail the containment, releasing radioactivity to the environment.

From this discussion, there are two major conclusions that can be drawn on the effects of liquid bonded fuel on Class IX accidents:

1. Liquid bonded fuel will lower the stored energy in the core. This causes the core to heat up less rapidly, and allows more time for operator mitigation. The higher the percentage of liquid bonded fuel in the core, the less severe the heat up of the core is likely to be following a large break LOCA.
2. After all the fuel is failed, the liquid bonded fuel will contribute additional heat and hydrogen generation due to the liquid metal reaction with water. Since the volume of liquid metal is much less than the zirconium, and the reaction is less vigorous, it is expected that this effect is not significant.

Manufacturing

Nuclear reactor fuel manufacturing has advanced to a highly automated state. To be considered a viable commercial option, the liquid metal bonded fuel must also lend itself to ease of manufacturing. After the fuel rods are sealed, the differences between the conventional and liquid bonded fuel must be minimal. Inherent differences such as somewhat higher weight per fuel rod and assembly

must be evaluated to determine whether fuel transportation equipment, refueling equipment, and in-reactor support structures are impacted.

A brief description of current LMR metal fuel manufacturing techniques is discussed, and possible application to current LWR fuel manufacturing is examined.

The manufacture of liquid sodium bonded metal fuel for liquid metal reactors is a complex procedure [1]. The pellets are stacked into the cladding tubes at room temperature and under "clean room" conditions. These tubes are sealed at one end, and the open end is attached to a vacuum pump through a tee fitting. After evacuating all gas from the tube, the fuel rod is heated to a temperature above the melting temperature of sodium (208°F), and the other end of the tee fitting is connected to a liquid sodium fill tank. The filling valve is opened and the tube is back-filled with liquid sodium. The tube is cooled and the end cap is welded in place to seal the rod. The liquid metal freezes upon cooling, but completely fills the interstitial spaces between the fuel pellets, and between the pellet stack and the cladding. During reactor start-up, the fuel temperature increases, and the liquid metal melts. When the coolant temperature reaches the melting temperature of the liquid metal, the liquid metal is completely melted, and the fuel rod operates as designed.

The manufacture of liquid bonded LWR fuel could be handled in much the same way as the liquid sodium bonded LMR fuel described above. Some reworking of existing LWR fuel manufacturing equipment and methods would be

required to handle liquid metals. Even so, the manufacturing of liquid metal bonded light water reactor fuel is technically feasible, and is capable of being automated to a high degree.

It is proposed that a simpler technique be considerd which involves placing all or a portion of the required bonding material in the form of a solid cylinder below the fuel pellet stack. The pellet hold-down spring is held in compression, and the fuel rod is evacuated. Upon heating, bond material liquifies and is forced into the diametral gap between the pellets and the cladding. The rod is then back-filled with helium and sealed.

Machining tolerances associated with the fuel pellets and cladding dimensions are extremely important for maintaining a predictable gap dimension and resulting thermal characteristics. No such constraint is placed on the liquid metal bonded LWR fuel due to the uniformly low thermal resistance across the gap.

Results of the LBLWR Feasibility Study

The results of this preliminary feasibility study indicated that LBLWR fuel exhibits sufficient merit to warrant further research. To accomplish this, a study was funded by the Department of Energy to conduct research in the following areas:

1. Laboratory testing of candidate liquid metals through material compatibility testing. This work is summarized in Chapters 3 and 4.

2. Detailed calculation of fuel rod steady-state and transient behavior. Calculations which integrate the effects of burnup dependent parameters such as fission gas release and fuel dimensional changes, to determine the fuel rod performance over a typical lifetime in a light water reactor. This work is summarized in Chapters 5, 6, and 7.

CHAPTER 3
MATERIAL COMPATIBILITY TESTING

As a result of the feasibility study, two candidate liquid metals, lead-bismuth eutectic (55.2w/oBi-44.8w/oPb) and a lead-bismuth-tin alloy (33w/oPb-33w/oBi-33w/oSn), were chosen to experimentally determine material compatibility between the liquid metals, Zircaloy-4 cladding, and the UO_2 pellets. For the purpose of light water reactor fuel, the compatibility between these materials is determined by the degree of reaction between the liquid metal, cladding, and pellets, synergistic effects of the three materials, and changes in the properties of the materials which would affect its function and the operation of the fuel rod.

This work was performed by Thad M. Adams and Mark Dubecky under the direction of Dr. Richard G. Connell, Jr., of the Materials Sciences and Engineering Department and Dr. Glen J.Schoessow of the Nuclear Engineering Sciences Department of the University of Florida [7, 8]. This work was accomplished by exposing the cladding material to the liquid metals at elevated temperatures for extended periods of time. The loss of wall thickness occurring in the cladding, and the degree of chemical reaction between the cladding and the liquid metal were determined. The results showed that lead-bismuth-tin alloy gave the best compatibility performance. A synopsis of this work is presented.

Discussion of Liquid Metal Attack

The phenomenon of liquid metal attack needs to be addressed differently from the standard idea of corrosion. Typically, corrosion is referred to as the chemical or electrochemical (galvanic) deterioration of a metal. However, when discussing liquid metal attack, this concept must be expanded to include solution of the solid metal in the liquid metal, the degree of attack being dependent upon the solubility in the liquid metal [15].

Solubility is an important factor in determining the extent of liquid metal attack of solid metals. Although simple solution of solid metals in liquid metals does occur, the majority of the attack associated with liquid metal corrosion involves more complicated concepts of solution and solubility. Solubility does seem to govern the rate of liquid metal attack on solid metals. Through early experimental work, it was determined that there are six basic types of liquid metal attack: simple solution, alloying/intermetallic compound formation, intergranular penetration, impurity reactions, temperature gradient mass transfer, and concentration gradient mass transfer [15, 16].

Simple solution of a solid metal by a liquid metal consists of the removal of surface metal from the solid until the solubility limit for the solid-liquid metal system is reached [16]. From the phase diagram for the solid-liquid metal system, one can predict the amount of solid metal that can be dissolved which, in turn, can be related to the amount of damage to the solid material. As expected, there is a strong coupling between the surface area of solid metal and the volume of liquid

metal [16]. In general, the smaller the volume of liquid metal, the less the depth to which attack can occur in the solid metal. In the simplest case, the attack will continue until the liquid metal becomes saturated with solute from the solid metal. Although solubility curves for the solid-liquid metal systems can give an accurate account of the amount of damage, they cannot supply any information as to the kinetics or rate of the solution process taking place. The kinetics of the process are of great concern since the liquid metal will be exposed to the cladding in liquid form for 4-5 years at temperatures over 600°F.

The formation of an intermetallic compound at the solid-liquid metal interface may be either beneficial or deleterious. Intermetallic layers forming at the solid-liquid metal interface can act as diffusion barriers that retard further deterioration of the solid by the liquid [17]. Additionally, metallic barrier layers are added to LWR fuel in order to improve pellet-clad interaction performance. On the other hand, since many intermetallic compounds are more brittle than the metal substrate, they can act to reduce the strength and/or toughness of the substrate metal.

Intergranular penetration/liquid metal embrittlement results from the preferential attack on the grain boundaries of the solid by liquid metal. Liquid metal preferential attack of grain boundaries is surface tension driven and causes the removal of solid metal along the grain boundaries by dissolving solid metal in the liquid metal [15, 16, 18]. From C. S. Smith's paper on interfaces and grains, it was shown that for a dihedral or spreading angle of 60° or less, a liquid will wet free

surfaces and penetrate toward the interior along grain boundaries [19, 20]. This particular manifestation of liquid metal attack is insidious; while no signs of apparent damage such as material loss or dimension change may be discernible, liquid metal embrittlement of the solid may reduce strength to such an extent that catastrophic failure occurs. Electron beam microprobe scanning is one of the methods used to detect such attack.

Impurities such as oxygen, nitrogen, hydrogen, and carbon have a pronounced effect on the reactions between solid and liquid metals [16, 18]. The most pronounced effect that these impurities have on solid-liquid metal systems relates to the kinetics of reactions, either increasing or decreasing the rate of attack. In addition, these impurity elements can change surface tension properties and suppress intermetallic compound formation.

The phenomenon of temperature gradient mass transfer can be related to a special case of the simple solution process. Temperature gradient mass transfer is observed in convection loops or heat exchanger tubes where the liquid metal is in motion through a solid metal channel. In convection loops or heat exchangers, some sections of the system are at higher temperatures than others. Because solubility generally increases with temperature, solid metal dissolves in the liquid in the hot zones, while in colder sections of the loop , it may plate out. By such a mechanism, partial or full blockage of coolant flow can occur. This phenomenon is characteristic of non-isothermal, dynamic systems, and will not occur in

isothermal systems, or static systems such as a thin layer of liquid metal between two concentric cylinders.

Concentration gradient mass transfer consists of solid metal dissolving into a liquid metal, then diffusing through the liquid metal and alloying with another solid metal [17, 18]. Concentration gradient mass transfer is most commonly seen in static liquid metal corrosion tests where the solid container material becomes alloyed with the test specimen or vice versa. The process is driven by a reduction in Gibb's free energy as the two metals alloy [17, 18].

The testing of liquid metal attack can be done by two methods: static or isothermal, and dynamic or non-isothermal. Static corrosion testing consists of placing a solid metal specimen into a liquid metal bath at a specified temperature. The specimen is exposed to the hot liquid metal for a prescribed period of time and then evaluated to ascertain the degree of attack. For a dynamic test, a forced or thermal convection loop is constructed to pump the liquid metal through the container material in order to simulate a heat exchanger, reactor piping, or similar component that is expected to experience temperature transients. Hot and cold sections are purposely built into the loop in order to examine solubility effects such as temperature gradient mass transfer.

The ability to determine quantitatively the amount of attack is often difficult [19]. The standard procedure used is to measure the weight loss or gain by the sample after exposure to the corrosive environment. For the case of liquid metal attack, simple weight loss/gain measurements may be misleading [19]. In order to

investigate the amount of attack when a solid metal is in contact with a liquid metal, four measurements are considered:

1. Dimensional Changes
2. Compositional changes
3. Weight changes
4. Depth of attack

One or more of these measurements may be used to quantify liquid metal attack. For this study, the dimensional changes and compositional changes at the liquid metal-solid interface was used to quantify the degree of attack.

The purpose of this study was to experimentally determine through the use of static, isothermal testing, the degree of attack experienced by the Zircaloy-4 cladding material when exposed to the candidate liquid metals at temperatures indicative of

1. Standard operating program (SOP) conditions. Temperatures expected during hot, full power operation of the fuel (750°F) for extended periods of time.
2. Limiting accident conditions. For reactor fuel, the highest temperatures expected during a design basis event are associated with loss of coolant accidents (LOCAs), where heat transfer to the coolant is significantly decreased leading to a rapid increase in the cladding temperature due to the stored energy in the fuel. For these tests the temperatures ranged from 1200°F to 1500°F for short periods of time. High temperature exposure for

short intervals was also viewed as a way to study accelerated attack since testing over a typical fuel lifetime (35,000 hours) was impractical.

Experimental Assessment of Bonding Liquid/Cladding Compatibility

The experimental studies at the University of Florida were performed over the course of two years in a joint effort between the Materials Science and Engineering Department, and the Nuclear Engineering Sciences Department. A discussion of the experimental procedures, including the materials, sample preparation, test matrix, determination and characterization of liquid metal attack is presented, as well as the interpolation of these results to determine the feasibility of the proposed liquid bonded LWR fuel design.

Materials Used in Experimental Samples

The Zircaloy-4 cladding used for this investigation was supplied by Babcock & Wilcox Nuclear Technology of Lynchburg, Virginia. The composition of this material is in accordance with the ASTM specification B350. Table 3-1 shows the specifications for reactor grade Zircaloy-4. The cladding was provided in 12 inch tube sections which were subsequently cut into 6 inch sections and sealed by welded stainless steel (type 304) end caps. The material provided consisted of

Table 3-1 ASTM B350 Chemical Composition Specification for Reactor Grade Zircaloy-4

ELEMENT	COMPOSITION RANGE (%)
Sn	1.20-1.50
Fe	.18-.24
Cr	.07-.30
Fe+Cr	.28
O	.10-.15
C	.010-.018
Si	.007-.012
Zr balance	

Table 3-2 Chemical Composition of Lead-Bismuth Eutectic Supplied by Cerro Metal Products, Inc.

ELEMENT	CHEMICAL ANALYSIS (%)
Cu	0.0001
Sb+Sn	0.005
Ni	0.0001
Pb	55.2
Bi	44.8

B&W 15x15 cladding (0.430 in. OD, 0.030 in. wall thickness), and B&W 17x17 cladding (0.375 in. OD and 0.025 in. wall thickness).

Eutectic lead-bismuth was purchased from Cerro Metal Products of Bellafonte, Pennsylvania, and was supplied as 0.25 in. diameter rod. The chemical composition of the lead-bismuth is shown in Table 3-2.

Alumina pellets were used to simulate fuel pellets in the cladding compatibility tests. Additional tests using depleted UO_2 pellets donated by Babcox & Wilcox Fuel Company to demonstrate the compatibility of the liquid metals with UO_2, and SIMFUEL simulated spent fuel donated by Atomic Energy of Canada, Ltd. were also used to determine compatibility with UO_2 and fission products. The pellet diameter is 0.366 in. for 15x15 fuel, and 0.322 in. for 17x17 fuel.

The ternary lead-bismuth-tin alloy used in this research was prepared from the eutectic lead-bismuth with additions of tin and lead stock. Tables 3-3 and 3-4 show the chemical compositions of the tin and lead stock, respectively. The lead-bismuth-tin alloy was produced by melting on a hot plate under flowing helium cover gas the proper amounts of lead-bismuth, tin, and lead in order to provide a ternary alloy composed of 33wt% Pb, 33wt%Bi, and 33wt%Sn. The approximate melting temperature of the alloy is 243°F [20, 21].

Sample Preparation

Zircaloy-4 cladding sections approximately 6 inches in length were sealed by welding a stainless steel end cap at one end. These sections were then filled with

Table 3-3 Chemical Composition of the Tin Stock Supplied by Ames Metal Products, Inc.

ELEMENT	CHEMICAL ANALYSIS (%)
Pb	0.0106
Sb	0.0036
Fe	0.055
Bi	0.0033
Al	0.001
S	0.001
Sn Balance	

Table 3-4 Chemical Composition of the Lead Stock Supplied by Fisher Scientific

ELEMENT	CHEMICAL ANALYSIS (%)
Cu	0.001
Sb+Sn	0.005
Bi	0.0001
Pb Balance	

one of the candidate liquid metal alloys. The tube sections were not filled completely so as to allow for the volumetric expansion of the liquid metal alloy when heated. Furthermore, from the study of past research in liquid metal attack, it was determined that there is a strong surface area-to-volume effect for liquid metals contacting solid metal surfaces [16]. In order to account for this effect, two studies were made, namely: tubes filled completely with liquid metal to represent a worst case scenario, and tubes containing simulated fuel pellets made of alumina (Al_2O_3) with liquid metal filling the gaps between the pellets and the cladding. A second stainless steel endcap was fitted into place to seal the tubes. Additional tests were run on tubes filled with UO_2 pellets to determine the compatibility between UO_2 and the liquid metal.

To minimize oxidation of the exterior of the tubes, the experiments were conducted in a helium atmosphere. The samples were loaded into the Barnstead-Thermolyne resistance wound tube furnace (Figure 3-1), and heated to the desired temperature. The samples remained at the target temperature for a prescribed period of time and were then allowed to cool to room temperature under a positive pressure of helium. The samples were then removed for analysis.

Test Matrix

Samples were subjected to two different temperature-time histories; representing standard operating program conditions (SOP), and typical loss of coolant accident (LOCA) conditions. SOP involves the day-to-day operation of the

Figure 3-1: Barnstead-Thermolyne Furnaces for Testing Samples

reactor during which liquid bond temperatures are expected to remain at approximately 750°F for the life of the fuel (30,000-40,000 hours with shut downs for scheduled refueling). To simulate the SOP conditions, samples were tested at 750°F for 100-3,500 hours.

During a LOCA, the temperature of conventional fuel cladding can reach 2200°F. Cladding remaining at these temperatures for even short periods of time experiences an energetic oxidation reaction with the steam which is present after the liquid coolant is lost. Calculations shown in Chapter 5 indicate that liquid bonded LWR fuel, due to the lower fuel operating temperatures, exhibits peak cladding temperatures in the range of 1200-1500°F for a LOCA. It was decided to test the samples at this temperature range for times between 6-24 hours to simulate the cladding response to a LOCA.

High temperature testing at short time intervals was also viewed as a way to study accelerated liquid metal attack, since testing over a typical fuel lifetime (35,000 hours) was impractical.

Metallographic Preparation of the Test Specimens

After the specimens had cooled to room temperature, they were removed from the furnace and sectioned using a diamond cut-off saw to produce 0.25 in. long cross-sections with flat surfaces. These sections were mounted in a 1 in. diameter mold using a quick setting resin. The mounted samples were polished prior to examination.

Measurement of the Loss of Tube Wall Thickness

Determination of the change in the tube wall dimensions as a result of exposure of the cladding to the liquid metal was measured directly from a series of photographs at a magnification of 100x. These photographs were measured using a dial caliper to 0.001 inches. Measurements from the tested samples were compared to as-manufactured standard tube wall thicknesses which were also measured from photographs. From this comparison, an average percent loss of wall thickness was determined as follows:

$$(\text{Standard wall} - \text{Tested wall} / \text{Standard wall}) \times 100 \qquad (3\text{-}1)$$

These average loss values were plotted versus testing time in order to generate plots that can be used to make predictions over the cladding lifetime.

Transition Layers at the Liquid Metal/Solid Interface

Early in the investigation, transition layers were found to form at the solid-liquid metal interface. As was discussed, the presence of these layers may have beneficial or harmful effects relative to the cladding performance. A technique that was used to characterize the transition layers is described below.

Electron beam microprobe analysis was performed using the JEOL SUPERPROBE 733 on the transition layers which formed at the liquid metal-solid

interface. The electron microprobe focuses an electron beam than impinges on the polished surface of the specimen producing characteristic x-rays, whose wavelengths report the quantitative chemical composition. The microprobe was used in the line scan mode by setting two end points and allowing the beam to move in a straight line in small periodic steps. The composition readings are plotted versus distance traveled in order to produce composition profiles necessary to study transition regions.

Liquid Metal Attack

Optical microscopy was used to determine the nature of the liquid metal attack. Polished specimens were anodized, then examined using a metallograph with a polarizer and full wavelength interference plate to view the microstructure of the cladding. Photomicrographs of the internal edge and the main tube wall of the cladding were made using magnifications of 200x to 500x.

Optical microscopy was also employed on the transition layer formed at the solid-liquid metal interface in an attempt to correlate thickness of the layer with length of time exposed, and to examine the integrity of the layer.

Results of the Material Compatibility Experiments

A total of 170 specimens from 79 tests were used to evaluate the liquid metal attack over a range of temperature-time histories. The specimens were tested

using both the lead-bismuth eutectic and the lead-bismuth-tin alloy. These specimens were evaluated for the amount of tube wall loss, and the interaction at the clad-liquid metal interface including the occurrence of liquid metal penetration of the grain boundaries.

Tube Wall Loss

The average loss of tube wall thickness measurements were made for both the SOP and LOCA specimens. Results for the LOCA samples are shown in Figures 3-2 to 3-7 for both candidate metals at three different temperatures. Results for the SOP samples are shown in Figures 3-8 and 3-9.

Figures 3-2 to 3-4 show the results for the eutectic lead-bismuth LOCA specimens. These specimens show a linear increase in tube wall loss with time for a specified temperature. Average loss data for specimens tested at 1215°F is shown in Figure 3-2. The two curves represent a specimen filled with liquid metal, and a specimen that contains alumina pellets and liquid metal. The specimen containing the large volume of liquid metal experienced a 14% decrease in the wall thickness after 24 hours. Nuclear Regulatory Commission (NRC) standards permit a 17% loss of tube wall thickness in one hour (due to clad oxidation). The second curve in Figure 3-2 representing the cladding tube containing pellets and a reduced liquid metal inventory, which is more indicative of an actual fuel rod, exhibits a 9.5% loss in 24 hours. These results demonstrate the surface area to liquid metal volume effect.

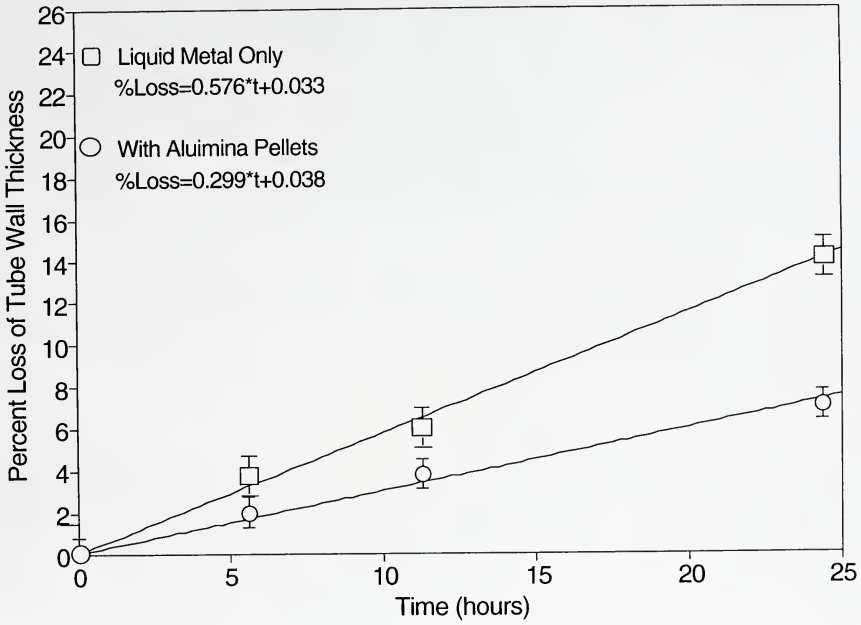

Figure 3-2: Loss of Wall Thickness, Lead-Bismuth Samples Tested at 1215°F for 24 hours [7]

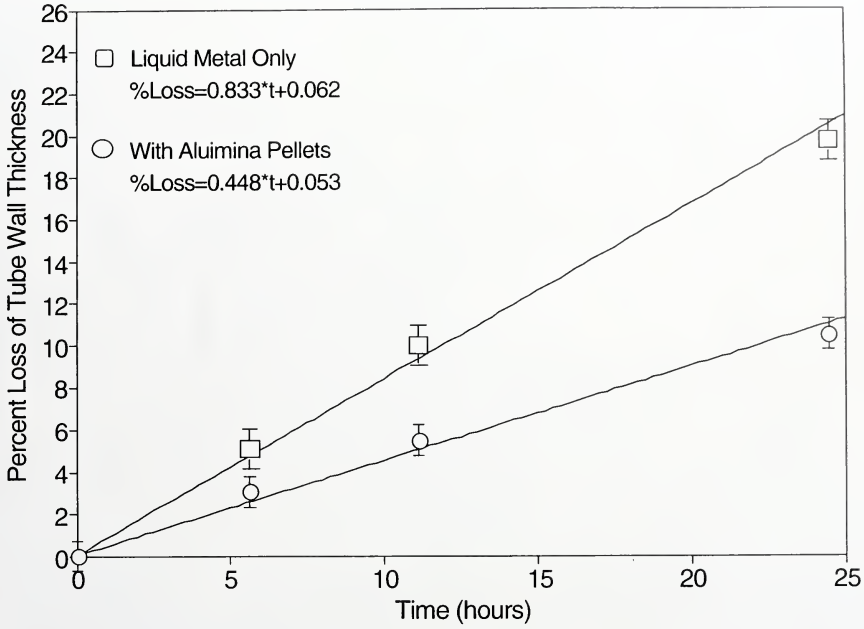

Figure 3-3: Loss of Wall Thickness, Lead-Bismuth Samples Tested at 1382°F for 24 hours [7]

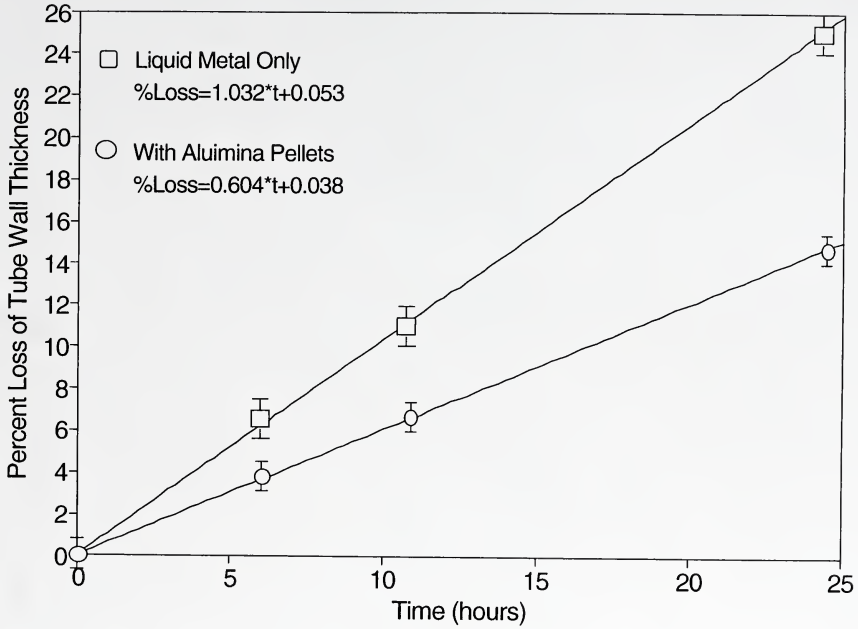

Figure 3-4: Loss of Wall Thickness, Lead-Bismuth Samples Tested at 1517°F for 24 hours [7]

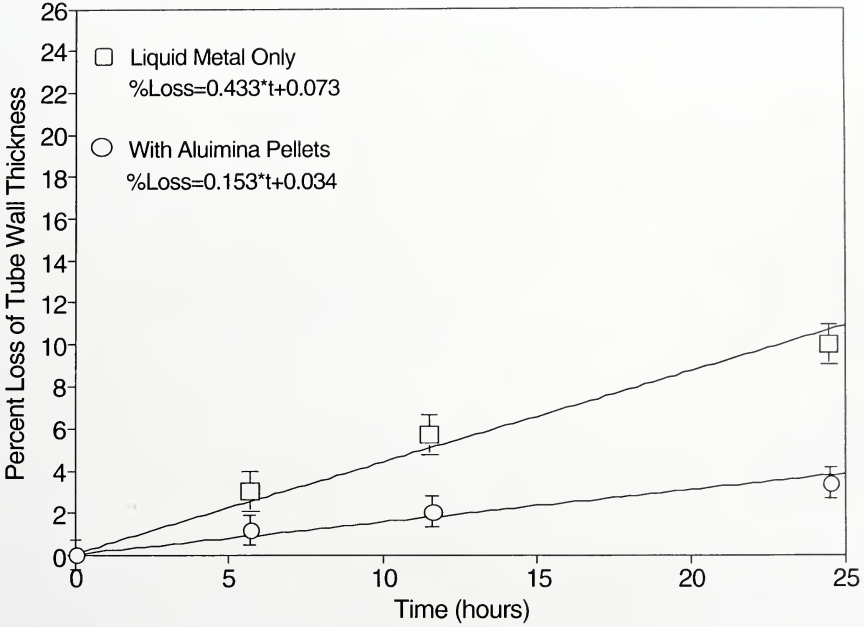

Figure 3-5: Loss of Wall Thickness, Lead-Bismuth-Tin Samples Tested at 1215°F for 24 hours [7]

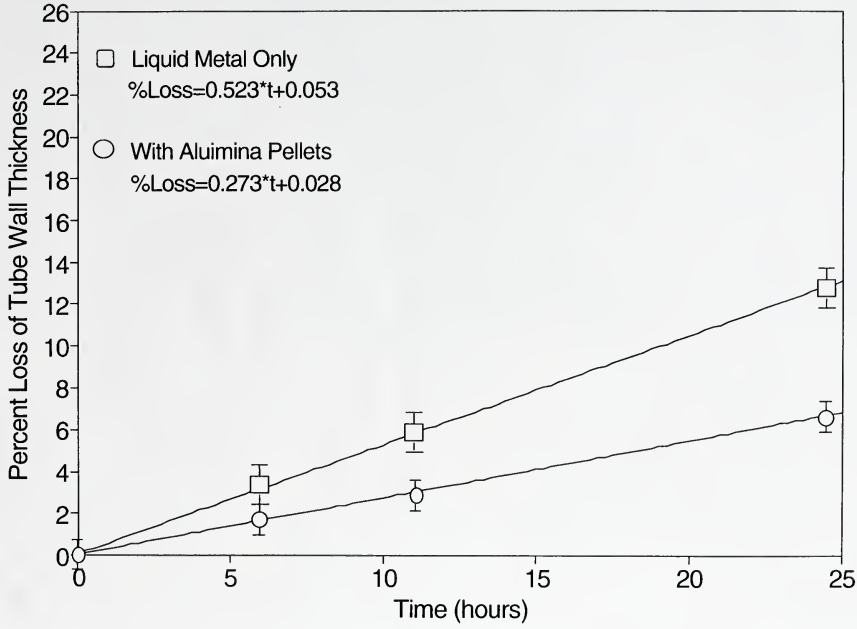

Figure 3-6: Loss of Wall Thickness, Lead-Bismuth-Tin Samples Tested at 1382°F for 24 hours [7]

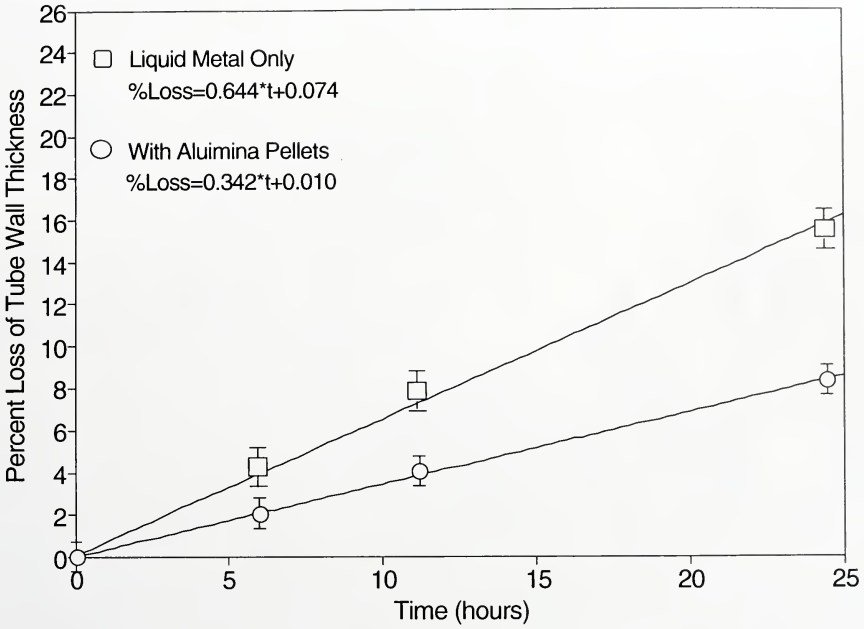

Figure 3-7: Loss of Wall Thickness, Lead-Bismuth-Tin Samples Tested at 1517°F for 24 hours [7]

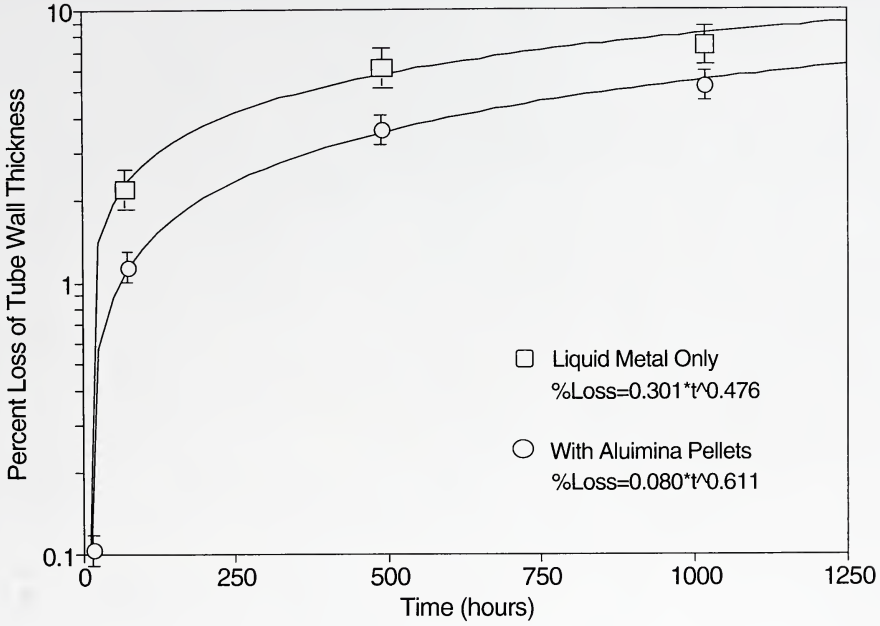

Figure 3-8: Loss of Wall Thickness, Lead-Bismuth Samples Tested at 750°F for 1000 hours [7]

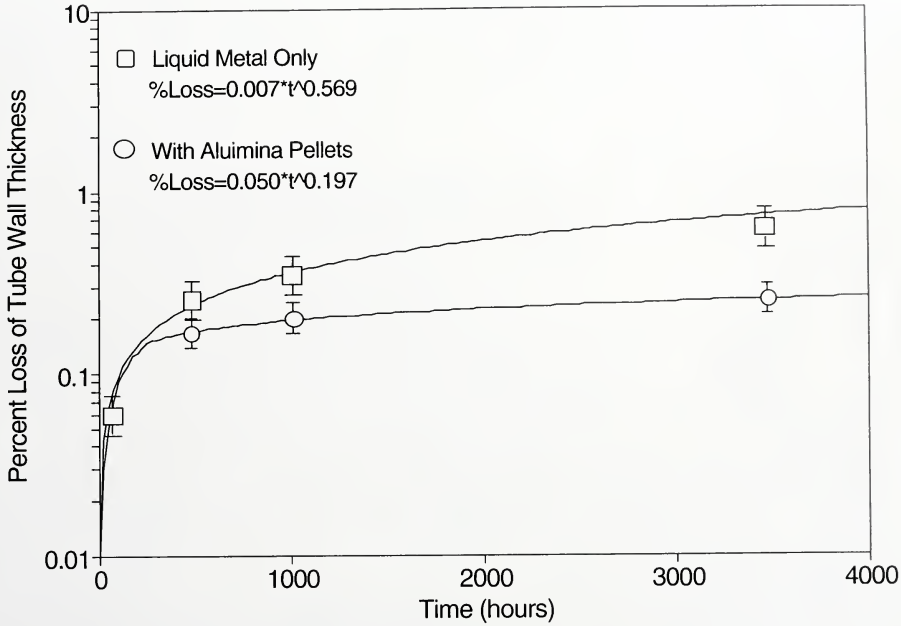

Figure 3-9: Loss of Wall Thickness, Lead-Bismuth-Tin Samples Tested at 750°F for 3500 hours [7]

Figures 3-3 and 3-4 show curves of tube wall thickness loss at 1382°F and 1517°F respectively. The average loss in tube wall thickness was found to be 19% in 24 hours for the tubes containing pellets for 1382°F, and 25% at 1517°F.

Figures 3-5, 3-6 and 3-7 shows curves of tube wall thickness loss at 1215°F, 1382°F, and 1517°F, respectively, for lead-bismuth-tin alloy. These specimens show a marked reduction in tube wall thickness loss over the lead-bismuth specimens, ranging from 4% for the 1215°F test with simulated fuel pellets at 24 hours to 10-15% for the 1517°F test. This may be explained by the transition layer formed at the solid-liquid metal interface.

For the SOP tests, specimens were tested at 750°F for longer period of time in order to simulate standard reactor operation. Figure 3-8 shows the results for the specimens containing lead-bismuth, while Figure 3-9 shows the results for the specimens containing lead-bismuth-tin. The lead-bismuth specimens were found to lose 7.5% average tube wall thickness in 1000 hours of operation. The lead-bismuth-tin specimens exhibit far lower wall thickness loss, with 0.2% measured for the simulated fuel rod after 3500 hours.

It can be concluded that for fuel lifetimes of 30,000-40,000, a LBLWR fuel rod using lead-bismuth-tin as the bonding liquid metal will exhibit favorable tube wall thickness loss characteristics. This is thought to be due to the formation of a zirconium-tin intermettalic reaction layer.

Evaluation of Reaction Layers

Photomicrographs of both the lead-bismuth and lead-bismuth-tin specimens tested for 1000 hours at 750°F are shown in Figures 3-10 and 3-11, respectively. Electron beam microprobe analysis of the reaction layer for both specimens is shown in Figures 3-12 and 3-13.

The reaction layer for the lead-bismuth specimen shown in Figure 3.10 appears black in color, and shows a lack of intimate contact with the cladding. The reaction layer is 3-4 mils thick. Compositional analysis of this layer shown in Figure 3-12 indicates that the reaction layer has an approximate composition of 70 weight percent bismuth and 30 weight percent zirconium, and formed a BiZr intermetallic compound.

The reaction layer for the lead-bismuth-tin specimen shown in Figure 3.11 appears lighter in color, and remains in contact with the cladding. The reaction layer is approximately 1 mil thick. Compositional analysis of this layer shown in Figure 3-13 indicates that the reaction layer has an approximate composition of 72.8 weight percent tin and 27.2 weight percent zirconium, and formed a $ZrSn_2$ intermetallic compound.

From the average loss of tube wall data, it has been shown that the eutectic lead-bismuth alloy exhibits much poorer compatibility with the Zircaloy-4 cladding, with losses 10-15 times that observed for the lead-bismuth-tin alloy. It is apparent that the $ZrSn_2$ intermetallic layer acts as a diffusion barrier, which, once formed, effectively stops the attack of the liquid metal on the cladding wall.

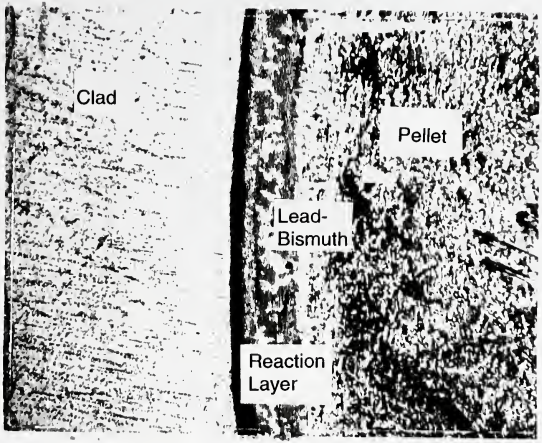

Figure 3-10: Photomicrograph of Reaction Layer, Lead-Bismuth Sample, 750°F for 1000 hours [7]

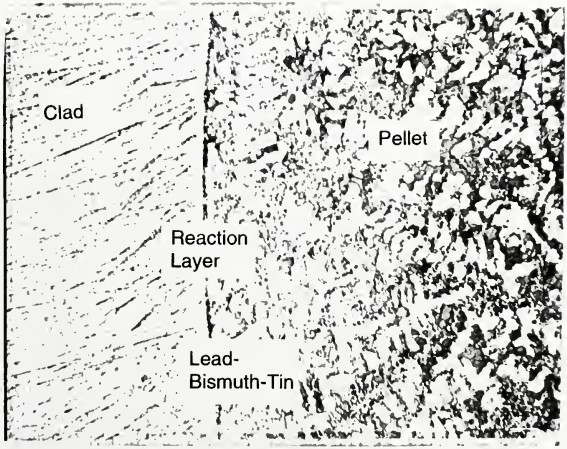

Figure 3-11: Photomicrograph of Reaction Layer, Lead-Bismuth-Tin Sample, 750°F for 3500 hours [7]

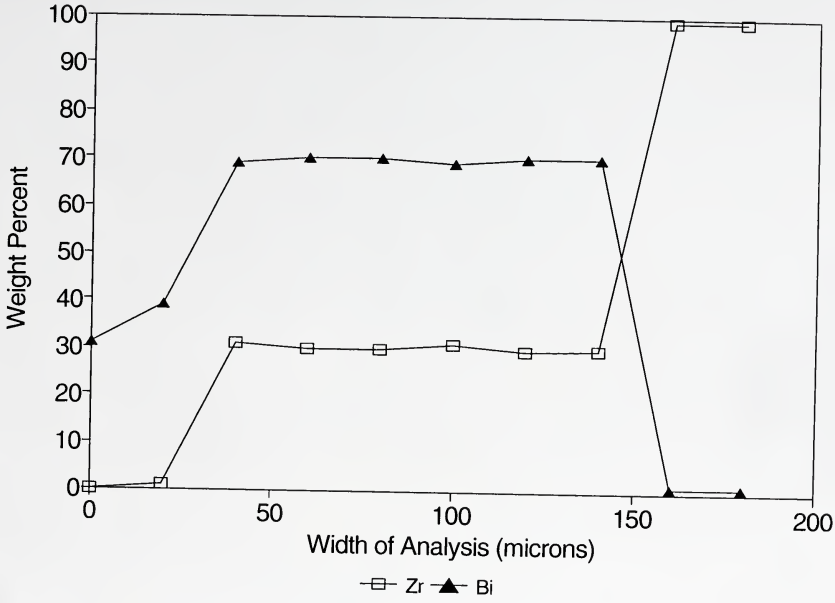

Figure 3-12: Electron Beam Microprobe Reaction Layer Analysis Lead-Bismuth Sample [7]

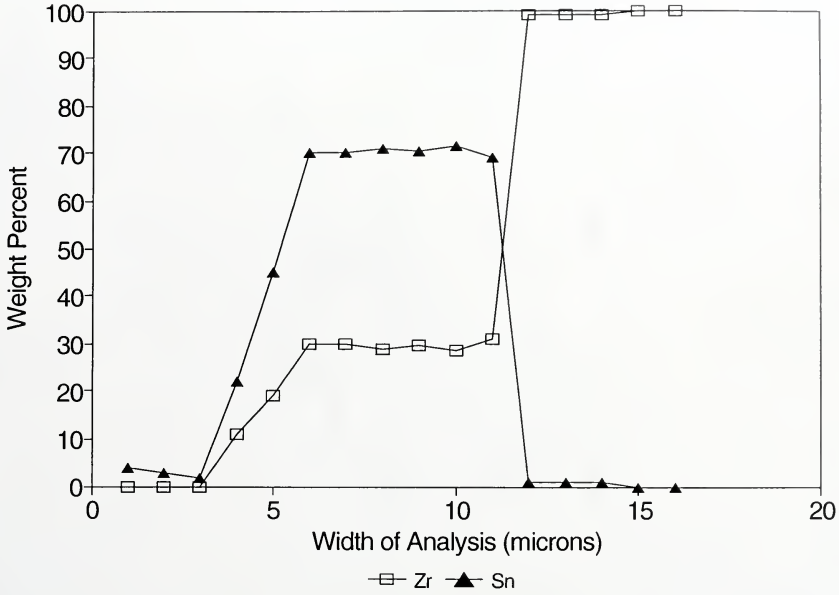

Figure 3-13: Electron Beam Microprobe Reaction Layer Analysis Lead-Bismuth-Tin Sample [7]

Liquid Metal Compatibility with UO_2

As discussed previously, compatibility tests were performed on Zircaloy tubes filled with liquid metal. Some of these tests included alumina pellets to simulate the effects of liquid metal volume reduction due to fuel pellets. A second set of tests were conducted to determine the effects of UO_2 pellets on the compatibility of liquid metal bonding material with other fuel materials. Two liquid metal alloys were tested; lead-bismuth-tin, and bismuth-tin-gallium. Tests were run with Zircaloy tubes containing depleted UO_2 pellets and filled with the liquid metal bonding alloy. The test specimens were tested at 750°F for 500 hours, representing standard operation procedure (SOP) conditions, and 1500°F for 24 hours representing loss of coolant accident (LOCA) conditions.

Slight differences were observed for the lead-bismuth-tin samples compared to the previous tests containing alumina pellets, namely, the formation of discernable $ZrSn_2$ crystals in the intermetallic layer as is shown in Figure 3-14. Previous tests, without UO_2, exhibited a uniform intermetallic layer with no observed crystal formation. Also shown in Figure 3-14 is an electron microprobe analysis of the intermetallic layer which shows a region of zirconium-uranium oxide which shows up as black. This oxide contains a large percentage of zirconium, and may be the precursor to the formation of the $ZrSn_2$ crystals.

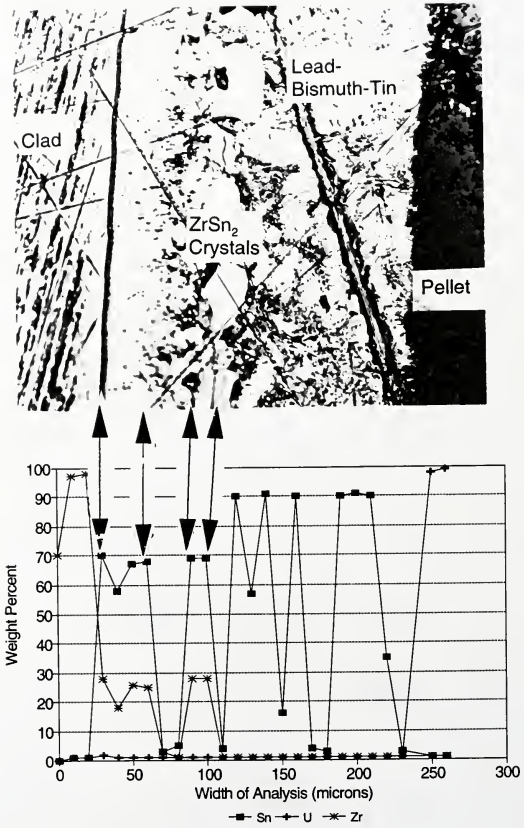

Figure 3-14: Optical Photomicrograph and Electron Microprobe results of Lead-bismuth-tin Sample with UO_2 pellets at 1500°F for 24 hours [8]

A hardness test was performed to determine the hardness of the $ZrSn_2$ layer relative to the substrate Zircaloy. These tests indicate that the intermetallic $ZrSn_2$ layer is significantly harder than Zircaloy (237 hV vs. 167 hV), and may add to the mechanical stability of the fuel rod and protect against pellet-clad interaction.

These tests shown that the properties of the UO_2 pellet are largely unaffected by the liquid bond, as no penetration into the pellet was observed, and no uranium was detected in the bulk liquid metal outside of the intermetallic layer.

Similar tests conducted using a bismuth-tin-gallium alloy indicate that the fuel matrix is soluble to some degree in the liquid metal, making this alloy unacceptable for long term compatibility with UO_2.

In summary, the presence of UO_2 pellets was found to have a definite effect on the morphology and abundance of intermetallic compounds. The lead-bismuth-tin alloy shows the formation of a zirconium-uranium oxide layer at the surface of the pellet, and a thin intermetallic layer made up of small crystals containing $ZrSn_2$.

The bismuth-tin-gallium alloy produced a larger amount of intermetallic compounds, as well as dissolving some of the UO_2. It is therefore deemed unacceptable for use as a bonding agent.

The results of these tests show that the lead-bismuth-tin alloy in the presence of UO_2 pellets does not affect the performance of the LBLWR fuel under standard operating and LOCA conditions.

Additional Experimental Studies

Additional experimental studies were conducted to determine the flow of fission gas through a small liquid metal-filled gap, and liquid metal-coolant at elevated temperatures. The results of these studies are summarized below.

Fission Gas Flow Through Liquid Metal

Experiments were conducted to determine the flow of fission gas through the liquid metal. These tests showed that helium and nitrogen gas readily rose through the liquid metal and did not blanket either the pellet or clad. These results confirm the data reported for fission gas release in sodium bonded fuel [22].

Liquid Metal - Coolant Interaction

Additional tests were run to confirm the non-reactive nature of the liquid metal with coolant water in case of a rod defected by a fretting mechanism. The tests with liquid lead-bismuth-tin at 600°F and water (<212°F) showed no reaction.

Summary of Experimental Studies

The following conclusions can be drawn from these experiments:

1. The lead-bismuth-tin alloy demonstrates better compatibility with Zircaloy-4 than lead-bismuth eutectic.

2. Extrapolation of the average loss of tube wall thickness data predicts 0.3% loss in 5,000 hours under standard reactor operating conditions using the lead-bismuth-tin alloy. This corresponds to less than 2% loss over the fuel lifetime assuming the correlation is valid over longer exposure times.
3. The lead-bismuth-tin alloy exhibits no significant reactions when exposed to UO_2 pellets at prototypic temperatures. Bismuth-tin-gallium, however, reacts with both the cladding and fuel and is deemed unacceptable for use in LBLWR fuel.
4. On the basis of the tests conducted to date, the lead-bismuth-tin alloy meets all of the material compatibility requirements for a candidate liquid metal to be used in a light water reactor fuel design.
5. Additional studies which examined gas bubble transport through small liquid filled gaps, and liquid metal-coolant interaction failed to produce any "show-stoppers" which would preclude the use of liquid metal in light water reactor fuel.
6. Experiments are currently underway to determine the compatibility of the lead-bismuth-tin with fission products. SIMFUEL, a simulated spent fuel obtained from Atomic Energy of Canada, Ltd. is being used in this study.

CHAPTER 4
LIQUID METAL WETTING IN ANNULAR GAPS

Experimental studies were conducted to determine the wetting characteristics of the liquid metal bond material, especially in small gaps. Such concerns arise due to the small diametral gaps, and eccentricities associated with the fuel manufacturing process. These eccentricities are a problem for conventional fuel rods as the unequal gas gap can result in local hot spots on the cladding.

Fabrication of LBLWR fuel rods involves the insertion of pellets into the cladding tube, and the introduction of the liquid metal into the cladding so that it fills the spaces between the pellets, and the annulus between the pellets and the cladding. As was discussed in Chapter 2, there are several methods for filling the tubes. One technique is to apply a vacuum to a loaded fuel rod at an elevated temperature, and back filling with liquid metal. A second method is to load solid metal slugs into cold tubes tube before loading pellets, using the spring to supply compression. As the rod is heated, the metal melts and is forced into the gaps by the force of the spring. In either case, the rods must be inspected to be sure that the liquid metal fills the gaps.

An experimental study was performed to characterize the wetting behavior of liquid metal in small gaps. The results of this experiment were used to determine

the effect of gas blanketing due to inhomogeneous distribution of the liquid metal on the fuel rod temperature profile.

Experimental Studies

Experiments were carried out under the direction of Dr. Glen J. Schoessow of the Nuclear Engineering Sciences Department of the University of Florida to confirm the fabrication and wetting behavior of the liquid metal/ UO_2/Zr bond. For these tests, UO_2 or Al_2O_3 pellets were loaded into quartz tubes approximating the cladding with solid lead-bismuth alloy on top of the pellets. The tubes were evacuated, the rods were heated to 400°F, and the liquid alloy was allowed to flow by gravity around the pellets. These tests showed that due to surface tension, the lead-bismuth alloy will not wet dimensions of one mil or less. An analytical study was performed to determine the effects of gas blanketing on the radial temperature profile, and the fuel centerline temperature.

Other liquid metals were tested to determine wettability, including non-lead alloys such as tin-bismuth-gallium. These studies showed similar results.

Analytical Predictions of Gas Blanketing due to Eccentricity

A two-dimensional (radial and circumferential) model of 180° section of a Westinghouse 15 x 15 fuel rod was modeled using the TRUMP generalized heat transfer computer code [23]. The rod, cladding, and gap material are all modeled,

and the pellet and cladding are assumed to be misaligned with a .001 inch gap on one side. One-tenth of the rod is assumed to be gas blanketed (i.e. the gap is assumed to be .001 inch wide and filled with helium), and the rest of the gap contains liquid metal bond. The rod is assumed to operate at an average power of 6 kW/ft, and the peak axial location has been modeled with a local peaking factor of 1.2. The fuel pellet and cladding dimension, as well as the reactor coolant thermal/hydraulic conditions are assumed to be at hot, full power conditions. The computer model used in this analysis is shown in Figure 4-1.

Results and Conclusions

Two separate runs were made

1. Symmetric gap is completely filled with liquid metal
2. Eccentric gap with gas blanketing the rod for < .001 inch gap

A comparison of the radial temperature profile for the symmetrical (completely liquid bonded) case, and the minimum and maximum gap eccentricity for the liquid/gas bonded case are shown in Figure 4-2. Also shown is the radial temperature profile for a conventional gas bonded fuel rod.

As shown in Figure 4-2, there is a local "hot spot" associated with gas blanketing in the minimum clearance area. Circumferential heat conduction mitigates this effect, however, and the net result is a radial temperature profile which is less than 100°F higher than the maximum clearance (liquid bonded)

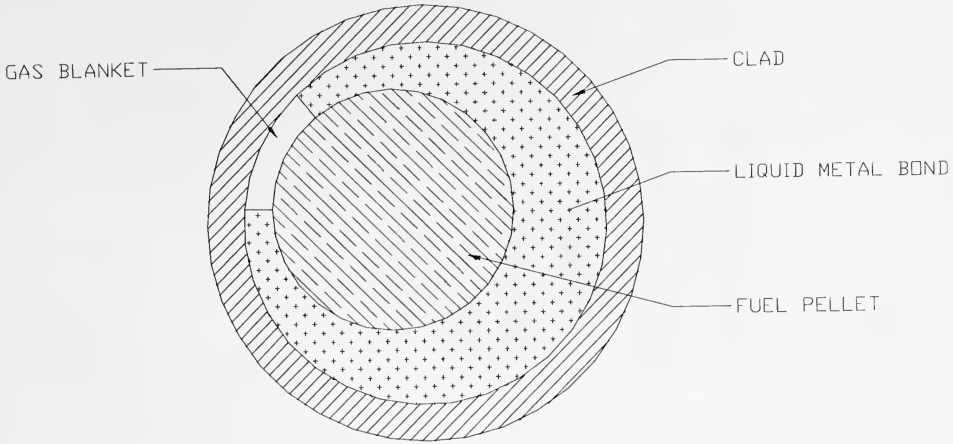

Figure 4-1: TRUMP Computer Model for Eccentric Rod Study

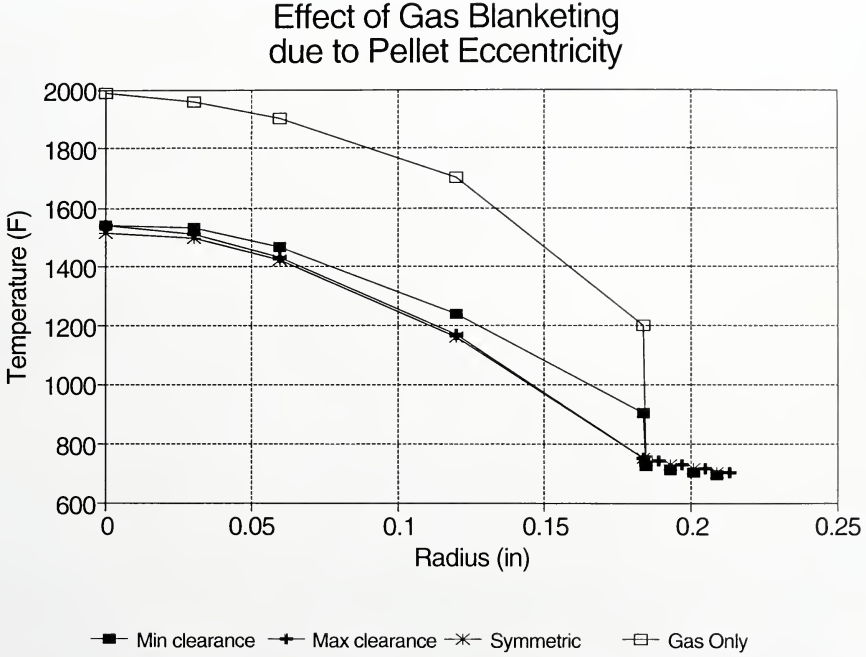

Figure 4-2: Eccentric Rod Study - With and Without Gas Blanketing

profile. In addition, the overall fuel temperatures are slightly higher (approximately 25°F at the centerline) for the eccentric rod than for the symmetrical rod, owing to the 10% reduction in high thermal conductance area.

Both cases exhibit far lower centerline temperatures and stored energy than the conventional fuel rod which is, in a sense, completely gas blanketed.

The results of this study indicate that

1. Liquid metal incorporated into the LBLWR fuel rod will fill the gaps between the pellets and cladding completely for any gap greater than approximately 0.001 inch.
2. In the event that small areas of the rod are gas blanketed due to rod eccentricity or other causes, the resultant increase in peak fuel temperatures is small due to circumferential heat conduction from regions of poor conductance (gas blanketed), to regions of high conductance (liquid bonded).

CHAPTER 5
LIQUID BONDED FUEL ROD THERMAL ANALYSIS

The potential benefit of liquid bonded LWR fuel lies in the reduction of the fuel centerline temperatures and the corresponding reduction in fuel stored energy. In order to evaluate the performance of the liquid metal bonded LWR fuel, detailed thermal analyses were performed using the TRUMP [23] generalized heat transfer computer code. In addition, a fuel thermal/mechanical computer code, ESBOND, was developed to assess the LBLWR fuel performance over a typical fuel cycle. The results of these calculations are discussed in Chapter 6.

Steady-State Fuel Temperatures

The steady-state operating characteristics of the liquid bonded LWR fuel were determined by constructing a simple one-dimensional radial heat conduction model. This analysis considers a typical PWR fuel rod design, (17 x 17 PWR rod) operating at average (6 kW/ft) and peak (13 kW/ft) linear power, with forced convection flow along the outside of the cladding. The LWR fuel dimensions are used with the gas gap replaced by liquid metal. Fuel rod dimensions are taken from Table 2-3. The forced convective heat transfer coefficient between the

cladding and the light water coolant is assumed to be 4000 Btu/hr-ft^2-°F, and uniform heat generation is assumed to occur throughout the fuel volume.

The TRUMP generalized heat transfer computer program was used to determine the steady-state radial temperature profiles for the liquid bonded fuel, and for conventional LWR fuel.

Over the life of a conventional LWR fuel rod, the thermal conductance that occurs in the gas gap varies from 500 to 3000 Btu/hr-ft^2-°F [9]. Liquid metal reactor fuel, on the other hand, which employs liquid metal bond material in the fuel-cladding gap, exhibits virtually zero thermal resistance across the gap throughout the fuel lifetime.

A radial heat conduction model consisting of 20 fuel nodes, and 6 cladding nodes was constructed using TRUMP. The effect of varying the thermal resistance between the fuel and cladding was studied by performing several steady-state calculations. The effect of varying the gap conductance for a typical fuel rod (Westinghouse 17x17), is shown in Figure 5-1 for a average linear power of 6 kW/ft. Figure 5-2 shows the effect of varying gap conductance for a peak linear power of 13 kW/ft. These results show that the centerline fuel temperature for a LBLWR rod can be reduced from 150°F-650°F for an average power rod, and 450°F-1600°F for a peak power rod by eliminating the gap resistance using the liquid metal bond.

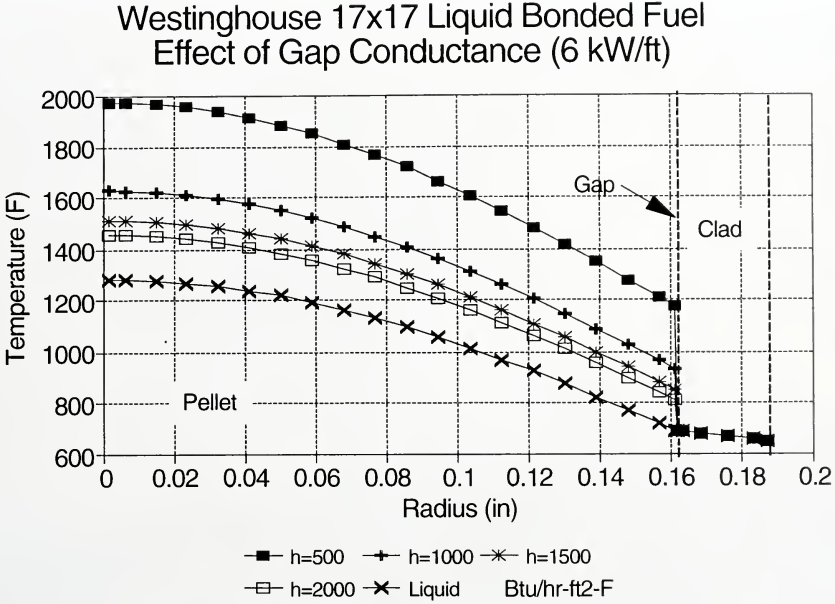

Figure 5-1: Fuel Temperature Profile vs. Gap Conductance (6 kW/ft)

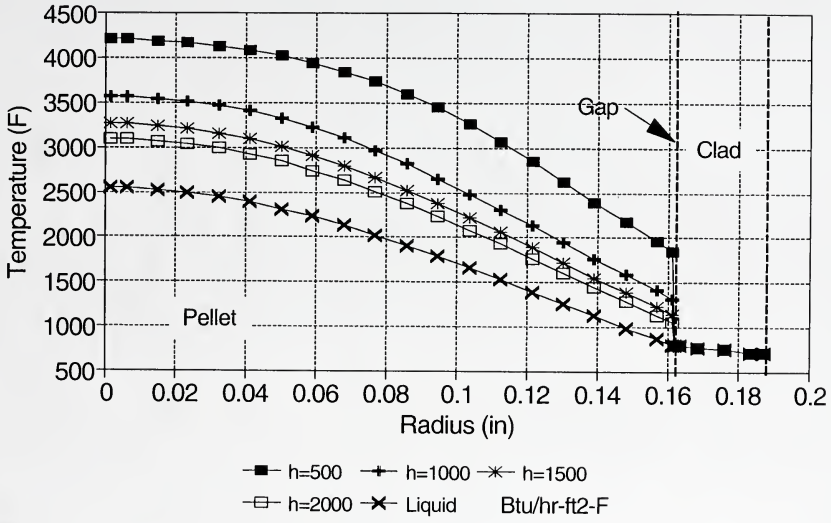

Figure 5-2: Fuel Temperature Profile vs. Gap Conductance (13 kW/ft)

Thus, a reduction of the fuel centerline temperatures translates directly into increased operating margins for LBLWR fuel, as compared to conventional LWR fuel.

Lower operating fuel temperatures also increase the fuel thermal conductivity, as is shown in Figure 2-3. Higher fuel thermal conductivity decreases the radial temperature gradient in the fuel pellet. The integrated effects of lower fuel temperatures and radial temperature gradient on operating fuel characteristics such as fission gas release, fuel cracking and swelling, fuel-cladding interaction, and clad integrity will be assessed using the fuel lifetime calculation code that is described in Chapter 6.

It can be concluded from this simple steady-state analysis that the liquid bonded fuel operates at far lower temperatures than the conventional LWR fuel, especially at the beginning of life when the maximum thermal resistance occurs for conventional fuel. This is primarily due to the lack of thermal resistance across the gas gap, and to a lesser extent, the improved thermal conductivity of UO_2 at these lower temperatures. For the 6 kW/ft case, the contribution of the reduced thermal impedance over the liquid metal gap to the reduction in centerline temperature at beginning of life is 66%, compared to 34% from the increased thermal conductivity.

Transient Performance

The TRUMP model used to determine the fuel steady-state operating temperatures can also be used to evaluate the LBLWR fuel performance in the event of a postulated accident. Two accident scenarios are examined:

1. Loss of coolant accident -- Instantaneous transition from forced convection heat transfer at the start of the event to steam cooling, coupled with an instantaneous reduction to zero power.
2. Transient overpower -- Step increase in fuel pin linear power resulting from a local reactivity excursion.

Loss of Coolant Accident

In a large number of design basis accidents, heat transfer to the coolant is sharply curtailed due either to loss of flow or loss of coolant. In these cases voids appear in the core, shutting down the nuclear reaction, but causing the cladding temperature to rise sharply due to the loss of heat transfer from the cladding surface. This rapid increase in clad temperature is due to the stored energy in the fuel which is given by

$$Q = \rho c_p \int_V [\, T(r) - T_w \,]\, dV \qquad (5\text{-}1)$$

where ρ is the fuel density

c_p is the fuel specific heat

V is the fuel volume

$T(r)$ is the radial temperature distribution

and T_w is the fuel rod outer surface temperature

For a cylinder with internal heat generation, the radial temperature profile is given by

$$T(r) = T_w + (T_o - T_w) [1 - (r/R)^2] \quad (5\text{-}2)$$

where T_o is the fuel centerline temperature

and R is the outer radius of the fuel rod

Substituting the temperature profile into equation 5-1 and integrating over the volume yields

$$Q/L = \pi \rho c_P (T_o - T_w) R^2/2 \quad (5\text{-}3)$$

where Q/L is the stored energy per unit length of fuel rod

A transient heat conduction calculation was performed to determine the effect of the stored energy on the cladding temperature after a loss of coolant event.

The steady-state temperature profiles for both liquid bonded and conventional fuel types were used as initial conditions for the transient. To simulate the power shutdown associated with the sudden loss of moderator, a step change in the fuel volumetric heat generation rate from 13 kW/ft to decay heat levels is assumed at the beginning of the transient. For simplicity, the decay heat is conservatively assumed to remain at 6% of operating power throughout the transient. To simulate the loss of coolant, a step change in the cladding surface heat transfer coefficient from 4000 Btu/hr-ft^2-°F (forced liquid convection) to 10 Btu/hr-ft^2-°F (steam cooling) is assumed at the beginning of the transient.

The steady state temperature profile in the fuel pellet is highly peaked due to the large heat generation rate, and the low thermal conductivity of the fuel. With the drastic reduction in the cladding surface heat transfer coefficient, the temperature profile is forced to assume a much flatter shape, which causes a large increase in the cladding surface temperature. The fuel and cladding quickly reach a quasi-equilibrium temperature which results in high cladding temperatures, as is shown for both liquid bonded and conventional 17 x 17 fuel in Figure 5-3. These temperatures are somewhat conservative due to the constant decay power level. For a more realistic decay heat curve, the rate of temperature increase would be continually less for both fuel types. The assumption of constant decay power is valid for comparisons over the first 40 seconds as is shown in Figure 5-3. Due to the lower average fuel temperature for the liquid bonded fuel, the maximum

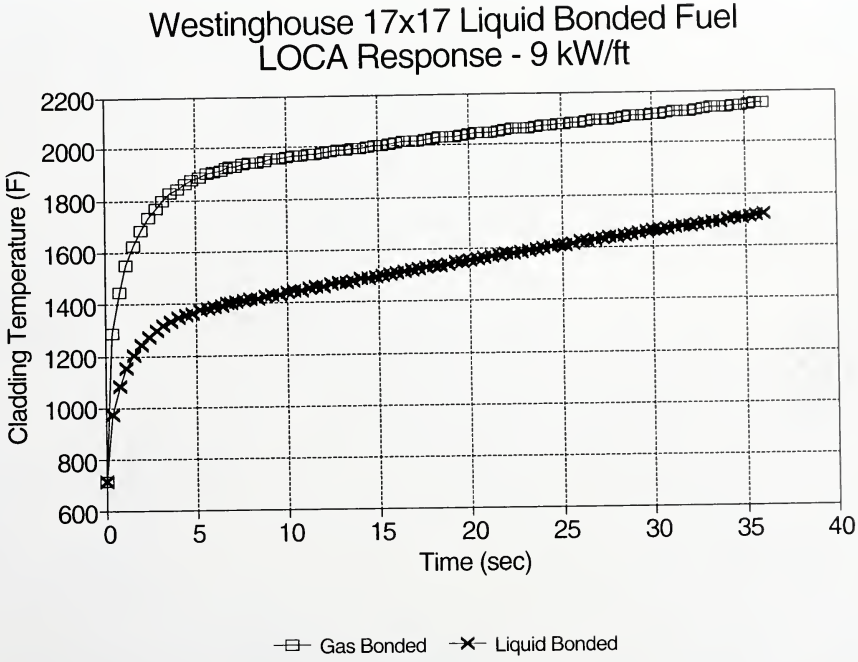

Figure 5-3: Transient Response to a Simulated LOCA

cladding surface temperature during the transient is significantly lower for the liquid bonded fuel than that calculated for the conventional fuel.

At high temperatures, the zirconium cladding reacts violently with water vapor creating additional heat, releasing hydrogen gas, and causing extensive damage to the fuel. The zirconium-water reaction is highly temperature dependent as is shown in Figure 5-4. Imposed upon this figure are the equilibrium temperatures reached by both of the fuel types (liquid bonded and gas bonded) after a loss of coolant event. The lower equilibrium fuel temperature experienced by the liquid bonded fuel during the transient results in approximately a factor of 50 reduction in the zirconium-water reaction rate constant when compared with conventional fuel, and assures that the zirconium-water reaction is dramatically lower. Similar results are expected for BWR fuel rods.

The time lag associated with reaching equilibrium temperature in the cladding following a LOCA is somewhat lower for the liquid bonded fuel. This is due to the smaller thermal resistance across the gap, which causes the cladding to heat up faster than the conventional gas gap design. Although the cladding for the liquid bonded fuel reaches an equilibrium temperature faster, the overall reduction in temperature is a far more important factor in mitigating clad damage.

Transient Overpower

Lower operating fuel temperatures similarly play a role in minimizing the effects of an unscrammed transient overpower event. For this case, the fuel rod is

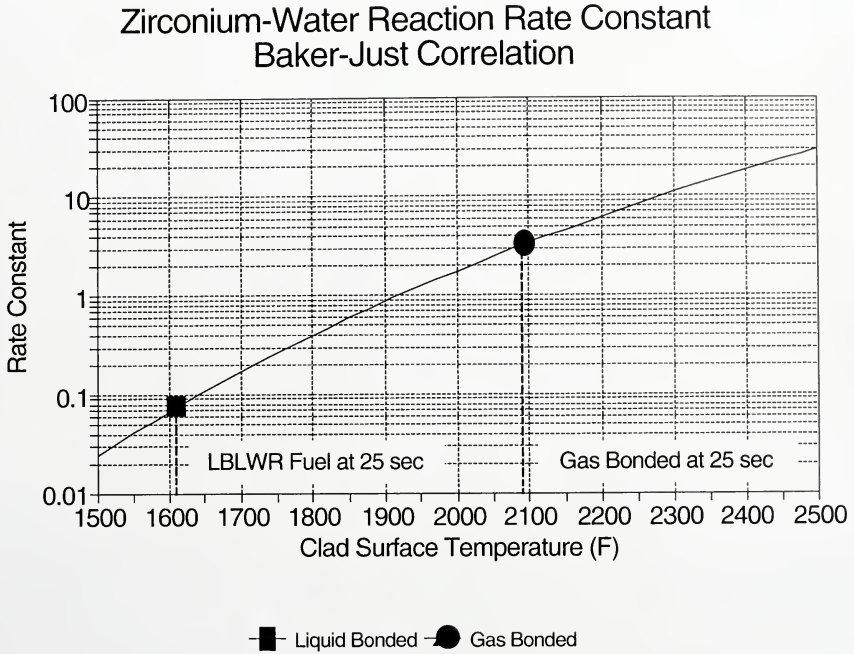

Figure 5-4: Zirconium-Water Reaction Rate Constant vs. Clad Temperature [7]

assumed to experience a 15% step increase in power at the start of the transient,and reach a new equilibrium temperature. For this simplified calculation, the effects of reactivity feedback from the increased fuel and moderator temperatures are not considered. However, this was a conservative assumption since the net effect is negative.

Figure 5-5 shows the centerline fuel temperature as a function of time for an LBLWR fuel rod and a conventional LWR fuel rod subjected to a 15% step increase in power. The rods are assumed to operate at 13 kW/ft peak power before the transient, and the conventional fuel rod gap conductance is assumed to be 500 Btu/hr-ft^2-°F. The peak centerline fuel temperature is 4600°F for the conventional LWR fuel, which is above the melting point of UO_2 (4500°F). By comparison, the peak centerline fuel temperature for the LBLWR pin is below 3000°F.

The fuel transient response to a LOCA and to an unscrammed transient overpower event indicate that the LBLWR fuel is potentially far safer than conventional LWR fuel, and may preclude severe accidents involving fuel damage and hydrogen generation, even for peak power rods. This simplified analysis does not include the effects of reactivity feedbacks. It is expected that the larger negative temperature coefficient for the LBLWR fuel rod would mitigate the power increase relative to the conventional fuel rod.

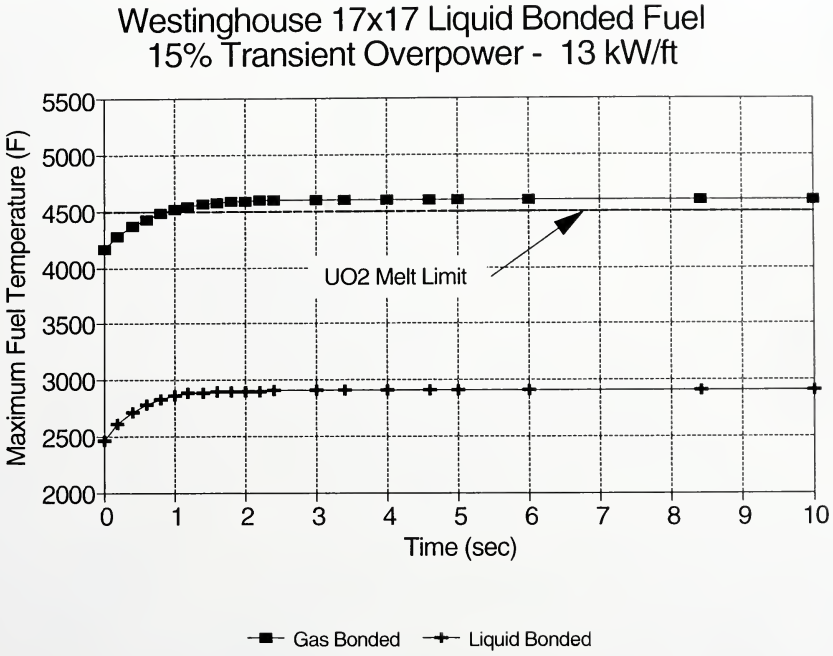

Figure 5-5: LBLWR Fuel Response to 15% Transient Overpower

Detailed Two-dimensional Fuel Rod Model

To prove the applicability of the simple radial heat transfer model, a detailed thermal analysis of the liquid bonded LWR fuel rod was performed to determine the effects of axial conduction on the peak clad temperatures during a postulated LOCA. The two-dimensional heat transfer model consisted of 15 radial fuel nodes, and 5 radial cladding nodes. One-half of the fuel rod length was modeled (6 ft.), with three-inch axial nodes. Internal heat generation in the fuel was modeled using two power levels, 6 kW/ft and 9 kW/ft. The axial power shape was approximated by a "clipped cosine" with a axial peaking factor of 1.2, as is shown in Figure 5-6. The radial power profile within the fuel rod was assumed to be uniform.

A steady-state two-dimensional analysis was performed for both liquid bonded and conventional fuel at both power levels. The gap conductance assumed for the conventional fuel rod is 1000 Btu/hr-ft^2-°F. The simulated LOCA transient calculation described in the previous section was also analyzed using the two-dimensional model.

The two-dimensional steady-state analyses show that the radial temperature profile is not significantly different from the one-dimensional radial heat conduction profiles calculated previously. This indicates that the heat transfer within the rod is predominately one-dimensional in the radial direction with little influence by axial heat conduction. Similarly, the two-dimensional transient analyses also showed no significant difference when compared to the one-dimensional analysis.

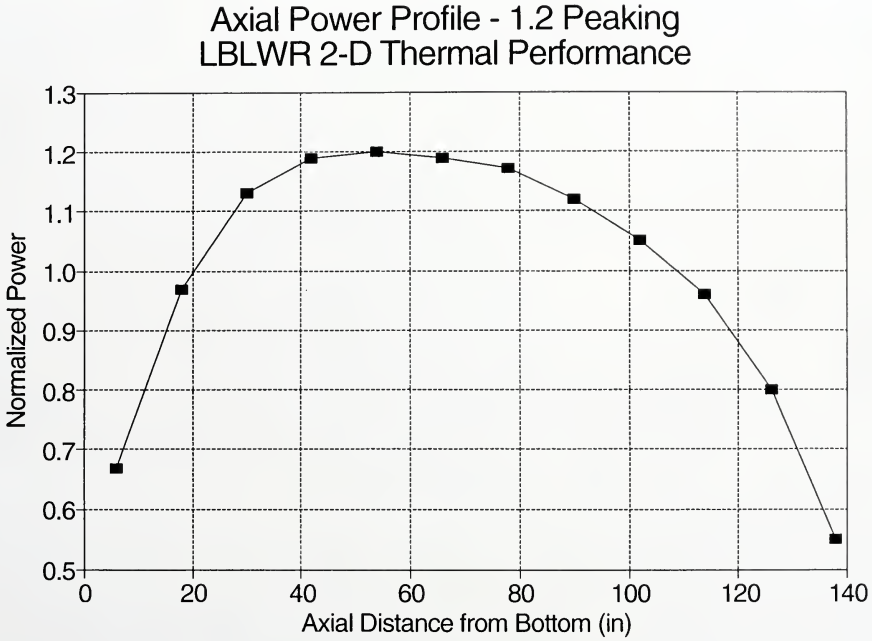

Figure 5-6: Cosine Axial Power Shape

The results of these thermal analyses of the fuel illustrate the benefits of incorporating the liquid metal bond into the fuel design. Lower fuel operating temperatures translate into increased operating margin and better fuel survivability in the event of an accident.

In Chapter 6, the LBLWR fuel is evaluated using more sophisticated methods to determine the operating characteristics and the expected fuel performance over a typical fuel rod lifetime in a light water reactor.

CHAPTER 6
FUEL ROD THERMAL/MECHANICAL PERFORMANCE ANALYSIS

To better characterize the performance of LBLWR fuel over a typical fuel lifetime, a methodology for predicting fuel rod performance as a function of fuel burnup is necessary. A study was made of all available fuel performance codes to determine the best basis for a code to predict the behavior of LBLWR fuel. To facilitate these predictions, a computer code, ESCORE [24], which was developed by the Electric Power Research Institute (EPRI), was modified to develop a tool to analyze the LBLWR fuel, determine operating limits, and optimize the design for use in both pressurized water reactors (PWRs) and boiling water reactors (BWRs). This resulting liquid metal bonded fuel analysis code named ESBOND, was developed on a UNIX workstation, and further modified to present the output graphically.

Background

The ability to predict the thermal-mechanical performance of a nuclear fuel rod over the rod lifetime is essential to predict behavior of fuel rod designs. Computer models, which predict phenomena such as fission gas release, swelling and densification, etc., have been derived and calibrated against test data. These

models can be integrated to determine the fuel temperature, fuel rod internal pressure, fuel structure, and fuel and cladding stress and strain, as a function of the fuel burnup. In this way, it is possible to assess fuel designs over the expected lifetime of the fuel.

Each of the fuel vendors has developed proprietary computer codes to predict fuel performance, for example the Westinghouse PAD code [9] and the General Electric GESTAR code [25]. In addition, several codes were developed by the DOE National Laboratories in support of both Light Water Reactor (LWR) fuel, and Liquid Metal Reactor fuel. These fuel performance codes include the LIFE code, MATPRO, and COMETH [26, 27, 28].

In the mid-1970s, nuclear utilities expressed the need for a best-estimate nuclear fuels performance code, containing the most up-to-date models. The Electric Power Research Institute (EPRI) was instructed to develop such a code, and contracted Combustion Engineering to evaluate existing public domain fuel performance codes, and to develop a new code, which could be used by utilities to evaluate fuel rod performance. This resulted in the ESCORE code [24].

An effort was initially made to modify the LIFE code for use in predicting LBLWR fuel performance. Since LIFE was developed by DOE, access to the code was easy to obtain. However, the code was originally developed for mixed oxide ($U+Pu\ O_2$) LMR fuel, and the applicability to LWR fuel was limited. It was decided to explore the possibility of using a dedicated LWR fuel code which led to EPRI's ESCORE code. The ESCORE code, and the modifications which were needed to analyze LBLWR fuel are described in the following sections.

ESCORE: Fuel Rod Thermal/Mechanical Performance Code

At EPRI, a 12-member utility advisory committee worked with the Combustion Engineering project team to develop, benchmark, and document the ESCORE fuel performance code. The ESCORE code, written in FORTRAN, was designed to meet all NRC licensing requirements, and was validated against an extensive database representing measured PWR and BWR fuel rod performance characteristics with a wide variety of irradiation histories. The code was developed on the CDC-7600 and IBM mainframe computers.

ESCORE was shown to be an effective tool in the determination of fuel rod performance. The code calculates parameters such as fuel temperatures, stored energy, swelling, fission gas release, cladding oxidation, and cladding stress and strain as a function of fuel burnup. The code analyzes individual fuel rods consisting of uranium dioxide fuel pellets enclosed in Zircaloy cladding. The fuel rod is discretized into several axial segments, for which the code performs radial thermal calculations, as a function of the local linear power. The fission gas released for each segment is assumed to mix within the rod to provide a prediction for the rod internal pressure as a function of burnup.

The code reads an input file containing fuel rod parameters such as dimensions, axial power shape, power history, and coolant conditions, as well as nuclear parameters such as flux profiles, and peaking factors. The code output

consists of a summary output file containing all calculated results. In addition, several files are generated which deal with specific parameters such as fuel temperatures, rod internal pressure, clad stress and strain, fission gas evolution and release, fuel and clad dimensions, and fuel and clad thermal characteristics. These files are extremely useful for examining specific results, and were used to create plot files with the aid of plotting programs.

The ESCORE code was used by the utilities to support the design and licensing of high-burnup fuel designs. It was decided that the ESCORE code be used as the basis for a new fuel rod performance calculation tool for analyzing Liquid Bonded Light Water Reactor (LBLWR) fuel, rather than modifying LIFE or other DOE fuel performance code.

ESBOND: LBLWR Fuel Rod Analysis Code

Through an agreement with EPRI and the Florida Power Corp., the University of Florida, Department of Nuclear Engineering Sciences was given access to the ESCORE source code. In addition, input and output files were included for several rod configurations to serve as a means of benchmarking the code. Several modifications were made to permit the analysis of LBLWR fuel rods. These included

1. Installation of the code on a UNIX platform
2. Development of a gap conductance model to simulate the liquid metal bond

3. Development of a methodology for calculating the free gas volume and liquid metal displacement as the clad creeps as a function of burnup

In addition, a graphical interface was created to graphically present calculational results. The program extracts fuel parameters such as fuel and cladding dimensions, fuel temperatures, fission gas release, clad creep, rod internal pressure, and gap conductance, and creates plot files to display them as a function of time. The program output is read into the QUATTRO PRO [29] spreadsheet program for plotting.

In order to become familiar with the structure of ESCORE, the major models and the sequence in which they are accessed during a typical run are shown in Figure 6-1. The modified ESCORE code was renamed ESBOND, and was used in the LBLWR fuel performance calculations. The basis for each modification is shown in the following sections.

Installation on the UNIX Platform

Due to the lack of availability of a mainframe computer and the trend toward UNIX-based computing, it was decided to port the code to a UNIX platform, specifically a Hewlitt-Packard 735 UNIX workstation. Several modifications of the ESCORE code were necessary in order to adapt it to the UNIX environment:

1. All non-standard FORTRAN-77 statements were modified or eliminated.

ESCORE LOGIC FLOW DIAGRAM

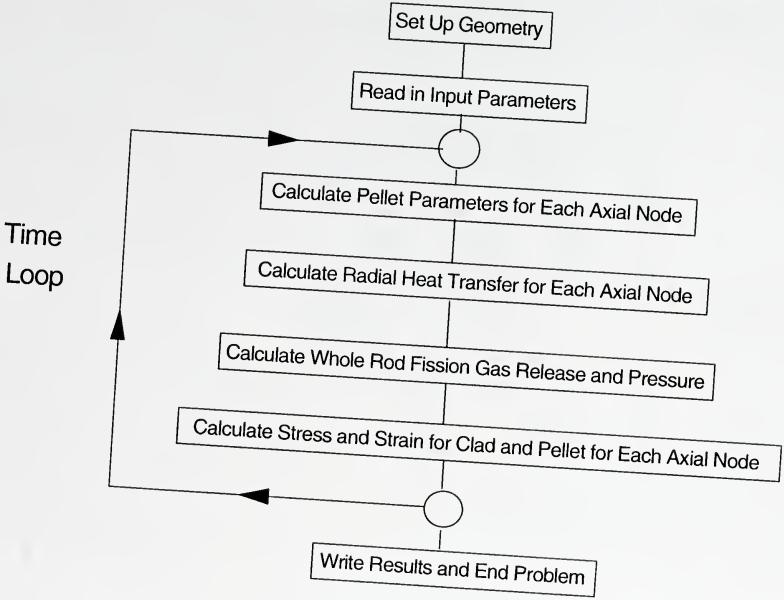

Figure 6-1: Program Logic Flow Diagram for ESCORE

2. All real variables were recast as DOUBLE PRECISION. This was necessary since the ESCORE code was developed on the CDC-7600, which uses 32 bit word lengths for real variables.
3. Interactive input/output logic was installed to allow the user to specify the input and output file name.

In all, nearly four hundred separate coding changes were necessary to successfully compile and run the ESCORE code on the HP-735 platform. The standard input decks were run using ESCORE, and the output files were successfully duplicated. The revised version of the ESCORE code formed the basis of the ESBOND code which was used to analyze the LBLWR fuel rods.

ESBOND Gap Conductance Model

The ESCORE code calculates one-dimensional heat transfer in the radial direction from the fuel pellet, across the gas gap, through the cladding, and into the coolant. The gap conduction model consists of heat conduction across a gas layer, radiation heat transfer from the outer surface of the pellet to the inner surface of the cladding, and, when applicable, contact conductance between the pellet and cladding. The model predicts a maximum gap conductance coefficient of 3000 Btu/hr-ft^2-°F when the gap is completely closed. Thus, the ESCORE code calculates a radial temperature profile which changes as a function of the local gap conductance, and the gap conductance changes as the fuel and cladding dimensions change.

The ESBOND gap conductance model is constructed in a similar manner. The conductance through the liquid metal bond is calculated by

$$h_{gap} = k_{liq\text{-}bond} / t_g \qquad (6\text{-}1)$$

where $k_{liq\text{-}bond}$ is the thermal conductivity of the bonding liquid

and t_g is the mean gap thickness

In the event that the gap is closed, the gap conductance is set to

$$h_{gap} = 1.E8 \text{ Btu/hr-ft}^2\text{-}^\circ\text{F}$$

which is consistent with LMR fuel experience [25] .

The model is invoked by specifying two input flags. The ESCORE code uses 32 logical input flags in Card Group A to set initial problem parameters. Two of these flags, 19 and 20, are currently unused. The first, logical flag 19 in Group A, is set to .TRUE. to invoke liquid metal bonding between the fuel pellet and the cladding.

Logical flag 19 =	.TRUE.	Liquid bond model switched on
	.FALSE.	Liquid bond model switched off

If the liquid bonding model is switched on, the user sets logical flag 20 to determine the liquid bonding material:

Logical flag 20 = .TRUE. for Lead-Bismuth Eutectic

.FALSE. for Lead-Bismuth-Tin Mixture

When logic flag 19 is set to .FALSE., the code performs original gap conductance calculations. In this way, the ESBOND code can be used to calculate both liquid bonded and conventional fuel rod performance depending on the choice of input flags.

Liquid Bond Displacement

For conventional fuel, as the fuel and cladding dimensions change, the available gas plenum volume also changes. Change in the fuel dimensions occurs as a function of burnup, and consists of both densification and swelling in the fuel pellet, and creep in the cladding due to the pressure difference across the cladding wall. The net result is that the gap between the fuel and cladding eventually closes causing a decrease in the fission gas plenum volume. To counter the rapid creep down of the cladding and delay the onset of pellet-clad interaction, fuel rods are often pre-pressurized with helium gas prior to irradiation [9].

The reduction in gas volume is magnified for the LBLWR fuel design. As the annular gap between the fuel pellet and the cladding is reduced, the incompressible liquid metal is displaced into the gas plenum above the fuel pellet stack. This action further reduces the fission gas plenum.

Several changes to the code were made to model the liquid bond displacement and subsequent change in the gas volume in the fuel rod. First, an input value is used to define the initial liquid metal fill level as a fraction of the active fuel height. The fuel rod is divided into axial segments, and the user has the option to allow the lower power upper region of the fuel rod to be "dry" at the beginning of life. Then, as the gap closes, the liquid metal level is tracked, and the gas volume calculated accordingly.

For hot, full power conditions at beginning-of-life, the total volume of liquid metal is calculated by determining the total open volume that exists below the prescribed liquid level:

$$V_{liq} = V_{lower\ plenum} + \sum V_{open} \qquad \text{for all "wet" nodes} \qquad (6\text{-}2)$$

Except for small changes due to volumetric expansion, this volume of liquid is assumed to remain constant throughout the fuel lifetime. At each time step, the change in the liquid level is calculated by determining the change in the open volume available for the liquid which changes as a function of the pellet and cladding dimensions.

$$V_{available} = \sum_{wet} V_{gap} + V_{dish} + V_{chamfer} + V_{hole} \qquad (6\text{-}3)$$

where V_{gap} is the volume of the annular gap

V_{dish} is the volume of the pellet dish

$V_{chamfer}$ is the volume of the pellet chamfer

and V_{hole} is the volume of the pellet central hole (if any)

The change in liquid level is defined as

$$\Delta L = (V_{liq} - V_{available})/A_{annulus} \quad (6\text{-}4)$$

where $A_{annulus}$ is the cross sectional area of the annulus between the fuel pellet and the cladding at the axial location of the level

Finally, the new level is calculated by

$$L_{new} = L_{old} + \Delta L \quad (6\text{-}5)$$

The axial nodes are then redefined as "wet" or "dry" depending on their location relative to the new level.

If an axial node is "wet" (i.e. liquid bonded), all available potential gas volume such as annular gap, dishes and chamfers, and central hole (for annular fuel pellets), are set to zero. For "dry" nodes, each of these volume components is added to the gas plenum volume above the fuel stack. This total gas volume is used to determine the internal rod pressure during a time step. For the next time

step, the fuel dimensions are updated, and the liquid level, gas volume, and rod pressure re-calculated.

For instance, a 17x17 PWR rod with 80% of its length filled with liquid metal at the beginning-of-life experiences maximum fuel temperatures at the core axial midplane in the "wet" region. At the end of the first 18 month cycle (~15,000 MWd/MT), the gap is reduced due to the combination of clad creepdown and fuel thermal expansion and swelling. At this point, the liquid metal completely fills the annular gap to the top of the active fuel, and the rod is completely "wet".

The change in the liquid metal volume due to thermal expansion is also calculated, although this change is small over the fuel lifetime.

The modified subroutines from the ESBOND code are shown in the Appendix.

ESBOND LBLWR Fuel Performance Calculations

To determine the performance characteristics of LBLWR fuel, several fuel rod designs were analyzed using the ESBOND code. Existing PWR and BWR fuel rod designs were examined using a liquid metal bond in place of the gas gap. Variations to these designs including changes in the rod pre-pressurization, and partially filled liquid metal are examined to optimize the fuel performance. An optimized pellet design, which takes the LBLWR technology to its fullest advantage is examined in Chapter 7.

ESBOND Analysis of the PWR Fuel Rod

The Westinghouse 15x15 fuel rod design was analyzed using liquid metal bonding. The fuel rod parameters are summarized in Table 2-3. The maximum rod average burnup is assumed to be 50,000 MWD/MT, which is typical for a fuel rod lifetime. The rod linear power is assumed to be constant 6 kW/ft over the fuel lifetime. Constant power, while not a practical power history over the life of a fuel rod, is useful for determining the basic performance parameters of the LBLWR fuel. Actual power histories would be applied to specific fuel designs for specific fuel cycles. The liquid metal level is assumed to be the top of the fuel stack at beginning-of-life.

Figure 6-2 shows the rod internal pressure as a function of time for a Westinghouse 15x15 fuel rod with liquid metal replacing the gas. Note that the large increase in rod pressure is due to the combination of high initial pressure (450 psia), and small gas volume available after the clad creep down. This fuel rod design is unacceptable, as the rod pressure exceeds the system pressure of 2200 psia.

A second calculation was performed using an initial pre-pressurization of 200 psia, which is above the minimum recommended pre-pressure value of 125 psia for Westinghouse fuel [9]. In addition, the liquid level is initially set to 80% of the active fuel height. As was illustrated previously, this value is chosen such that the maximum centerline fuel temperature occurs in the "wet" (liquid bonded) region. The combination of these two design features assure that rod pressure due to

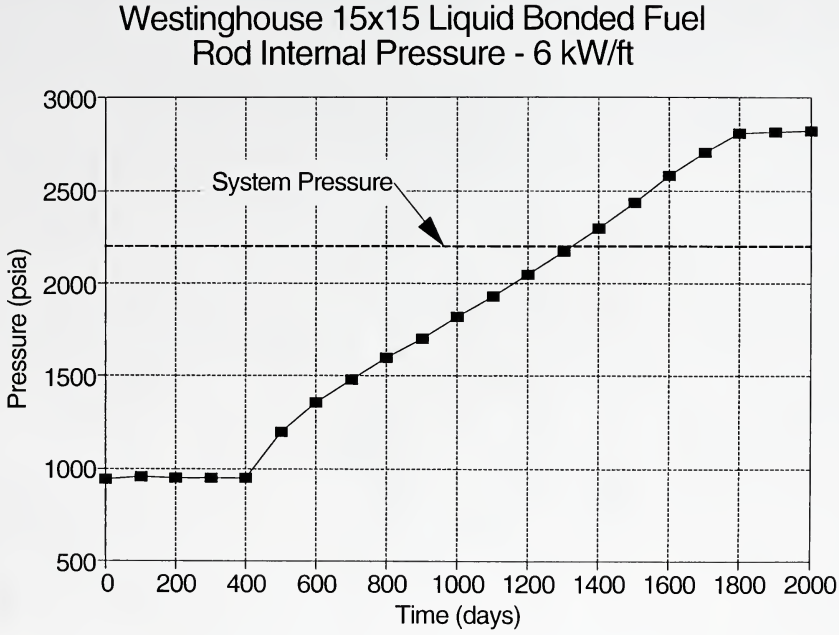

Figure 6-2: Rod Internal Pressure vs. Time For Unmodified PWR Fuel Rod

fission gas release is well within the design limits. The results of this calculation are presented in Figures 6-3 to 6-13. Also presented are the results from a conventional gas bonded fuel rod subject to the same conditions for comparison to the LBLWR fuel.

Figure 6-3 shows the fuel and cladding dimensions for the peak axial node as a function of time. Both rods exhibit similar behavior as the fuel pellet first shrinks due to densification, then swells over the remainder of the fuel lifetime. The LBLWR fuel pellet diameter is consistently less than the conventional rod by about 1 to 1.5 mils smaller because of lower thermal expansion due to the lower fuel temperatures. The conventional gas bonded fuel rod cladding creeps down onto the fuel pellet due to the difference between the internal gas pressure and the external reactor pressure. At about 700 days, the cladding contacts the pellet, and the gap is closed. For the LBLWR rod, lower internal pressure causes the gap to close in about 200 days. After gap closure, the fuel/cladding gap remains closed with a thin layer of liquid metal bond between them over the remainder of the fuel lifetime.

Figure 6-4 shows the gap conductance averaged over the fuel rod length as a function of time. The conventional gas bonded fuel rod gap conductance increases from about 900 Btu/hr-ft^2-°F at beginning of life (BOL) to about 2600 Btu/hr-ft^2-°F at end of life (EOL). At BOL, the thermal resistance due to the gas gap represents 40% of the total thermal resistance between the fuel pellet and the reactor coolant. At EOL, the resistance is reduced to 15% of the total.

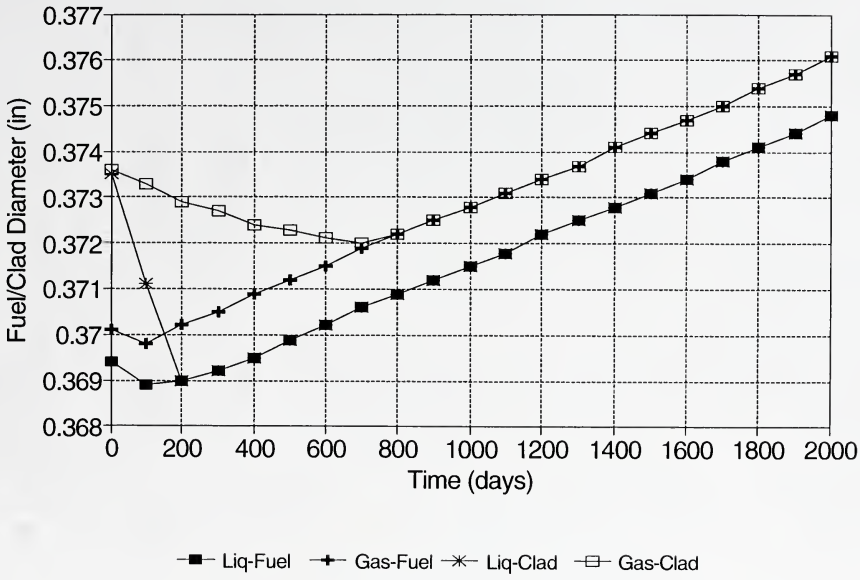

Figure 6-3: Westinghouse 15x15 Fuel - 6 kW/ft: Rod Dimensions Peak Node

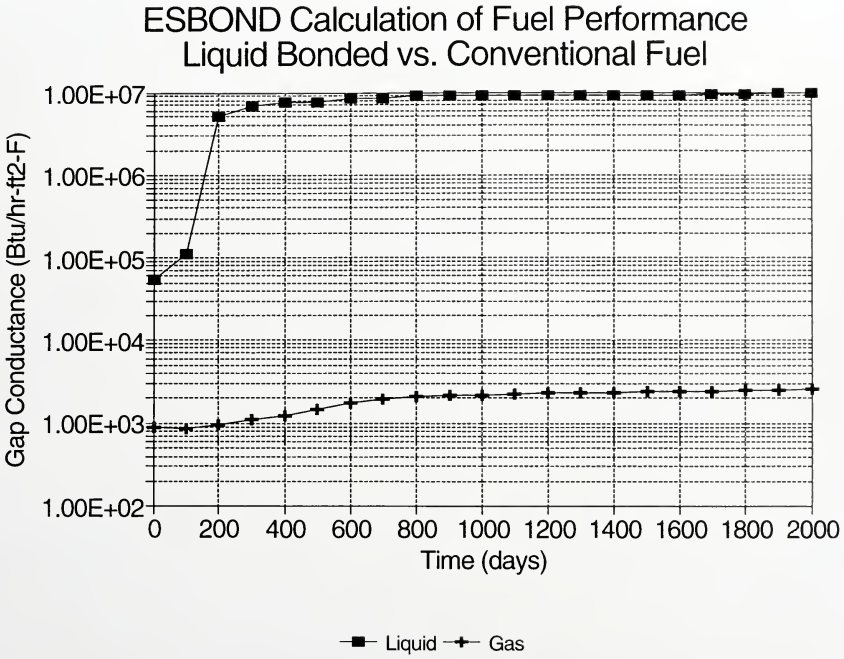

Figure 6-4: Westinghouse 15x15 Fuel - 6 kW/ft: Average Gap Conductance

For the LBLWR rod, the gap conductance is consistently several orders of magnitude greater than for conventional fuel. The thermal resistance due to the liquid metal gap is insignificant over the life of the fuel rod.

Figure 6-5 shows the average and peak fuel temperatures for both fuel types. The greatest difference in temperature occurs at BOL where the fuel centerline temperature at the maximum axial power node is over 350°F higher for conventional fuel than for the LBLWR fuel rod. For both fuel rods, the thermal resistance in the fuel increases as a function of burnup due to the accumulation of fission products. At the same time, the gap for both fuel types is closing, resulting in an increase in the gap conductance as was mentioned above. The net result of these two competing phenomena is a decrease in the fuel temperature for the conventional fuel rod, as the increase in gap conductance dominates the reduction in fuel thermal conductivity. Conversely, the LBLWR rod experiences an increase in fuel temperature as the fuel conductivity change dominates the minute change in the thermal resistance.

At about 600 days, the difference in centerline temperature between the two designs reaches about 160°F, and remains the same for the duration of the fuel lifetime. Thus, the benefits of the liquid metal bond are most apparent at BOL, and slowly decrease over the fuel lifetime.

Figure 6-6 shows the internal rod pressure as a function of time. The initial fill gas pressure for the LBLWR fuel rod was chosen such that the rod internal pressure for both designs is equal at EOL. As was shown, the main result of the

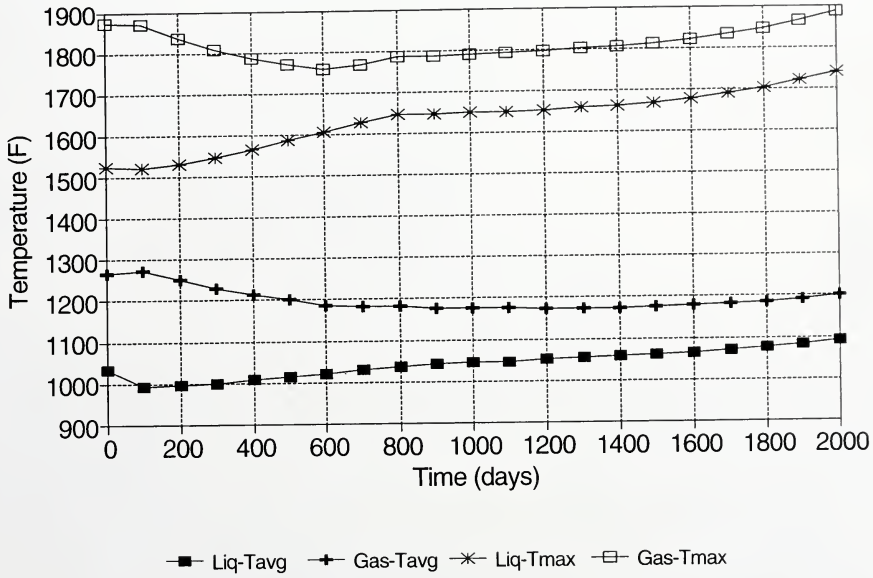

Figure 6-5: Westinghouse 15x15 Fuel - 6 kW/ft: Fuel Temperatures

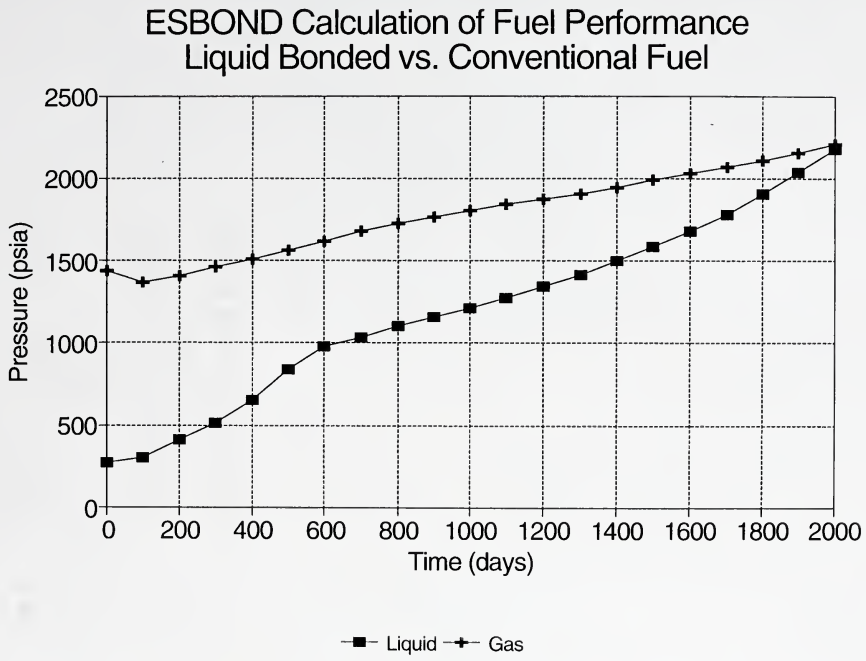

Figure 6-6: Westinghouse 15x15 Fuel - 6 kW/ft: Rod Internal Pressure

lower initial gas pressure is the faster clad creep down time. This pressure profile is similar to later Westinghouse fuel designs which employ an integral ZrB_2 burnable absorber [9]. The pre-pressurization for these rods is specified at 125 psia to accommodate both fission gas and accumulated helium from the absorber over the fuel lifetime.

The beginning-of-life pressure at the hot, full power condition is 1500 psia for the conventional fuel rod. This increase from the cold pressure of 450 psia is accounted for by an increase in the gas temperature from room temperature to approximately 800_oF, and a 40% decrease in the available gas plenum volume. Similarly, the beginning-of-life pressure for the liquid metal bonded fuel rod increases to 350 psia from the cold fill pressure of 200 psia. However, for this case, the pressure change is almost entirely due to the temperature change as the gas plenum volume remains nearly constant from the cold to the hot condition. This results from the gas volume being located in a relatively low temperature axial position, at which the fuel pellets do not experience a large amount of thermal expansion.

As a result of lower fuel temperature, temperature dependent phenomena such as fission gas release are significantly lower for the LBLWR fuel, as is shown in Figure 6-7. The ESBOND code assumes that 0.2% of the fission gas is deposited outside of the fuel pellet [24], which results in the lower limit in Figure 6-7. At the end-of-life, nearly 250% more fission gas is released from a conventional fuel rod as compared to the LBLWR design.

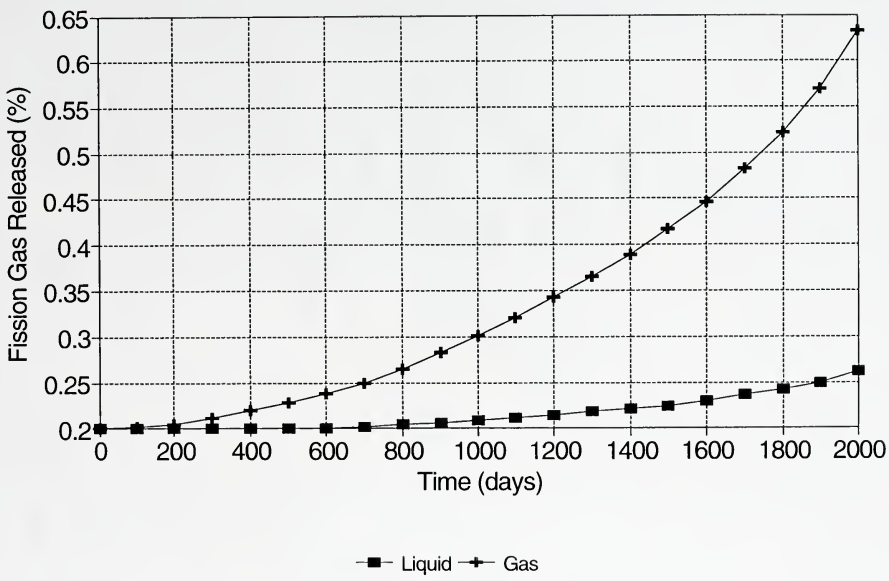

Figure 6-7: Westinghouse 15x15 Fuel - 6 kW/ft: Fission Gas Released

Figure 6-8 shows the clad diametral strain due to creep as a function of the axial fuel length at EOL. The clad strain is still negative for the LBLWR rod at EOL, while the conventional rod exhibits a positive strain.

Several conclusions can be drawn from this analysis:

1. ESBOND analysis of the LBLWR indicates that the fuel temperatures are significantly lower than those calculated for conventional fuel rods.
2. Maximum benefit for the LBLWR rod occurs at beginning of life. This is primarily due to the large thermal resistance posed by the gas gap in the conventional fuel rod. This benefit is decreased as the fuel burnup increases due to the closure of the gap.
3. Temperature dependent parameters such as fuel thermal expansion, fission gas release, and clad strain are all lower because of the lower temperature associated with the LBLWR fuel.
4. The ESBOND calculations for the PWR fuel rod were performed on a design which replaces the gas gap with a liquid metal bond. The increased margins demonstrated in these calculations represent a minimum of what can be achieved if the design is optimized to take full advantage of the liquid metal bond. An optimized LBLWR fuel design is presented in Chapter 7.
5. The clad strain, which is still negative at the end-of-life allows the LBLWR fuel to achieve higher burnups over the current conventional limits of 50,000

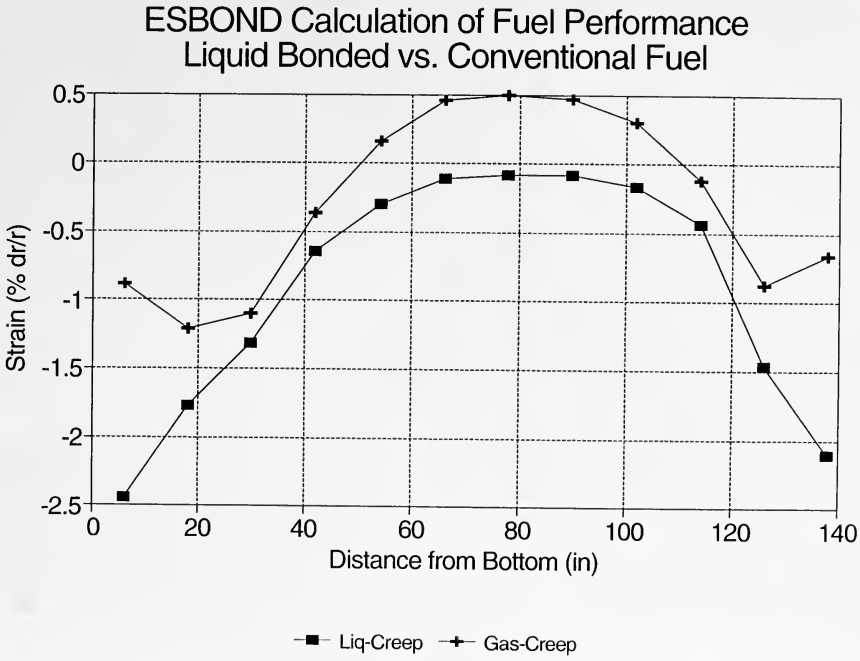

Figure 6-8: Westinghouse 15x15 Fuel - 6 kW/ft: Clad Strain at EOL

MWD/MT, provided that the additional fission gas can be accommodated. This is a key advantage over conventional fuel designs.

ESBOND Analysis of the BWR Fuel Rod

The General Electric 8x8 fuel rod design was also analyzed incorporating a liquid metal bond. The fuel rod parameters are summarized in Table 2-3. The maximum rod average burnup is assumed to be 50,000 MWD/MT, which is typical for a fuel rod lifetime. For this analysis, the rod linear power is assumed to be constant 9 kW/ft over the fuel lifetime. The liquid metal level is assumed to be the top of the fuel stack at beginning of life.

For these calculations, an initial pre-pressurization of 3 atmospheres (45 psia) is assumed for both the LBLWR and conventional fuel designs. The results of the ESBOND calculations for both designs are presented in Figures 6-9 to 6-14.

Figure 6-9 shows the fuel and cladding dimensions for the peak axial node as a function of time. The major difference between the BWR rods and the PWR rods analyzed earlier is the thicker cladding (.15 in vs .25 in). Thicker cladding coupled with a larger gap results in longer times for the gap to close. As with the PWR fuel, both rods exhibit similar behavior first densifying, then swelling over the remainder of the fuel lifetime. The LBLWR fuel pellet diameter is consistently less than the conventional rod by about 2 mils because of lower thermal expansion due to the lower fuel temperatures. As with the PWR fuel, both the LBLWR and conventional BWR fuel cladding creeps due to the difference between the

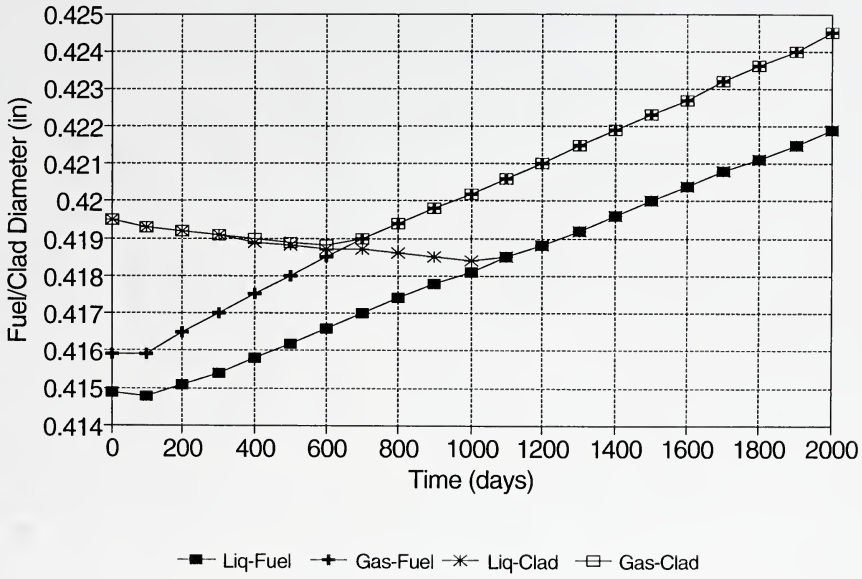

Figure 6-9: BWR 8x8 Fuel - 9 kW/ft: Rod Dimensions for Peak Node

internal gas pressure and the external reactor pressure. For the gas bonded fuel, the gap closes in about 700 days, and for the LBLWR rod, due to the lower fuel thermal expansion, the gap closes in about 1100 days. After gap closure, the fuel and cladding remain in contact over the remainder of the fuel lifetime.

Figure 6-10 shows the gap conductance averaged over the fuel rod length as a function of time. The conventional gas bonded fuel rod gap conductance is much lower for the BWR fuel rod than for the PWR fuel rod. This is because of the larger gap at BOL. The gap conductance for the conventional rod increases from about 690 Btu/hr-ft^2-°F at BOL, to about 1800 Btu/hr-ft^2-°F at EOL. As for the PWR LBLWR rod, the gap conductance is consistently several orders of magnitude greater than for conventional fuel, and the thermal resistance due to the liquid metal gap is insignificant over the life of the fuel rod.

Figure 6-11 shows the average and peak fuel temperatures for both fuel types. Once again, the greatest difference in temperature occurs at BOL where the fuel centerline temperature at the maximum axial power node is over 400°F higher for conventional fuel than for the LBLWR fuel rod. For both fuel rods, the thermal resistance in the fuel increases as a function of burnup due to the accumulation of fission products. At the same time, the gap for both fuel types is closing, resulting in an increase in the gap conductance as was mentioned above. As for the PWR fuel, the net result of these two competing phenomena is a decrease in the fuel temperature for the conventional fuel rod, as the increase in gap conductance dominates the reduction in fuel thermal conductivity.

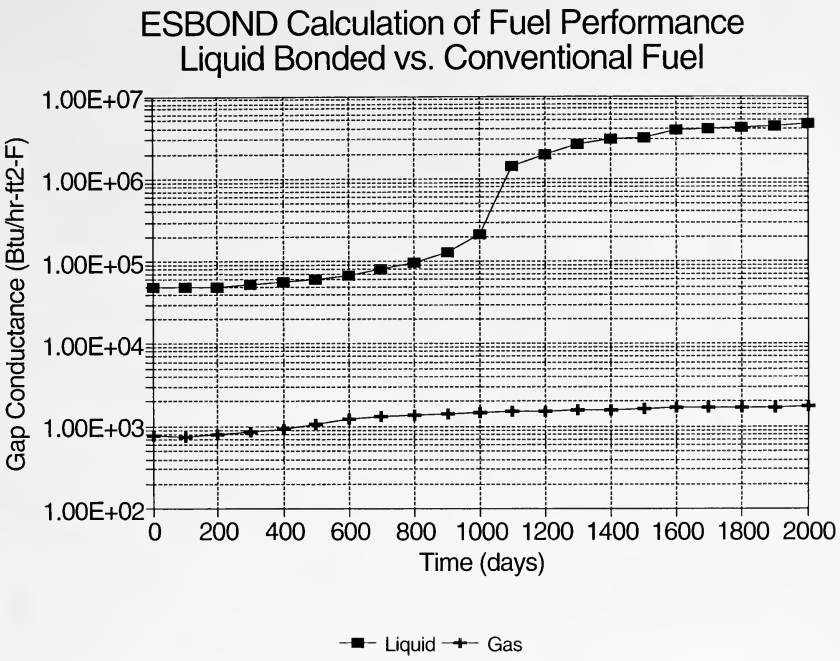

Figure 6-10: BWR 8x8 Fuel - 9 kW/ft: Average Gap Conductance

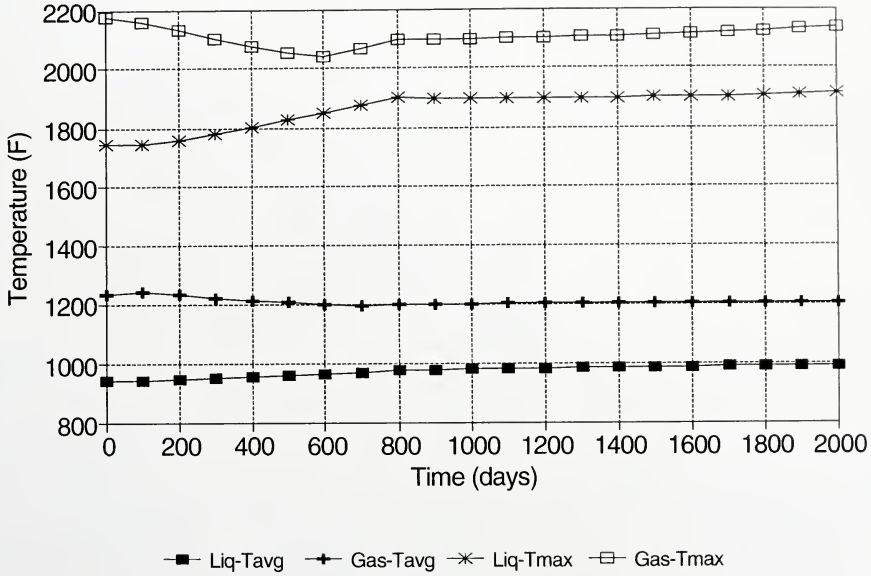

Figure 6-11: BWR 8x8 Fuel - 9 kW/ft: Fuel Temperatures

Conversely, the LBLWR rod experiences an increase in fuel temperatures as the fuel conductivity change dominates.

At about 600 days, the difference in centerline temperature between the two designs reaches about 200°F, and remains the same for the duration of the fuel lifetime. As with PWR fuel, the benefits of the liquid metal bond are most apparent at BOL, and slowly decrease over the fuel lifetime.

Figure 6-12 shows the internal rod pressure as a function of time. The lower initial fill gas pressure for BWR fuel does not challenge the rod internal pressure limit of 1065 psia for either the LBLWR or conventional fuel. Thus, the clad creep down is similar for both fuel designs as is shown in Figure 6-9.

As was shown for the PWR fuel, temperature dependent phenomena such as fission gas release are significantly lower for the LBLWR fuel due to lower fuel temperatures.

Figure 6-13 shows that this difference is more dramatic for the BWR fuel than for the PWR fuel. This is due to the higher fuel power level, coupled with a larger temperature difference between the LBLWR and conventional fuel designs.

Figure 6-14 shows the clad diametral strain due to creep as a function of the axial fuel length at EOL. The clad strain is similar for the two designs, but is more highly positive for the conventional fuel rod.

Several conclusions can be drawn from the analysis of BWR fuel:

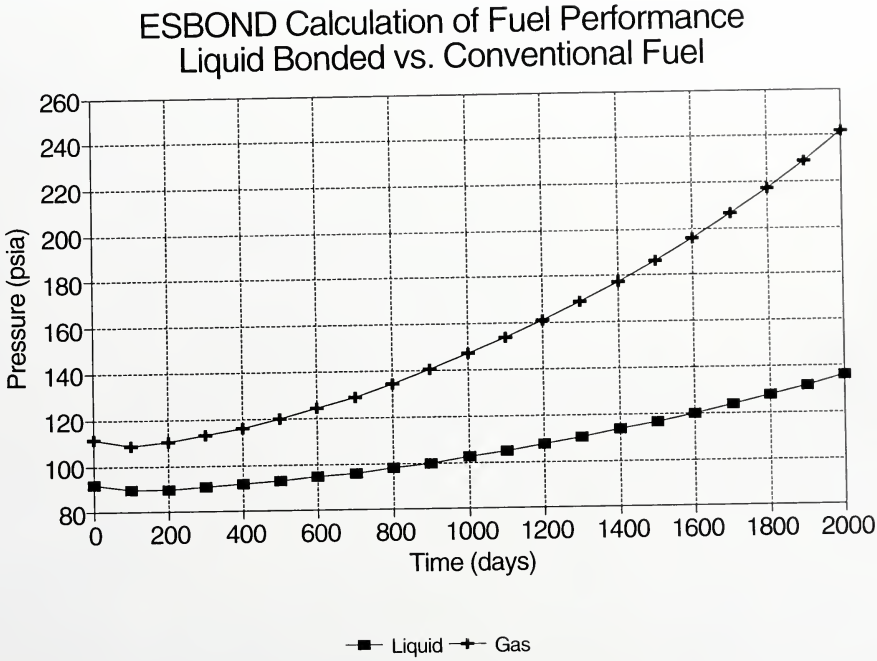

Figure 6-12: BWR 8x8 Fuel - 9 kW/ft: Rod Internal Pressure

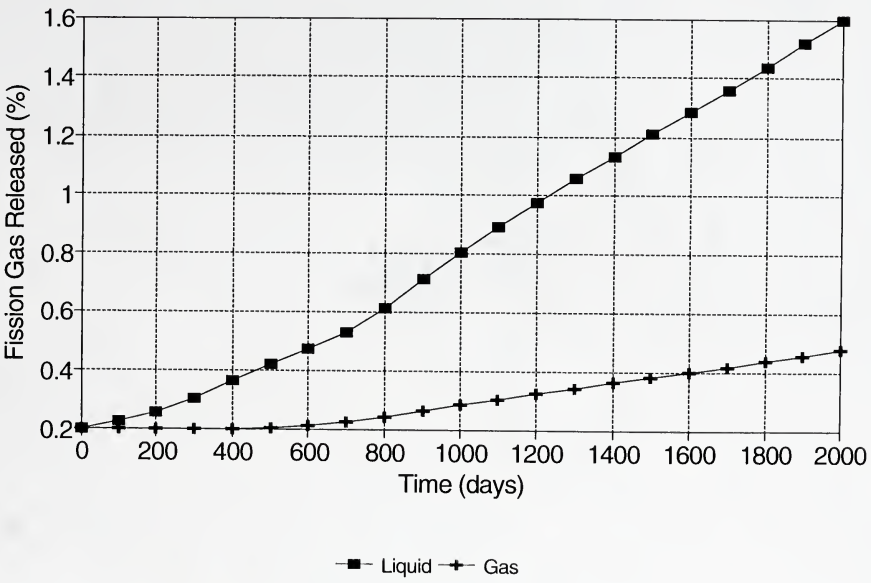

Figure 6-13: BWR 8x8 Fuel - 9 kW/ft: Fission Gas Released

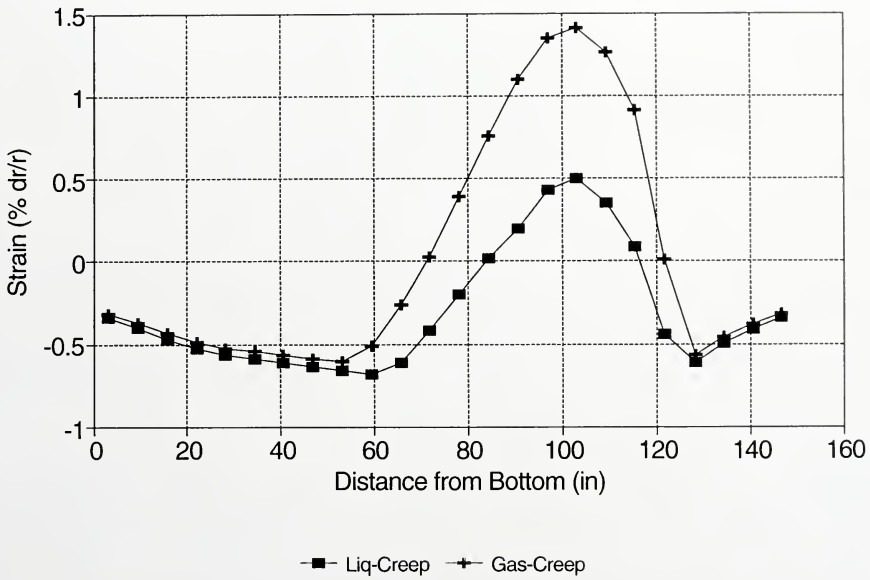

Figure 6-14: BWR 8x8 Fuel - 9 kW/ft: Clad Strain for Peak Node at EOL

1. As for the PWR fuel, ESBOND analysis of the liquid bonded BWR fuel rod indicates that the fuel temperatures are significantly lower than those calculated for conventional fuel rods.
2. As for the PWR fuel, maximum benefit for the liquid bonded BWR rod occurs at beginning-of-life. This is primarily due to the large thermal resistance posed by the gas gap in the conventional fuel rod. This benefit is decreased as the fuel burnup increases due to the closure of the gap.
3. Temperature dependent parameters such as fuel thermal expansion, fission gas release, and clad strain are all lower because of the lower temperature associated with the LBLWR fuel. The end-of-life clad strain is significantly lower for the LBLWR fuel, which indicates that burnup limits associated with clad strain may not be limiting for liquid metal bonded BWR fuel.
4. The BWR liquid bonded fuel performance characteristics are significantly better than those for the PWR when compared to conventional fuel rods. Specifically, the liquid bonded BWR fuel temperatures are significantly lower than conventional BWR fuel over a larger fraction of the fuel lifetime than was observed for the PWR fuel. This is primarily due to the thicker cladding in the BWR rod which, combined with the lower system pressure, resists creepdown far longer than the PWR rod, which keeps the gap between the pellets and the cladding open wider during the fuel lifetime.

ESBOND LBLWR Fuel Analysis- Conclusions

The ESBOND code has been used in these analyses to perform calculations on fuel rods which represent modifications to existing LWR fuel designs. The availability of such a tool makes it possible to optimize liquid metal bonded fuel designs reducing fuel operating temperature, increasing the margin for safe operation, and increasing the fuel rod lifetime.

CHAPTER 7
IMPROVED DESIGNS TO ENHANCE LWR FUEL SAFETY

The fuel design improvements described in the previous chapters allow for a modest decrease in the fuel temperature due to enhanced radial heat transfer across the liquid metal gap between the fuel pellet and the cladding. Typically, the poor thermal conductivity of the UO_2 fuel accounts for over 50% of the total thermal resistance in a conventional fuel rod. For liquid bonded fuel, the pellet thermal resistance is over 80% of the total. To take greater advantage of the liquid bonded fuel technology, it would be beneficial to modify the fuel pellet design to allow for more effective heat transfer within the fuel pellet. Such a fuel design offers the opportunity to minimize the fuel temperatures while maintaining the fuel rod power level.

To reduce fuel operating temperatures, two fuel pellet designs are proposed. The first consists of a standard 15x15 fuel pellet with a 0.1 inch diameter center hole. For the second design, radial grooves are cut into the annular pellet forming direct channels for heat transfer from the fuel center to the cladding. The volume of fuel in the annular pellet design is 10% less than the standard pellet, and the volume of fuel in the annular, grooved pellet design is 22% less than the standard pellet. It is proposed that the interstitial volume for both designs be filled with liquid metal. The grooved, annular fuel pellet design is shown in Figure 7-1.

To provide a similar power level, it is necessary to increase the power density in the proposed fuel pellet. This can be accomplished by increasing the enrichment, and hence, the volumetric heat generation by the ratio of the volume of the pellet to that of a standard 15x15 fuel pellet. For the proposed pellet designs, an increase in the volumetric power of 10% for the annular pellet, and 22% for the annular, grooved pellet is needed to provide the same linear power rating as a solid pellet.

Three-Dimensional Heat Transfer Model

To analyze the proposed fuel design, a three-dimensional computer model was constructed using the TRUMP general purpose heat conduction code. The model consists of a 45° section of the pellet, with one half of the pellet height. Volumetric heat generation rates are specified in the fuel pellet to simulate 6 kW/ft rod linear power. The pellet is clad in Zircaloy tubing of standard 15x15 dimensions, and the outer cladding surface is subjected to a forced convection boundary condition which assumes 4000 Btu/hr-ft^2-°F for the film coefficient and a coolant temperature of 650°F.

Six separate cases were analyzed

1. Solid pellet--gas bonded
2. Solid pellet--liquid bonded
3. Annular pellet--gas bonded

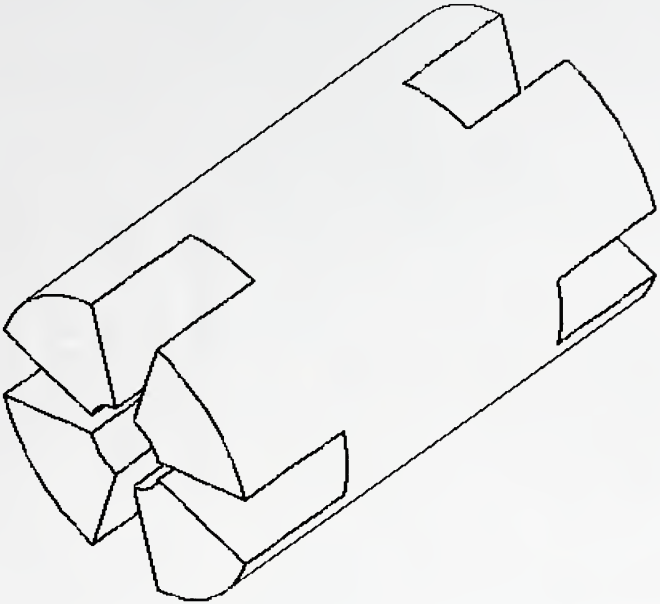

Figure 7-1: Proposed LBLWR Fuel Pellet Design for Optimized Performance

4. Annular pellet--liquid bonded
5. Annular, grooved pellet--gas bonded
6. Annular, grooved pellet--liquid bonded

The peak fuel temperature for each case is summarized in Table 7-1. In addition, a contour plot of the temperature distribution for each case is shown in Figures 7-2 to 7-7.

Figure 7-2 shows the temperature contours for a solid pellet with gas bonding between the fuel pellet and the cladding. The contour lines are uniform indicating strictly one-dimensional radial heat transfer. The maximum fuel temperature, 1672°F, occurs at the fuel centerline.

Figure 7-3 shows the temperature contours for a solid pellet with liquid metal bonding between the fuel pellet and the cladding. Once again the contour lines indicate radial heat transfer, but the maximum fuel temperature is reduced to 1364°F.

Figure 7-4 shows the results for an annular pellet containing gas in the center hole, and in the pellet/cladding gap. As described above, the fuel volumetric power generation rate was increased to provide 6 kW/ft linear power rating. The maximum fuel temperature for this case was calculated to be 1497°F and occurs along the inside surface of the hole.

Figure 7-5 shows the results for an annular pellet, with liquid metal in the center hole and in the pellet/cladding gap. The maximum fuel temperature for this case is 1211°F.

Table 1: Maximum Fuel Temperatures for LBLWR Pellet Designs		
Case Number	Description	Maximum Fuel Temperature
1	Solid Pellet, Gas Bonded	1672°F
2	Solid Pellet, Liquid Bonded	1364°F
3	Annular Pellet, Gas Bonded	1497°F
4	Annular Pellet, Liquid Bonded	1211°F
5	Annular, Grooved Pellet, Gas Bonded	1615°F
6	Annular, Grooved Pellet, Liquid Bonded	1183°F

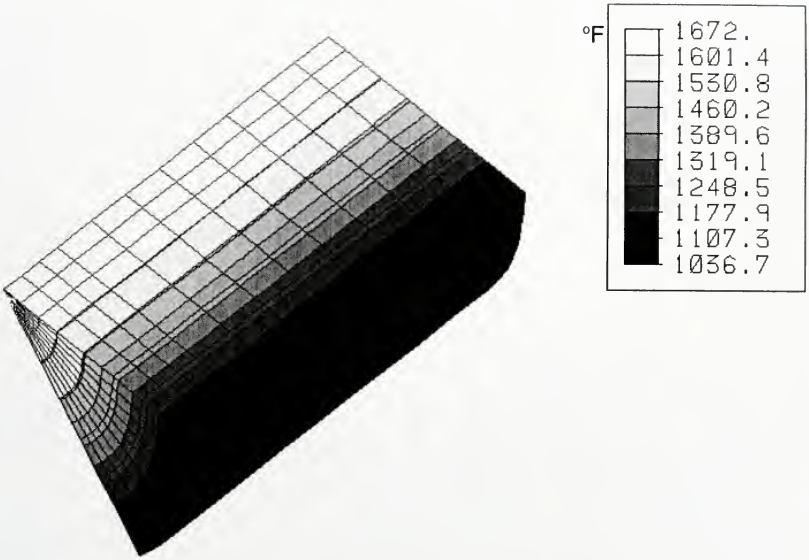

Figure 7-2: Temperature Contours, Solid Pellet, Gas Bonded

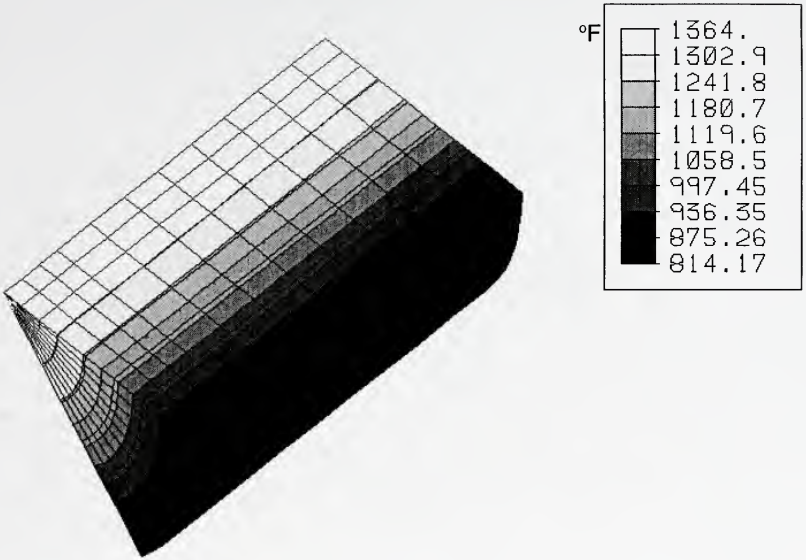

Figure 7-3: Temperature Contours, Solid Pellet, Liquid Bonded

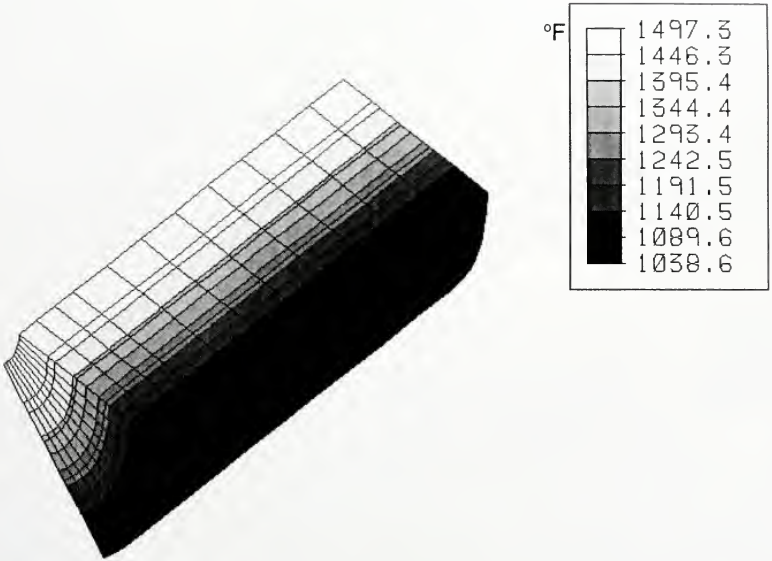

Figure 7-4: Temperature Contours, Annular Pellet, Gas Bonded

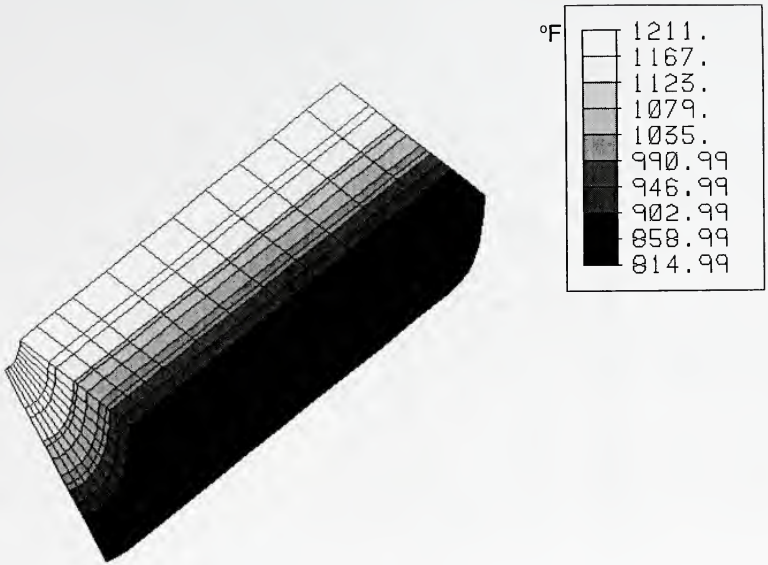

Figure 7-5: Temperature Contours, Annular Pellet, Liquid Bonded

Figure 7-6 shows the temperature contours for the proposed grooved, annular pellet design with gas filling the interstitial volume. Once again, the volumetric power generation rate is increased to maintain 6 kW/ft linear power rating. The maximum fuel temperature for this case is 1615°F, and occurs along the center hole at a point furthest away from the grooves. It is interesting to note that the maximum fuel temperature for this case is higher than that calculated for the gas bonded annular pellet. This is due to the higher volumetric heat generation rate coupled with little or no benefit from increased heat transfer through the grooves due to the poor thermal conductivity of the gas.

Finally, the temperature contours for the liquid metal bonded grooved, annular pellet are shown in Figure 7-7. In this case, the liquid metal in the center hole and the grooves provides a heat transfer paths which reduces fuel temperatures by more efficiently transferring heat from the hot fuel regions to the cladding. Figure 7-7 shows the three-dimensional effects caused by increased heat transfer through the grooves. Subsequently, the maximum fuel temperature for this case is 1183°F, and occurs at the fuel center hole at a point furthest away from the grooves.

Optimized LBLWR Fuel Design--Conclusions

The three-dimensional analyses of an optimized fuel design employing a center void and grooves to more efficiently transfer heat indicate that the maximum fuel temperatures can be substantially reduced. It should be noted, however, that the

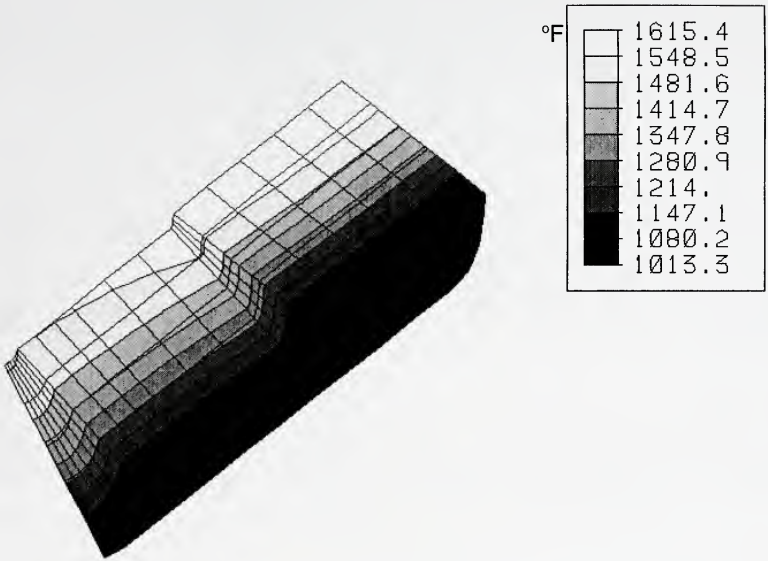

Figure 7-6: Temperature Contours, Annular, Grooved Pellet, Gas Bonded

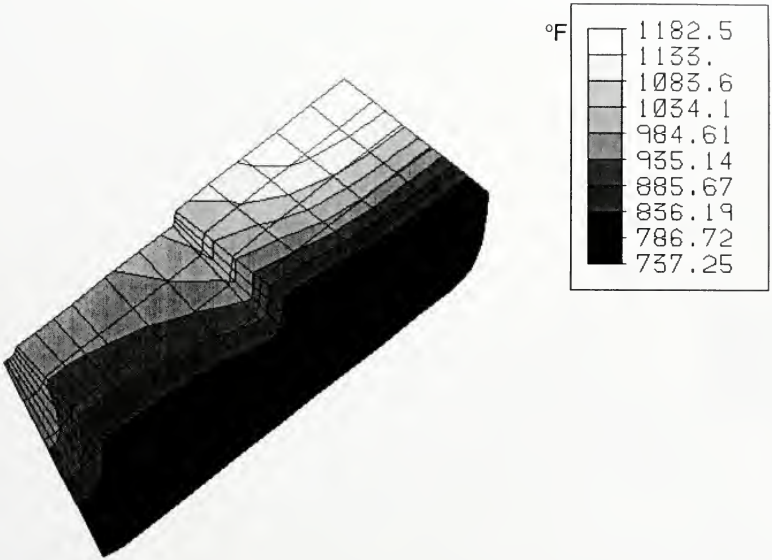

Figure 7-7: Temperature Contours, Annular, Grooved Pellet, Liquid Bonded

reduction in fuel volume which is replaced by liquid metal necessitates a proportional increase in the specific power. The largest part of the observed benefits occurs due to the reduction of centerline temperatures due to the addition of the center hole, and a smaller benefit occurs because of the enhanced radial heat transfer due to the grooves.

By increasing the enrichment for the modified pellet designs, the fuel burnup would also need to be increased to achieve the same power history as a solid pellet design. Thus, burnup dependent performance parameters such as fuel swelling and fission gas generation will be increased compared to a solid pellet design with similar power rating. Balanced against the increased burnup are the benefits associated with lower fuel temperatures including fission gas release, fuel thermal expansion, high thermal conductivity, and lower thermal gradients.

The level of detail in the pellet heat transfer model of the ESBOND code was deemed inadequate for predicting performance for these optimized fuel designs. It is expected that, despite the effects of increased burnup, the lower fuel operating temperatures would result in across the board improvements in the fuel performance based on the ESBOND results for the LBLWR fuel analyzed in Chapter 6.

CHAPTER 8
CONCLUSIONS AND RECOMMENDATIONS

It has been shown that liquid bonded LWR fuel provides thermal advantages over conventional LWR fuel. These advantages are particularly important in the areas of safety and thermal/mechanical margin. The improvement results from the lower operating temperature of the UO_2 fuel pellet and the corresponding lower stored energy in the fuel. The lower stored energy precludes the onset of zirconium-water reaction in even the most severe postulated accidents, as the parabolic rate constant for the reaction is reduced as much as three orders of magnitude relative to conventional fuel.

It was determined that liquid metal is the best choice of bonding liquid because of the temperature range over which liquid metals remain liquid and chemically stable. Either lead-bismuth-tin, or lead-bismuth eutectic was identified as the best candidate, and lithium-7 was identified as the backup candidate from the standpoint of thermal, nuclear, and material compatibility. Major criteria leading to these choices include temperature range, thermal neutron interaction, corrosion of zircaloy cladding, and interaction with water at high temperatures.

Preliminary thermal analyses have been completed to determine the steady-state radial temperature profile for liquid bonded fuel, and the results are compared to conventional LWR fuel. The liquid bonded fuel was shown to operate

at significantly lower temperatures than the conventional fuel, improving the margin for the design criteria associated with maximum fuel temperature. The lower operating temperature was also found to yield lower stored energy in the fuel pellet. Transient response of the fuel to a severe loss-of-coolant event indicated that the lower stored energy precluded significant reaction between the zircaloy cladding and steam. It is expected that the liquid bonded fuel will mitigate severe accidents (Class IX) by reducing the stored energy in the fuel pellets and reducing the incidence of zirconium-water reaction.

The liquid metal bonded fuel response to fuel rod clad failure and severe accidents has been qualitatively discussed. It is felt that fuel rod failure exposing the bonding liquid metal to the light water coolant would result in a slow chemical reaction releasing heat and hydrogen gas. Research into the nature of the reaction between lead-bismuth-tin and water has been performed by Dr. Glen J. Schoessow. These tests showed that the reaction between this liquid metal and water at 600°F is negligible.

It has been demonstrated that the manufacturing of liquid bonded LWR fuel is technologically feasible. Current LMR liquid metal bonded fuel manufacturing techniques can be adapted for LWR fuel application, although the process is slightly more complex than for current LWR fuel.

Based on the establishment of the technical feasibility of LBLWR fuel, several developmental areas were identified to support the fuel design effort. These efforts were funded by the Department of Energy and included

1. Experimental assessment of the unique aspects of LBLWR fuel. Namely: the interaction of the liquid metal and the fuel and/or cladding.
2. Analytical assessment of the performance characteristics of LBLWR fuel. This task included the detailed thermal analysis of the fuel, and the development of a computer program to determine the lifetime performance of the LBLWR fuel designs.

Experimental Results

Foremost in demonstrating the feasibility of LBLWR fuel is ascertaining the compatibility between the candidate liquid metal(s) and the fuel, cladding, and water coolant. Extensive testing has been conducted by Thad Adams and Mark Dubecky under the supervision of Dr. Glen J. Schoessow and Dr. Richard Connell at the University of Florida to determine the corrosion characteristics of lead-bismuth eutectic and lead-bismuth-tin ternary alloy and Zircaloy-4 cladding. It was concluded that for the lead-bismuth-tin alloy, the liquid metal interaction with the cladding does not pose a significant problem at the expected operating temperature range over the proposed fuel lifetime. The chemical compatibility of the lead-bismuth-tin alloy is primarily due to the formation of a $ZrSn_2$ reaction layer between the cladding and the liquid metal which enables the cladding to resist further attack. This is similar to fuel manufacturers using tin metallurgically bonded

to the inside of the cladding to decrease the effects of pellet-cladding interaction [30].

Separate tests were run with UO_2 pellets included in the test samples. These tests show that the lead-bismuth-tin alloy is compatible with both the fuel and cladding at prototypic temperatures over the fuel lifetime.

Tests were also conducted by Dr. Schoessow to characterize the transport of fission gas through thin liquid metal layers. In addition, the extent of reaction between the proposed liquid metal bond material and water at high temperature and pressure was investigated. Both of these tests showed that the liquid metal bonded fuel will perform well during both operating and transient conditions.

Additional experimental efforts by Dr. Schoessow to determine the wetting characteristics of liquid metal in small gaps indicated that gas gaps could occur during fabrication of LBLWR for gaps of 1 mil or less. Subsequent thermal analysis showed that small variations in the circumferential heat transfer due to gas blanketing did not significantly affect fuel performance.

As a result of these experiments, a large body of data has been accumulated which will be instrumental in licensing fuel designs utilizing liquid metal bonding.

Analytical Fuel Performance Results

Detailed thermal calculations were performed to determine the operating characteristics of the LBLWR fuel during both steady-state and transient

conditions. These calculations showed that the level of benefit for LBLWR fuel as compared to conventional fuel depend on the value of the gap conductance for the conventional fuel, which can change significantly over the life of the fuel. Typical values of gap conductance for beginning-of-life when the fuel/cladding gap is open exhibit much higher fuel temperatures for the conventional fuel rod, than for the LBLWR rod which has virtually an infinite gap conductance. However, as the gap conductance for the conventional fuel rod increases, and as the fuel/cladding gap is reduced, the relative benefit of the liquid bond decreased.

At this point, the need for a mechanistic tool for use in calculating the LBLWR fuel performance over a typical fuel lifetime became apparent. An extensive review of available computer codes led to the development of a fuel performance code for LBLWR fuel based on the ESCORE code which is used to calculate LWR fuel performance. This code has all the pertinent models needed to determine the fuel performance characteristics over the fuel lifetime including

1. Detailed fuel heat transfer
2. Gap conductance model
3. Fission gas evolution and release
4. Fuel densification and swelling
5. Clad strain and creep
6. Temperature and burnup dependent thermal properties for the fuel and cladding

The ESCORE code was obtained from the Florida Power Corporation, and modified to run on the Hewlitt-Packard-735 UNIX workstation. Models and upgrades were added to the code to analyze LBLWR fuel. These include:

1. Liquid metal gap conductance model
2. Methodology for determining the displacement of the liquid metal as the cladding creeps down onto the fuel pellet. An option to allow the user to specify the level of liquid metal fill was also included.
3. Input/output changes to invoke the new models, and to allow the code to analyze conventional fuel by bypassing the new models
4. A graphical interface to present the results graphically

The modified code, named ESBOND, was used to analyze both PWR and BWR liquid bonded fuel rods. In both cases, the results of the analyses were compared to conventional fuel rods at the same conditions to determine the relative merit of the liquid bonded technology.

The ESBOND code provides a vital tool for analyzing the performance of advanced fuel designs. Based on a proven, licensed, methodology, the code is capable of assessing a wide range of fuel designs which utilize liquid metal to enhance reactor safety.

PWR Fuel Rod

The Westinghouse 15x15 fuel rod was analyzed using the ESBOND code. All fuel design parameters such as fuel rod dimensions, average linear power, axial

power shape, thermal/hydraulic conditions, and fuel rod pre-pressurization were specified to match those used on conventional fuel rods. Initial calculations indicated that the resultant internal fuel rod pressure exceeded design criteria due to the use of the recommended pre-pressurization (450 psia), and the resultant smaller gas plenum due to the incompressible liquid metal. Subsequent calculations were performed which employed a lower value of pre-pressurization (200 psia) similar to rods employing integral burnable absorbers, and a partial fill of the liquid metal (80% of the annulus filled at beginning-of-life). These results show that the fuel rod pressure at end of life falls within the acceptable range.

The results of the analysis of the liquid bonded PWR fuel rod show that the benefits of the liquid bond to reduce the fuel temperatures is maximized at the beginning-of-life when the gap conductance for conventional fuel is at a minimum. The calculations also show that temperature dependent parameters such as fuel swelling, fission gas release, and clad strain are all mitigated by the use of the liquid metal bond.

BWR Fuel Rod

More impressive results were observed during the analysis of BWR fuel. The decrease in the fuel temperatures for the liquid bonded fuel relative to conventional fuel is more pronounced than was shown for PWR fuel. This is primarily due to the larger gap which occurs in BWR fuel, which results in an decreased gap conductance at the beginning of life as compared to the PWR fuel rod. In addition,

the combination of rod pre-pressurization, thicker cladding, and lower reactor coolant system pressure keeps the gap from closing until very late in the fuel lifetime. This factor allows the liquid bonded BWR fuel rod to exhibit lower fuel temperatures relative to conventional fuel which do not significantly diminish over the fuel lifetime.

To take full advantage of the heat transfer ability of the liquid metal, a fuel rod design was proposed which includes an annular pellet with grooves to allow thermal communication between the high temperature regions and the cladding. The results a three-dimensional thermal analysis of this design indicate that the fuel temperatures can be significantly decreased using an annular fuel pellet, when compared with a solid pellet design. Analysis of the grooved pellet design showed that the marginal decrease in fuel temperature resulting from the grooves do not justify the additional manufacturing complication.

Recommendations

The Liquid Metal Bonded Light Water Reactor Fuel Program has successfully demonstrated that liquid metal bonding can reduce fuel operating temperatures; resulting in safer and more efficient fuel performance for both steady-state and transient conditions. Based on the results of this program, it is recommended that the design be optimized to take full advantage of the heat transfer characteristics of the liquid metal. Based on the results of the material testing conducted at the

University of Florida, the fuel design is considered sufficiently reliable to initiate irradiation testing to provide a demonstration of the benefits of LBLWR fuel, and to provide a data base for the qualification of the performance models.

APPENDIX
ESBOND LBLWR FUEL PERFORMANCE CODE SUBROUTINES

The ESCORE computer program was modified to perform fuel performance calculations on liquid bonded light water reactor (LBLWR) fuel. While serveral subroutines were modified, five in particular contain extensive modifications to calculate LBLWR fuel performance. The source code listing for these five subroutines are included in this appendix. The subroutines are:

1. MAIN The initial program segment, contains the upgrade history
2. PGAS Calculates the rod pressure
3. SFILE Sets up ESBOND input options
4. DTGAP Calculates gap conductance
5. BEGIN Sets up initial gas volumes

MAIN PROGRAM SEGMENT SOURCE CODE LISTING

```
C.. MAIN PROGRAM SEGMENT
C
C     + (C-CODE, VERSION BETA-2)
C
C*********************************************************************C
C*                                                                   *C
C*     ============================================================  *C
C*      THIS NOTICE MAY NOT BE REMOVED FROM THE CODE BY ANY USER     *C
C*     ============================================================  *C
C*                                                                   *C
C*                                                                   *C
C*                ELECTRIC POWER RESEARCH INSTITUTE, INC.            *C
C*                        COPYRIGHT NOTICE                           *C
C*                                                                   *C
C*                                                                   *C
C* ELECTRIC POWER RESEARCH INSTITUTE, INC. (EPRI) RESERVES ALL RIGHTS *C
C* IN THE CODE AS DELIVERED.  THE CODE OR ANY PORTION THEREOF MAY NOT *C
C* BE REPRODUCED IN ANY FORM WHATSOEVER EXCEPT AS PROVIDED BY LICENSE *C
C* WITHOUT THE CONSENT OF EPRI.  SUCH CONSENT HAVING BEEN OBTAINED,   *C
C* CHANGES OR MODIFICATIONS MAY BE MADE IN THE CODE PROVIDED THAT     *C
C* WRITTEN NOTICE AND A DETAILED DESCRIPTION OF ANY SUCH CHANGES OR   *C
C* MODIFICATIONS SHALL BE TRANSMITTED TO EPRI AND EPRI PROVIDES       *C
C* WRITTEN PERMISSION TO MAKE SUCH CHANGES OR MODIFICATIONS PRIOR TO  *C
C* SUCH CHANGES OR MODIFICATIONS BEING MADE TO THE CODE; AND,         *C
C* PROVIDED FURTHER THAT, UPON THE WRITTEN REQUEST OF EPRI, THE CODE, *C
C* AS CHANGED OR MODIFIED, SHALL BE GIVEN A NEW DESIGNATION           *C
C* SUFFICIENTLY DIFFERENT FROM ITS CURRENT DESIGNATION AS TO PREVENT  *C
C* MISTAKE, CONFUSION, OR DECEPTION AS BETWEEN THE CURRENT CODE AND   *C
C* THE CODE AS CHANGED OR MODIFIED.                                   *C
C*                                                                   *C
C* A LICENSE UNDER EPRI'S RIGHTS IN THE CODE CAN BE OBTAINED DIRECTLY *C
C* FROM EPRI.  THE CODE AND SUPPORTING MATERIALS MAY BE INDEPENDENTLY *C
C* AVAILABLE FROM ELECTRIC POWER SOFTWARE CENTER.                     *C
C*                                                                   *C
C* NEITHER EPRI, ANY MEMBER OF EPRI NOR ANY PERSON OR ORGANIZATION    *C
C* ACTING ON BEHALF OF THEM:                                          *C
C*                                                                   *C
C*   1. MAKES ANY WARRANTY OR REPRESENTATION WHATSOEVER, EXPRESS OR   *C
C*      IMPLIED, INCLUDING ANY WARRANTY OF MERCHANTABILITY OR FITNESS *C
C*      OF ANY PURPOSE WITH RESPECT TO THE CODE; OR                  *C
C*                                                                   *C
C*   2. ASSUMES ANY LIABILITY WHATSOEVER WITH RESPECT TO ANY USE OF   *C
C*      THE CODE OR ANY PORTION THEREOF OR WITH RESPECT TO ANY       *C
C*      DAMAGES WHICH MAY RESULT FROM SUCH USE.                      *C
C*                                                                   *C
C* RESTRICTED RIGHTS LEGEND: USE, DUPLICATION, OR DISCLOSURE BY THE   *C
C* GOVERNMENT IS SUBJECT TO RESTRICTIONS AS SET FORTH IN PARAGRAPH    *C
C* (B) (3) (B) OF THE RIGHTS IN TECHNICAL DATA AND COMPUTER SOFTWARE  *C
C* CLAUSE IN DAR7-104.9 (A).                                          *C
C*                                                                   *C
C*********************************************************************C
C - -
C - - MODIFICATION LOG:
C - -   DATE    VERSION  MOD  DESCRIPTION
C - - --------  -------  ---  ----------------------------------------
C - -   2/86       1      A   INITIAL SINGLE SOURCE RELEASE (BASE UPDATE
C - -                          IDENTIFIERS AND MJA0286)
C - -
C - - - - - - - - - - - - - - - - - - - - - - - - - - - - - - - - - - - -
C
C*********************************************************************C
C - -
```

```
C - - MODIFICATION LOG:
C -    DATE    VERSION  MOD  DESCRIPTION
C - - -------- -------- --- ------------------------------------------
C - -   8/93    ESBOND    A  MODIFICATION OF ESCORE V1A TO PERFORM
C - -                        LIQUID METAL BONDED LIGHT WATER REACTOR
C - -                        FUEL PERFORMANCE ANALYSIS
C
C - -
C - - - - - - - - - - - - - - - - - - - - - - - - - - - - - - - - - - -
C
C.. CALLS:
C       BEGIN
C       PREHOT
C       HOTGAP
C       PROGRAM ESCORE(INPUT,OUTPUT,TAPE40,TAPE41,TAPE5=INPUT
C     2  ,TAPE6=OUTPUT)
C       POHOT
C       CREOUT
C       REASON
C
C..CALLED BY:(-)
C
C
C
C
C.. ESTABLISH AN ARRAY MEMORY(  ) IN BLANK COMMON TO CONTAIN ALL THE
C     INFORMATION NEEDED FOR AN AXIAL NODE WHICH IS PARTICULAR TO THE
C     AXIAL NODE AND WHICH MAY CHANGE WITH TIME.  EXPLICITLY LABEL
        COMMON TIME,TIME0,NITER,NITER0,MEM(1496),DUM(1234)
        COMMON/BB/B(72)
        COMMON /AA/ A(3),A1(2),A2(2),A3(2),A4(3),A5,A6,A7,A8(2),A9(2)
       +  ,A10(2)
        CHARACTER*4 A,A2,A4,A10,IVERS
        CHARACTER*5 A1,A5,A8,A9
        CHARACTER*6 A6
        CHARACTER*7 A3,A7
C.. BLANK COMMON USED BY:
C     FCOD,BEGIN,PREHOT,HOTGAP,FHOT1,REASON,POHOT,CREOUT
        DIMENSION MEMORY(1500)
        EQUIVALENCE (MEMORY(1),TIME)
        COMMON/CREP/AY1(16)
        COMMON/IFILE/ICH,JCH,KCH,LCH,MCH,NCH,NNCH
        COMMON/EXX/ CRFACT,SPTYM,FGPRO,FGREL,
       +TPOWJ(24),HLJ(24),TCOJ(24),POJ(24),ATT(24),QOLD(24),MAXAX
       +,HLJ2(24),FLUX(24),TCOOL(24),RABUT,DBURT,HLRA
       +,REPJ(24)
        COMMON/PLAIN/XPL1(21)
        COMMON/PLAOUT/XPL2(18)
        COMMON/PLATE/LPL1(11)
C-2.4QF ADD COMMON TRANS
        COMMON/TRANS/AK,BK,CK,TXX(2)
        LOGICAL OK,SENS,STEP1,PFIRST,IFIRST,CONT,LAST,RSTRT
       ',SPRNT,NOMELT,NOAUXP
C
C.. USE LABELED COMMON BLOCKS FOR CONSTANTS AND FOR VARIABLES
C   WHICH ARE THE SAME FOR ALL AXIAL NODES
C
C   LABELED COMMON BLOCKS ARE SET IN AUXIALIARY ROUTINE FBLOK.FR
C
        REAL MSUM
CREV1.3 REVISION FOR FORTRAN77. NEW TYPE FOR STERM
C-2.6QF I/O ENHANCEMENTS CHANGE TYPE FOR TITLE,IDAY,ITYM
```

```
      CHARACTER*10 CLOCK,IDAYZ,ITYMZ,DATE
      DIMENSION TF0(24)
      COMMON/HOLD/HOLDIT(1500,24)
C     LEVEL 2,/HOLD/
      COMMON/PHI/PPP(25)
      COMMON/PRE/PP1(22)
      COMMON/PRE2/PP2(15)
      COMMON/GASDAT/GRFRFX(11)
      COMMON/AAA/AA33(109)
      COMMON /ROD/ TITLE(10),IDAY,ITYM,IVERS
      CHARACTER*10 IDAY,ITYM
      CHARACTER*8 TITLE
C     REAL IDAY,ITYM
C JSTCK IS USED FOR STACKING CASES:0=FIRST CASE,1=ALL OTHER CASES
      COMMON/CFEAT/CFS(7)
      COMMON/PRNT/IDD
      COMMON/GASP/TF1,TCI1,MSUM,PLENVO,
     -PLENT,PVOPT,RODHT,HOTSTK,
     +HRODHT,S1,S2,STHEGT,
     -PLENHT,PIFAB,PO,GHTOT,GTOT,GXTOT,PIOLD,DPOLD,PLENV0,FFGREL
     +,DELVV0,V0,PLNVL1,EFFVOL,VOLCLD
      COMMON/REKY/ZRON(27)
      COMMON/TERM/NTERM,STERM,IWORD
C-2.1QF ADD COMMON CCOD
      COMMON/CCOD/CDAT(11),FRELOC,TRELOC
C-2.2QF ADD COMMON GAP
      COMMON/GAP/EXX(69)
      COMMON/WID/YYY(24,7)
      COMMON/JUNK/JUNK1,JUNK2,JUNK3,PFAILA,JUNK4,JUNK5
      REAL JUNK1,JUNK2,JUNK3,JUNK4,JUNK5
      COMMON/CDT/N11(5),RESET1
      LOGICAL RESET1
C-2.6QF I/O REVISIONS; ADD COMMON EDIT
      COMMON/EDIT/IXCH(20),ENGOUT,TAB(10),SPRNT,DAYS,ITC1,ITC2
CREV1.3 REVISION FOR FORTRAN77
      CHARACTER*4 NULWRD,IWORD,NTERM,STERM
      DATA NULWRD/'    '/
      DATA ATR,DSPTYM,FOPEN,PTIME,SPTIME,TF0,XE0 /30*0./
      DATA IDDD,II,JCTR,JSTK,MFLAG,MSIZE,NAX,NMEM,NOCREP,NOGASR,NORELO
     +  ,NTRYR /12*0/
      DATA CONT,IFIRST,LAST,NOAUXP,NOMELT,OK,PFIRST,RSTRT,SENS,STEP1
     +  /10*.FALSE./
C
C     DATA NTERM/'####'/
C     DATA STERM/'    '/
      OPEN(UNIT=81,FILE='ftn81')
      OPEN(UNIT=50,FILE='ftn50')
      OPEN(UNIT=5,FILE='inin')
      OPEN(UNIT=6,FILE='outout')
      TIME = 0.
      TIME0 = 0.
      NITER = 0.
      NITER0 = 0.
      DO 5 I = 1, 1496
      MEM(I) = 0.
    5 CONTINUE
      DO 7 I = 1, 1234
      DUM(I) = 0.
    7 CONTINUE
      JSTK=0
      IFIRST=.TRUE.
500   CONTINUE
```

```
      IWORD=NULWRD
C
      REWIND 81
      WRITE(81,10)
   10 FORMAT('ABORT ',2X,24X)
      REWIND 81
C
      NMEM=1500
      MSIZE=NMEM
C - - CALLS TO DATE AND TIME FUNCTIONS
C     IDAYZ = DATE()
C     ITYMZ = CLOCK()
C     IDAY = '          '
C     IDAY(2:9) = IDAYZ(2:9)
C     ITYM = '   :  :   '
C     ITYM(2:3) = ITYMZ(2:3)
C     ITYM(5:6) = ITYMZ(5:6)
C     ITYM(8:9) = ITYMZ(8:9)
C
C     IBM VS-FORTRAN VERSION 2 CALL TO GET DATE AND TIME
C
      CALL TIMDAT(IDAY,ITYM)
      CALL BEGIN(MEMORY,1500,NMEM,NAX,IDDD,NOGASR,NORELO,NOCREP,
     +NOMELT,NOAUXP,PTIME,SPTIME,SENS,PFIRST,DSPTYM,CONT,STEP1,SPTYM,
     +FGPRO,FGREL,TF0,FOPEN,IFIRST,RSTRT,JSTK,JCTR)
      IDD=MIN0(0,IDDD)
      XE0=1.E-6
      II=0
C-2.6QF I/O ENHANCEMENTS REMOVE NEXT 4 LINES
C
C
C.. RETURN HERE FOR NEW TIME STEP
CTTTTTTTTTTTTTTTTTTTTTTTTTTTTTTTTTTTTTTTTTTTTTTTTTTTTTTTTTTTTTTTTTTTTTTT
100   IF(TIME.GE.PTIME) IDD=IDDD
      IF(TIME.GE.SPTIME) IDD=MIN0(0,IDDD)
      DO 150 IAX=1,NAX
      IF(NAX.GT.1)CALL GET(MEMORY,4,-4,IAX)
      NITER0=NITER
      NITER=0
      NTRYR=0
      TIME0=TIME
      IF(NAX.GT.1)CALL PUT(MEMORY,4,-4,IAX)
150   CONTINUE
C
      IF(IDD.GE.0)WRITE(NCH,25)TIME
25    FORMAT(' NEW TIME STEP, TIME =',F13.4,' HRS')
C
C-----------------------------------------------------------------------
C
C   RETURN HERE FOR CUTTING TIME-STEP
200   CONTINUE
C
C
C
C..READ IN POWER HISTORY,COMPUTE TIME STEP, AND PREPARE FOR HOTGAP
C
      CALL PREHOT(MEMORY,1500,NAX,TPOWJ,HLJ,TCOJ,MAXAX,PFIRST,ATT,
     +QOLD,LAST,HLJ2,FLUX,TCOOL,RABUT,DBURT,HLRA,POJ,NOCREP,NORELO,
     +NOAUXP,REPJ)
      IF(IWORD.EQ.STERM.AND.CONT) GO TO 600
      IF(IWORD.EQ.STERM.AND..NOT.CONT)IFIRST=.FALSE.
      IF(IWORD.EQ.STERM.AND..NOT.CONT) GO TO 500
```

```
      IF(IWORD.EQ.NTERM.AND.CONT) GO TO 600
      IF(IWORD.EQ.NTERM) STOP
C
CXXXXXXXXXXXXXXXXXXXXXXXXXXXXXXXXXXXXXXXXXXXXXXXXXXXXXXXXXXXXXXXXXXXXXXXXXXXXXXX
C.. INPUT VALUE FOR XENON CONCENTRATION
C
300       DO 400 IAX=1,NAX
      IF(NAX.GT.1) CALL GET(MEMORY,1500,-4,IAX)
C
C.. SOLVE HOTGAP PROBLEM
      CALL HOTGAP(IAX,NAX,NORELO)
      CALL REASON(OK,ATR,IAX,NAX,NTRYR,TF0(IAX))
C
C
C.. CHECK REASONABLENESS OF SOLUTION
      ATT(IAX)=ATR
C
      IF(.NOT.OK)GOTO 200
C
C.. IF UNREASONABLE (FOR ANY NODE), CUT TIME-STEP AND TRY AGAIN
C
C-------------------------------------------------------------------
C
      IF(NAX.GT.1) CALL PUT(MEMORY,1500,-4,IAX)
400       CONTINUE
C
C.. COMPUTE FISSION GAS RELEASE & ROD INTERNAL PRESSURE
C-2.6QF I/O REVISIONS ADD TITLE,FTAB TO CALL.
      CALL POHOT(MEMORY,NMEM,NAX,MFLAG,FGPRO,FGREL,FOPEN,XE0)

C
      IF(MFLAG.EQ.1)GOTO 300
C
C
      IF( SPRNT .AND. ( TIME.LT.TPOWJ(1) ) ) GO TO 700
C
CXXXXXXXXXXXXXXXXXXXXXXXXXXXXXXXXXXXXXXXXXXXXXXXXXXXXXXXXXXXXXXXXXXXXXXXXXXXXXXX
C
C
C  COMPUTE POWER-TO-CENTERLINE-MELT AND INCREMENTAL CLAD STRAIN
C  DUE TO FUEL MELTING AND FUEL TEMPERATURES BASED ON THE
C  AUXILIARY POWER SHAPE
C
C
      IF( NOMELT ) GO TO 2000
      CALL MOLTEN(NAX,NORELO)
 2000 IF( NOAUXP ) GO TO 1000
C
C  CALCULATE FUEL TEMPERATURES BASED ON AUXILIARY
C  POWER CURVE
C
      CALL AUXPWR( NAX,NORELO )
1000  CONTINUE
C
C
C**********************************************************************
C
C
C.. COMPUTE CLAD CREEP AND THERMAL CONTRACTION. THEN
C.. OUTPUT RESULTS FOR THIS TIME STEP
C
 700  CALL CREOUT(MEMORY,1500,NAX,FGPRO,FGREL,II,STEP1,
```

```
     +TF0,RSTRT,HLRA,NOCREP,NORELO)
C
      STEP1=.FALSE.
      IF(.NOT.LAST) GO TO 100
600   CONTINUE
      IF(.NOT.CONT)STOP
C
C.. STORE RESULTS FOR THIS TIME-STEP
      CALL ASTORE(NMEM,NAX,IFIRST)
      IFIRST=.FALSE.
      IF(IWORD.EQ.STERM) GO TO 500
CTTTTTTTTTTTTTTTTTTTTTTTTTTTTTTTTTTTTTTTTTTTTTTTTTTTTTTTTTTTTTTTTTTTTTTTTTTTTTTT
C
      STOP
      END
```

SUBROUTINE PGAS SOURCE CODE LISTING

```
      SUBROUTINE PGAS(NMEM,NAX,PICLD,PLNHT0)
C
C   THIS SUBROUTINE CALCULATES THE ROD PRESSURE
C
      DIMENSION MEMORY(1500)
      EQUIVALENCE (MEMORY(1),TIME)
C
C  LIQUID BONDED CODE CHANGES ARE DELIMITED BY ********
C
C*********************************************************************
      COMMON /BOND/NBOND,BONDCOND,VLBCOLD,BONDEXP,NPAD,XLLIQ,FRACFIL,
     +IWET(50)
      LOGICAL NBOND,NPAD
C*********************************************************************
C
      COMMON TIME,TIME0,N1(3),RCIOUT,N2(150),PFABO,PFABC,A101(2),
     -DISH,N2A(5),RELOC,N21(107),NRING,N21A(40),GRELTT,N3(3),
     -NNODE,PC,RF,
     -RCOLD(20),N4(6),
     -ECZ,T(20),DT(20),VFOLD,VFNEW,FOP,FCP,FOP0,
     -RHONEW,AFF,ACSWL0,DNSWL0,DLOPVL,TEMP20(4),
     -VFRAC0,VFRAC,Y113(4),
     -N5(50),RCHOT,NCRACK,N6,BUT,N6A(4),FNODHT,
     +TCO,RHOT(20),TG,N7(18)
      COMMON N8(3),RCIFAB,N8A(4),RFFAB,ESWAVG,TFCL,TCI,TF,
     'N9(2),ADEN,N9A(3),DENSWL,N9B(33),RELOCR,
     -QS1,FRELT,N10(62),CVAF,DVAF,OPVAF,VVAF,
     -CRKVUP,DSHVUP,CTRVUP,
     -OPVUP,CVAF0,DVAF0,OPVAF0,VVAF0,CRKFIL,DSHFIL,OPFIL,
     'CTRFIL,OPVOL,ECR,DSHNTH,CTRNTH,
     -N10A(140),
     -ACC1,N101(2),GFPSWL,RFINUP,LHOLE,RFIN01,FL,REP,
     +KGG(5),Y110(2),
     -ACCVLC,ACCVL1,ACCVLH,ACCVL5,
     -N101B(40),
     'GZ,FHOT(20),RFC,GAPVH,GAPTEM,VOVTPG,CRKV04,CRKTMP,
     +CVLVCT,N11(21),FREL,N11A1,RFCOLD,N11C(33),
     +TPOW,N11A(7),
     -RCICLD,N11B(103),NODELC,NODELH,N11E(54),DRRMAX,
     -N13A(24),TAVG,N13B(6)
      COMMON TSWGR(20),FMIN(20),FDPC,RHOIN,RHOOUT,BUCOM,FTYP,
     -RFIN,FPL,HDISH,RLAND,RBOT,VDISH,VCHAM,VHOLE,VTC,TCLNT,
     -RABU,RABU0,HL2,DUMMEN(311)
      COMMON/IFILE/ICH,JCH,KCH,LCH,MCH,NCH,NNCH
      COMMON/GAP/AG,PI,DP,XGAS(5),XMGAS(5),C(5),FGAP(25)
     +,AGAP(5),RGAP(5),AAGAP(5),BBGAP(5),NNNCH
     -,PREVC(5)
      COMMON/PRNT/IDD
      COMMON /GASDAT/ YF,XEFRAC,XMEVF(7),FGRIN,DUMMY
      COMMON/BB/B(23),VF,VFUEL(24),VRAT(24)
      COMMON/GASP/TF1,TCI1,MSUM,PLENVO,
     -PLENT,PVOPT,
     -RODHT,HOTSTK,HRODHT,S1,S2,STHEGT,PLENHT,PIFAB,PO
     +,GHTOT,GTOT,GXTOT,PIOLD,DPOLD,PLVFAB,FFGREL
     -,TEMP21,V0,PLNVL1
     +,EFFVOL,VOLCLD
      REAL MSUM
      REAL LHOLE,NETVLC,NETVLH,HOTHOL,NODELC,NODELH
      DATA ACCNTC,ACCNTH,ACCVL2,ACCVL3,ACCVL4,ACCVL6,ATCC,CHMV01
     +  ,CHMV02,CLDHOL,CLDNOD,CLDPLN,CLDSTK,CRKNTC,CRKNTH,CRKVLC,CRKVLH
     +  ,CRKV01,CRKV02,CRKV03,CRKV05,CRKV06,CROD,CRODHT,CTRNTC,CTRTMP
     +  ,CTRVLC,CTRVLH,CTRV01,CTRV02,CTRV03,CTRV04,CVLCVT,DELND1,DELND2
```

```
     +   ,DELTAT,DNSFRC,DSHNTC,DSHTMP,DSHVLC,DSHV01,DSHV02,DSHV03,DSHV04
     +   ,FACT,FACTC,FACT1,FAFT,FAFTC,GAPVC,GAPV01,GAPV02,HDISHC
     +   ,HOTHOL,HOTNOD,HOTPLN,HROD,NETVLC,NETVLH,OPVL01,OPVL02,PLNVLC
     +   ,PORNTC,PORNTH,PORVLC,PORVLH,PORV01,PORV02,PORV03,PORV04,PY,R
     +   ,RADFRC,RATIO1,RATIO2,RCI1,RCLADC,RINHOT,RTC,STAKLC,STAKLH
     +   ,SUMACC,SUMAF,SUMVLC,SUMVLH,S3,S4,TAVGC,TAVG1,TAVG11,TCI11
     +   ,TFAVG,TLAND,VACC1,VCHVT,VCTRVT,VDSHVT,VOPVT,VTC1 /99*0./
C*********************************************************************
C
C  LIQUID BONDED CODE CHANGES
C
C      DATA IFLAG/0/
C
C*********************************************************************
C
      IF(IDD.GE.1) WRITE(NCH,25)
25    FORMAT(' ,' PGAS')
      PY=3.14159
      R=8.2921
      HOTSTK=0.
      MSUM=0.
      GAPV01=0.
      GAPV02=0.
      CRKV03=0.
      CRKV06=0.
      DSHV02=0.
      CHMV02=0.
      CTRV02=0.
      CTRV04=0.
      PORV02=0.
      PORV04=0.
      STAKLH=0.
      STAKLC=0.
      CHMV01=0.
      DSHV04=0.
      OPVL02=0.
      CLDSTK=0.
      ACCVL3=0.
      ACCVL6=0.
      GFPTC=0.
      GFPTH=0.
C
      IF(TIME0 .GT. 2.) GO TO 50
         PLENHT=(PLVFAB-PLNVL1)/(PY*RCIFAB*RCIFAB)
   50 CONTINUE
C*********************************************************************
C
C  LIQUID BONDED CODE CHANGES
C
      VLBHOT=0.
C*********************************************************************
C
      DO 1000 IAX=1,NAX
      IF(NAX.GT.1)CALL GET(MEMORY,NMEM,-4,IAX)
      IF(IDD.GE.2) WRITE(NCH,26) PC,RCIOUT,PLENHT,
     +FNODHT,RCHOT,RFC,XGAS(3),PO
      IF(IDD.GE.2) WRITE(NCH,27) NCRACK
26    FORMAT(' ',5E15.7)
27    FORMAT(' ',I4)
      CRKV02=0.
      CRKV05=0.
      CTRNTC=0.
```

```
      DSHV03=0.
      CTRV03=0.
      PORV03=0.
      DSHV01=0.
      CTRV01=0.
      PORV01=0.
      GFPVLC=0.
      GFPVLH=0.
      TF1=TF+273.
      TCI1=TCI+273.
      TFAVG=TAVG
      TAVG1=TFAVG+273.
      VACC1=ACC1*VFUEL(IAX)
C     FUEL AXIAL THERMAL EXPANSION
        IF(RLAND.LE.0.) GO TO 16
        DO 13 I=1,NRING
        IF((RLAND .LT. RCOLD(I+1)) .OR. (RLAND .GE. RCOLD(I))) GO TO 55
           RADFRC=(RLAND-RCOLD(I+1))/(RCOLD(I)-RCOLD(I+1))
           DELTAT=T(I)-T(I+1)
           TLAND=RADFRC*DELTAT+T(I+1)
           GO TO 16
     55 CONTINUE
     13 CONTINUE
     16   AFF=AF(TAVG)
C     CLADDING AXIAL THERMAL EXPANSION--INPUT TEMPERATURE IN 'K
     15 TAVGC=(TCI+TCO)/2.
        ATCC=4.44E-6*(TAVGC+273.) - 1.24E-3
        FACT=(1.+ATCC)*(1.+GZ)*(1.+ECZ)
        FACTC=( 1.+GZ ) * ( 1.+ECZ )
        IF(IAX.EQ.1)CRODHT=PLENHT*FACTC
        IF(IAX .NE. 1) GO TO 60
            RCLADC=RCICLD
            FACT1=FACTC
           HRODHT=PLENHT*FACT
           PLNHT0=PLENHT
     60 CONTINUE
        HROD=FNODHT*FACT
        HRODHT=HRODHT+HROD
        FAFT=(1.+AFF)*(1.+ESWAVG)
        FAFTC=(1.+ESWAVG)
        HOTNOD=FNODHT*FAFT
        STAKLH=STAKLH+HOTNOD
        CROD=FNODHT*FACTC
        CRODHT=CRODHT+CROD
        CLDNOD=FNODHT*FAFTC
        STAKLC=STAKLC+CLDNOD
        MSUM=GRELTT+MSUM
        IF(IDD.GE.2) WRITE(NCH,26) GHTOT,GRELTT,MSUM
C
C     GEOMETRIC VOLUMES ARE CALCULATED AND THEN ADJUSTED BY THE
C     CHARACTERISTIC TEMPERATURE TO DERIVE THE EFFECTIVE VOLUMES
C
C     FUEL/CLAD ANNULUS VOLUME CALCULATION
C
C      HOT COMPONENT -- GAPVH=NODAL HOT ANNULUS VOLUME
C                       GAPTEM=CHARACTERISTIC ANNULUS TEMPERATURE
C                       VOVTPG=NODAL VOLUME/CHARACTERISTIC TEMPERATURE
C                       GAPV02=SUM ( VOVTPG ) FOR FUEL PIN
C
        IF(PC.LE.0.) GO TO 10
        GAPVH=0.
        VOVTPG=0.
```

```
      GAPTEM=0.0
      GOTO 11
   10 GAPVH=PY*(RCIOUT**2-(RCIOUT-TG)**2)
      GAPVH=GAPVH*HOTNOD
      GAPTEM=(TF1+TCI1)/2.
      VOVTPG=GAPVH/GAPTEM
C*********************************************************************
C
C  LIQUID BONDED CODE CHANGES
C
      IF(NBOND) THEN
      IF(IWET(IAX).EQ.1) THEN
      VLBHOT=VLBHOT+VOVTPG*GAPTEM
      VOVTPG=0.
      ENDIF
      ENDIF
C*********************************************************************
C
      GAPV02=GAPV02+VOVTPG
C
C     COLD COMPONENT -- GAPVC=NODAL COLD ANNULUS VOLUME
C                       GAPV01=TOTAL COLD ANNULUS VOLUME FOR PIN
C
   11 GAPVC=PY*(RCICLD*RCICLD-RFCOLD*RFCOLD)*CLDNOD
C*********************************************************************
C
C  LIQUID BONDED CODE CHANGES
C
      IF(NBOND) THEN
      IF(IWET(IAX).EQ.1) THEN
      GAPVC=0.
      ENDIF
      ENDIF
C*********************************************************************
C
      GAPV01=GAPV01+GAPVC
C
C   CVAF =    CRACK     VOLUME ACCOMMODATION FACTOR
C   DVAF =    DISH          "          "          "
C   OPVAF=  OPEN POROSITY   "          "          "
C   VVAF =  CENTRAL VOID    "          "          "
C
C  CRACK VOLUME CALCULATION ** DUE TO RELOCATION ONLY
C
C    COLD COMPONENT --- CRKV01=NODAL CRACK VOLUME
C                       CRKV02=   "      "     "    TO BE ACCOMMODATED
C                                 IN THE PLENUM
C                       CRKV03=TOTAL CRACK VOLUME IN THE FUEL PIN
C
      CRKVLC=PY*CLDNOD*(RFCOLD*RFCOLD-(RFCOLD-RELOC)**2)
      CRKNTC=CRKVLC+CRKFIL
      CRKV01=CRKNTC+VACC1*CVAF
C*********************************************************************
C
C  LIQUID BONDED CODE CHANGES
C
      IF(NBOND) THEN
      IF(IWET(IAX).EQ.1) THEN
      CRKV01=0.
      ENDIF
      ENDIF
C*********************************************************************
```

```
C
      IF(CRKV01 .GE. 0.) GO TO 65
         CRKV02=CRKV01
         CRKV01=0.
   65 CONTINUE
      CRKV03=CRKV03+CRKV01
      CRKVUP=CRKFIL+VACC1*CVAF-CRKV02
C
C     HOT COMPONENT -- CRKV04=NODAL CRACK VOLUME
C                      CRKV05=NODAL CRACK VOLUME TO BE ACCOMMODATED
C                                IN THE PLENUM
C                      CVLCVT=  "     "     "   /FUEL AVERAGE TEMPERATURE
C                      CRKV06=TOTAL SUM OF ( CVLCVT ) FOR FUEL PIN
C
      CRKVLH=PY*HOTNOD*(RF*RF-(RF-RELOC)**2)
      RATIO1=1.
      CRKNTH=CRKVLH+CRKFIL*RATIO1
      CRKV04=CRKNTH+VACC1*CVAF*RATIO1
C*********************************************************************
C
C  LIQUID BONDED CODE CHANGES
C
      IF(NBOND) THEN
      IF(IWET(IAX).EQ.1) THEN
      VLBHOT=VLBHOT+CRKV04
      CRKV04=0.
      ENDIF
      ENDIF
C*********************************************************************
C
      IF(CRKV04 .GE. 0.) GO TO 70
         CRKV05=CRKV04
         CRKV04=0.
   70 CONTINUE
      CRKTMP=TAVG1
      CVLCVT=CRKV04/CRKTMP
      CRKV06=CRKV06+CVLCVT
C
C    CHAMFER VOLUME CALCULATION -- VCHAM IS THE AS-FAB VOLUME
C    HOT AND COLD CHAMFER VOLUMES ARE TAKEN TO BE THE SAME
C
C       COLD COMPONENT -- VCHAM=NODAL COLD CHAMFER VOLUME
C                         CHMV01=TOTAL COLD CHAMFER VOLUME IN FUEL PIN
C
C*********************************************************************
C
C  LIQUID BONDED CODE CHANGES
C
      IF(NBOND) THEN
      IF(IWET(IAX).EQ.1) THEN
      VCHAM=0.
      ENDIF
      ENDIF
C*********************************************************************
C
      CHMV01=CHMV01+VCHAM
C
C    HOT COMPONENT -- VCHAM=HOT NODAL CHAMFER VOLUME
C                     VCHVT=HOT CHAMFER VOLUME/CHARACTERISTIC TEMP
C                     CHMV02=SUM OF ( VCHVT ) FOR FUEL PIN
C
C*********************************************************************
```

```
C
C  LIQUID BONDED CODE CHANGES
C
      IF(NBOND) THEN
      IF(IWET(IAX).EQ.1) THEN
      VLBHOT=VLBHOT+VCHAM
      VCHAM=0.
      ENDIF
      ENDIF
C*********************************************************************
C
      VCHVT=VCHAM/TF1
      CHMV02=CHMV02+VCHVT
C
C   DISH VOLUME CALCULATION
C
C   COLD COMPONENT---DSHNTC=NODAL COLD DISH VOLUME
C                    DSHV01=NODAL COLD DISH VOLUME TO BE ACCOMMODATED
C                           IN THE PLENUM
C                    DSHV02=TOTAL COLD DISH VOLUME FOR THE FUEL ROD
C
      IF(RLAND .GT. 0.) GO TO 75
          DSHNTC=0.0
          DSHNTH=0.0
          DSHTMP=0.0
          GO TO 12
   75 CONTINUE
      DSHVLC=VDISH+DSHFIL
      DSHNTC=DSHVLC+VACC1*DVAF
C*********************************************************************
C
C  LIQUID BONDED CODE CHANGES
C
      IF(NBOND) THEN
      IF(IWET(IAX).EQ.1) THEN
      DSHNTC=0.
      ENDIF
      ENDIF
C*********************************************************************
C
      IF(DSHNTC .GE. 0.) GO TO 76
         DSHV01=DSHNTC
         DSHNTC=0.
   76 CONTINUE
      DSHV02=DSHV02+DSHNTC
      HDISHC=HDISH*DSHNTC/VDISH
      DSHVUP=DSHFIL+VACC1*DVAF-DSHV01
C
C   HOT COMPONENT---TLAND=FUEL TEMPERATURE AT PELLET LAND RADIUS
C                   DSHNTH=NODAL HOT DISH VOLUME
C                   DSHV03=NODAL HOT DISH VOLUME TO BE ACCOMMODATED
C                          IN THE PLENUM
C                   VDSHVT=NODAL DISH VOLUME/CHARACTERISTIC TEMPERATURE
C                   DSHV04=SUM OF ( VDSHVT ) FOR ROD
C
      DSHTMP=(TFCL+TLAND)/2.
      DSHNTH=DSHNTC
      IF(DSHNTH .GE. 0.) GO TO 80
         DSHV03=DSHNTH
         DSHNTH=0.
   80 CONTINUE
C*********************************************************************
```

```
C
C    LIQUID BONDED CODE CHANGES
C
      IF(NBOND) THEN
      IF(IWET(IAX).EQ.1) THEN
      VLBHOT=VLBHOT+DSHNTH
      DSHNTH=0.
      ENDIF
      ENDIF
C*********************************************************************
C
      VDSHVT=DSHNTH/(DSHTMP+273.)
      DSHV04=DSHV04+VDSHVT
C
C    CENTRAL VOID VOLUME CALCULATION (CORRECTED FOR TC VOLUME)
C
C       COLD COMPONENT -- RTC=EFFECTIVE COLD TC RADIUS
C                         VTC=COLD TC VOLUME (INPUT)
C                         CTRNTC=NODAL COLD HOLE VOLUME
C                         CTRV01=EXCESS VOLUME TO BE ACCOMMODATED
C                                IN PLENUM
C                         CTRV02=TOTAL COLD HOLE VOLUME IN ROD
C                         RFINUP=UPDATED COLD HOLE VOLUME (ALWAYS
C                                .GE. RTC)
C
   12 IF(RFIN01.LE.0.) GO TO 19
      CLDHOL=LHOLE*(1+ESWAVG)
      RTC=SQRT( VTC/(PY*LHOLE) )
      VTC1=PY*RTC*RTC*CLDHOL
      CTRVLC=VHOLE*(1.+ESWAVG)+CTRFIL
      CTRNTC=CTRVLC+VACC1*VVAF
C*********************************************************************
C
C    LIQUID BONDED CODE CHANGES
C
      IF(NBOND) THEN
      IF(IWET(IAX).EQ.1) THEN
      CTRNTC=0.
      ENDIF
      ENDIF
C*********************************************************************
C
      IF(CTRNTC .GE. 0.) GO TO 85
         CTRV01=CTRNTC
         CTRNTC=0.
   85 CONTINUE
      CTRV02=CTRV02+CTRNTC
      IF(CTRNTC .LE. 0.) GO TO 90
      RFINUP=SQRT( (CTRNTC+VTC1)/(PY*CLDHOL) )
      GO TO 95
   90 CONTINUE
         RFINUP=RTC
   95 CONTINUE
      CTRVUP=CTRFIL+VACC1*VVAF-CTRV01
C
C       HOT COMPONENT -- CTRNTH=NODAL HOT CENTRAL VOID VOLUME
C                        CTRV03=EXCESS VOLUME TO BE ACCOMMODATED IN
C                               THE PLENUM
C                        VCTRVT=NET HOT VOLUME/CHARACTERISTIC TEMP
C                        CTRV04=TOTAL SUM OF ( VCTRVT ) FOR FUEL PIN
C
      HOTHOL=FNODHT*(FAFT-2.*HDISHC/FPL)
```

```
      RATIO2=1.0
      RINHOT=RFINUP
      CTRVLH=PY*RINHOT*RINHOT*HOTHOL
      CTRNTH=CTRVLH
C*********************************************************************
C
C  LIQUID BONDED CODE CHANGES
C
      IF(NBOND) THEN
      IF(IWET(IAX).EQ.1) THEN
      VLBHOT=VLBHOT+CTRNTH
      CTRNTH=0.
      ENDIF
      ENDIF
C*********************************************************************
C
      IF(CTRNTH .GE. 0.) GO TO 100
         CTRV03=CTRNTH
         CTRNTH=0.
  100 CONTINUE
      CTRTMP=T(NNODE)+273.
      VCTRVT=CTRNTH/CTRTMP
      CTRV04=CTRV04+VCTRVT
C
C   OPEN POROSITY VOLUME
C
C        COLD COMPONENT -- PORNTC=NET COLD OPEN POROSITY VOLUME FOR NODE
C                          PORV01=NODAL POROSITY VOL TO BE ACCOMMODATED
C                                 IN THE PLENUM
C                          PORV02=SUM OF POROSITY VOLUMES IN  FUEL PIN
C
   19 DNSFRC=ABS( DENSWL/ADEN/(PFABO+PFABC) )
      OPVL01=DLOPVL*(1.-DNSFRC)
      OPVL02=OPVL02+OPVL01
      PORVLC=OPVOL+OPFIL
      PORNTC=PORVLC+VACC1*OPVAF
C*********************************************************************
C
C  LIQUID BONDED CODE CHANGES
C
      IF(NBOND) THEN
      IF(IWET(IAX).EQ.1) THEN
      PORNTC=0.
      ENDIF
      ENDIF
C*********************************************************************
C
      IF(PORNTC .GE. 0.) GO TO 105
         PORV01=PORNTC
         PORNTC=0.
  105 CONTINUE
      PORV02=PORV02+PORNTC
      OPVUP=OPFIL+VACC1*OPVAF-PORV01
C  COLD POROSITY VOLUME CALCULATION -- DUE TO GASEOUS
C  SWELLING COMPONENT
      GFPVLC=GFPSWL*VFUEL(IAX)*FRELT
      GFPTC=GFPTC+GFPVLC
C  HOT POROSITY VOLUME CALCULATION (GASEOUS SWELLING)
      GFPVLH=GFPVLC
      GFPTH=GFPTH+GFPVLH/TAVG1
C
C        HOT COMPONENT -- PORNTH=NET NODAL HOT OPEN POROSITY VOLUME
```

```
C                          PORV03=EXCESS SWELLING VOL TO BE ACCOMMODATED
C                                 IN THE PLENUM
C                          VOPVT=NET HOT VOL/CHARACTERISTIC TEMPERATURE
C                          PORV04=SUM OF ( VOPVT ) FOR FUEL PIN
C
      PORVLH=OPVOL+OPFIL*RATIO1
      PORNTH=PORVLH+VACC1*OPVAF*RATIO1
C*********************************************************************
C
C  LIQUID BONDED CODE CHANGES
C
      IF(NBOND) THEN
      IF(IWET(IAX).EQ.1) THEN
      VLBHOT=VLBHOT+PORNTH
      PORNTH=0.
      OPVL01=0.
      GFPTH=0.
      ENDIF
      ENDIF
C*********************************************************************
C
      IF(PORNTH .GE. 0.) GO TO 110
         PORV03=PORNTH
         PORNTH=0.
  110 CONTINUE
      PORNTH=PORNTH+OPVL01
      VOPVT=PORNTH/TAVG1
      PORV04=PORV04+VOPVT
C
      IF(IAX .NE. 1) GO TO 115
          TAVG11=TF1
          RCI1=RCIOUT
          TCI11=TCI1
  115 CONTINUE
C
C   UPDATE NODAL LENGHTS TO ACCOUNT FOR ACCOMMODATION OF THE EXCESS
C   SWELLING VOLUME
C
C   COLD LENGHTS
C
      ACCVL2=ABS( CRKV02+DSHV01+CTRV01+PORV01 )
      SUMAF=CVAF+DVAF+VVAF+OPVAF
      IF(SUMAF .GT. 0.) GO TO 120
         ACCNTC=ABS(VACC1)
      GO TO 125
  120 CONTINUE
         ACCNTC=ACCVL2
  125 CONTINUE
C   DON'T ALLOW ACCOMMODATION IN PLENUM
      ACCNTC=0.
      ACCVL1=ACCNTC+ACCVLC
      DELND1=ACCVL1/PY/(RFCOLD*RFCOLD-RFIN*RFIN)
      NODELC=CLDNOD+DELND1
      CLDSTK=CLDSTK+NODELC
      ACCVL3=ACCVL3+ACCVL1
C
C   HOT LENGHTS
C
      ACCVL4=ABS( CRKV05+DSHV03+CTRV03+PORV03 )
      IF(SUMAF .GT. 0.) GO TO 130
         ACCNTH=ABS(VACC1*RATIO1)
      GO TO 135
```

```
  130 CONTINUE
          ACCNTH=ACCVL4
  135 CONTINUE
      ACCVL5=ACCNTH+ACCVLH
      DELND2=ACCVL5/PY/(RF*RF-RFIN*RFIN)
      NODELH=HOTNOD+DELND2
      HOTSTK=HOTSTK+NODELH
      ACCVL6=ACCVL6+ACCVL5
C
C   CALCULATE UPDATED (COLD) VOLUME ACCOMMODATION FRACTIONS
C
      SUMACC=CRKV01+DSHNTC+CTRNTC+PORNTC
      IF(SUMACC .GT. 0.) GO TO 140
         CVAF0=0.
         DVAF0=0.
         VVAF0=0.
         OPVAF0=0.
         VFRAC=0.
      GO TO 145
  140 CONTINUE
         CVAF0=CRKV01/SUMACC
         DVAF0=DSHNTC/SUMACC
         VVAF0=CTRNTC/SUMACC
         OPVAF0=PORNTC/SUMACC
         VFRAC=SUMACC/VFUEL(IAX)
  145 CONTINUE
C
C   NODAL VOID VOLUMES
C
      NETVLC=GAPVC+CRKV01+DSHNTC+VCHAM+CTRNTC+PORNTC+OPVL01
      NETVLH=GAPVH+CRKV04+DSHNTH+VCHAM+CTRNTH+PORNTH
      IF(IDD.GE.2) WRITE(NCH,26) VOVTPG,CVLCVT,VDSHVT,VCHVT,
     -VCTRVT,NETVLH,NETVLC
      IF(NAX.GT.1)CALL PUT(MEMORY,NMEM,-4,IAX)
      CALL GPED1(TIME,TIME0,IAX,
     #EFFVOL,VOLCLD,FFGREL,CRKV01,CRODHT,DSHTMP,HRODHT,TF1,
     #HOTSTK,TAVG1,CTRNTH,CTRTMP,GAPVC,DSHNTC,VCHAM,PORNTC,NAX,
     #CTRNTC,PLNVLC,CLDSTK,CRKV04,PORNTH,DSHNTH,GAPVH,BUT,
     +GAPTEM,CRKTMP,PLENVO,
     +PLENT,PI,PICLD,1,GTOT,RABU,TPOW)
 1000  CONTINUE
       S3=PY*RCI1*RCI1
       S1=PY*RCI1*RCI1
       S4=PY*RCLADC*RCLADC
C
C   CALCULATE HOT ROD PRESSURE
C
       HOTPLN=HRODHT-STAKLH
C
C
C  TEST ON INSTANTANEOUS HOT PLENUM LENGTH
C
       IF(HOTPLN .GT. 0.) GO TO 150
       WRITE(NCH,14)
 14    FORMAT(1X,'IN SUBROUTINE PGAS --',
      1       'HOT FUEL STACK LENGTH EXCEEDS HOT CLAD LENGTH')
       STOP
   150 CONTINUE
C*********************************************************************
C
C
C  LIQUID BONDED CODE CHANGES
```

```
C
C  THIS RATIOS THE SPRING VOLUME BY THE AMOUNT OF THE PLENUM LIQUID FILLED
C
C      IF(NBOND) THEN
C         IF(VLBANN.LT.VLBCOLD) THEN
C            PLENVO=HOTPLN*S1+PLNVL1*VLBANN/VLBCOLD-ACCVL6
C         ELSE
C            PLENVO=HOTPLN*S1+PLNVL1-ACCVL6
C         ENDIF
C      ELSE
C         PLENVO=HOTPLN*S1+PLNVL1-ACCVL6
C      ENDIF
C*********************************************************************
      S2=2.*PY*HOTPLN*RCI1
      PLENT=(S1*TAVG11+S2*TCI11+S3*TCI11)/(S1+S2+S3)
C*********************************************************************
C
C  LIQUID BONDED CODE CHANGES
C
C
      IF(NBOND) THEN
        VOLDIFF=VLBCOLD-VLBHOT
        XLDIFF=VOLDIFF/(PY*(RCIOUT**2-(RCIOUT-TG)**2))
        IF((XXLIQ+XLDIFF).GE.STHEGT) THEN
          DO 6262 I=1,NAX
          IWET(I)=1
 6262     CONTINUE
          XTOTOP=STHEGT-XLLIQ
          VOLTOTOP=XTOTOP*PY*(RCIOUT**2-(RCIOUT-TG)**2)
          VOLINPL=VOLDIFF-VOLTOTOP
          PLENVO=HOTPLN*S1+PLNVL1-VOLINPL-ACCVL6
          XLLIQ=STEGT
        ELSE
          XLLIQ=XLLIQ+XLDIFF
          DO 6263 I=1,NAX
          IF(I*STHEGT/NAX.LE.XLLIQ) THEN
            IWET(I)=1
          ELSE
            IWET(I)=0
          ENDIF
 6263     CONTINUE
          PLENVO=HOTPLN*S1+PLNVL1-ACCVL6
        ENDIF
      ELSE
          PLENVO=HOTPLN*S1+PLNVL1-ACCVL6
      ENDIF
C
C*********************************************************************
      SUMVLH=GAPV02+CRKV06+DSHV04+CHMV02+CTRV04+PORV04
     '      +GFPTH
      EFFVOL=SUMVLH*PLENT+PLENVO
      PI=R*GTOT*PLENT/EFFVOL
C
C   CALCULATE COLD ROD PRESSURE
C
      CLDPLN=CRODHT-STAKLC
      PLNVLC=CLDPLN*S4+PLNVL1-ACCVL3
      SUMVLC=GAPV01+CRKV03+DSHV02+CHMV01+CTRV02+PORV02+OPVL02
     '      +GFPTC
      VOLCLD=SUMVLC+PLNVLC
      PICLD=R*GTOT*298/VOLCLD
      DP=PI-PO
```

```
C
C  LOAD PREVIOUS GAS FRACTIONS INTO /GAP/
C
      DO 17 I=1,5
   17 PREVC(I)=C(I)
C
      C(1)=XMGAS(1)/GTOT
      C(3)=XMGAS(3)/GTOT
      C(4)=XMGAS(4)/GTOT
      C(2)=(XGAS(2)*GHTOT+MSUM*XEFRAC)/GTOT
      C(5)=(XGAS(5)*GHTOT+MSUM*(1.-XEFRAC))/GTOT
      IF(C(1).LT.0.) C(1)=0.
      IF(IDD.GE.1) WRITE(NCH,26) TF1,TCI1,TFAVG,TAVG1,
     -AFF,TAVGC,ATCC,PLENVO,GAPVH,GAPTEM,CRKV04,
     +CRKTMP,(C(I),I=1,5),DP,PI,PO,HOTSTK,HRODHT,HOTPLN,S1,S2,
     +PLENT,PVOPT,(XGAS(I),I=1,5)
      CALL GPED1(TIME,TIME0,NAX,
     #EFFVOL,VOLCLD,FFGREL,CRKV01,CRODHT,DSHTMP,HRODHT,TF1,
     #HOTSTK,TAVG1,CTRNTH,CTRTMP,GAPVC,DSHNTC,VCHAM,PORNTC,NAX,
     #CTRNTC,PLNVLC,CLDSTK,CRKV04,PORNTH,DSHNTH,GAPVH,BUT,
     +GAPTEM,CRKTMP,PLENVO,
     +PLENT,PI,PICLD,2,GTOT,RABU,TPOW)
      RETURN
      END
```

SUBROUTINE SFILE SOURCE CODE LISTING

```
      SUBROUTINE SFILE(IDD,IDDD,PTIME,SPTIME,NOGO,NOGASR,
     +NOMELT,NOAUXP,
     +NORELO,NOCREP,CONT,NAX,DTLIM,STHEGT,PIFAB,FLXMUL,
     +PLVFAB,CROUGH,SYAUI,COXY,CFE,CTANN,CLADL,
     +APSI,OVALTY,ECCENT,IFIRST,RSTRT,RCOFAB,RCIFAB,
     +XGAS,HEABS,PCTPWR,RPFMUL,AASMUL,ENGIN,
     +JAS,JRINGS,TORBU,CTORBU,CHIN,TCOIN,ZIRC,KKKCH,JTCO,JSTK,
     +HBOIL,HCONV,PLNVL1,OXSW,JVDFR)
      LOGICAL IA2(32),CONT,RSTRT,IFIRST,DEFALT,BTCH,DAYS,NOGO,
     +NOGASR,NORELO,NOCREP,NOMELT,NOAUXP
      CHARACTER*4 A1
C     INTEGER A1
      DIMENSION XGAS(5)
C-2.6QF I/O ENHANCEMENT CHANGE TYPE FOR TITLE
      COMMON /ROD/ TITLE(10),IDAY,ITYM,IVERS
C
C  LIQUID BONDED CODE CHANGES ARE DELIMITED BY ********
C
C*********************************************************************
C
C
      COMMON /BOND/ NBOND,BONDCOND,VLBCOLD,BONDEXP,NPAD,XLLIQ,FRACFIL,
     +IWET(50)
      LOGICAL NBOND,NPAD
C*********************************************************************
C
      CHARACTER*10 IDAY,ITYM
      CHARACTER*8 TITLE
      CHARACTER*4 IVERS
C     REAL IDAY,ITYM
      CHARACTER*8 DUMMY(10)
C     DIMENSION DUMMY(10)
      COMMON/EDIT/IXCH(20),ENGOUT,TAB1,TAB2,TAB3,TAB4,TAB5,TAB6,TAB7,
     +TAB8,TAB9,TAB0,SPRNT,DAYS,ITC1,ITC2
      LOGICAL TAB1,TAB2,TAB3,TAB4,TAB5,TAB6,TAB7,TAB8,TAB9,TAB0
     +,SPRNT,TDENS
      COMMON/GRODAT/K0,GE,PTH,PZ,PR
      REAL K0
      COMMON/GASDAT/F101(9),FGRIN,RELFAC
      COMMON/SWLDAT/SWLDT(11),TDENS
      LOGICAL ENGIN,ENGOUT,TORBU,CTORBU,CHIN,TCOIN
      DIMENSION AB(50)
      COMMON/IFILE/ICH,JCH,KCH,LCH,MCH,NCH,NNCH
CREV1.3 REVISION FOR FORTRAN77
      CHARACTER*4 ITEST,IWORD
      CHARACTER*4 F1,F2,F3,F4,F5,F6,F7,F8,F9,F10,F11,F12,F13,F14,B1,B2
     +  ,B3,B4,B5,B6,B7,B8
C     INTEGER F1,F2,F3,F4,F5,F6,F7,F8,F9,F10,F11,F12,F13,F14,B1,B2,B3
C    +  ,B4,B5,B6,B7,B8
      CHARACTER*4 XXX(20),XTXTX
C     DIMENSION XXX(20)
      CHARACTER*4 RCHAR(2)
C     INTEGER RCHAR(2)
      DATA RCHAR /'HRS ','DAYS'/
      DATA XTXTX/'$$$$'/
      DATA F14/'KSI '/
      DATA F1,F2,F3,F4,F5,F6,F7,F8,F9,F10,F11,F12,F13
     +/'IN  ','CM  ','PSIA','MPA ','IN3 ','CM3 ','M   ',
     +'W/CM','2/C ','BTU/','HR/F','T2/F','    '/
      DATA ITEST/'****'/
      DATA AB,ECV,G1,G2,G3,G4,G5,PY,SDD,SPL,SPV,XAB /61*0./
      DATA IAB,IDUM,IEN,JAB,JJJCH /5*0/
```

```
      DATA BTCH,DEFALT,IA2 /34*.FALSE./
C INPUT ECHO IS MOVED FROM CHANNEL JJJCH TO NCH
      JJJCH=NCH
      ICTR=0
C
C     READ IN THE MODE THAT INFORMATION WILL BE FEED IN.
C     IF BTCH = TRUE THAN THIS WILL BE A BATCH JOB,
C     IF BTCH = FALSE THAN THIS JOB WILL BE RUN FROM A TERMINAL.
      IF(.NOT.IFIRST) GO TO 557
C
   64 READ(5,101,END=65) DUMMY
      WRITE(MCH,101) DUMMY
      GO TO 64
   65 REWIND MCH
 4100 READ(MCH,4081,END=999) XXX
      ICTR=ICTR+1
      IF(XXX(1) .EQ. XTXTX) GO TO 4100
      REWIND 50
      WRITE(50,4081) XXX
      REWIND 50
      READ(50,558) BTCH,ITC1,ITC2
  558 FORMAT(L1,2I3)
      IF(BTCH) NNCH=NCH
      IF(BTCH) GO TO 90
      DO 100  I=1,32
100   IA2(I)=.FALSE.
      WRITE(NNCH,1000)
1000  FORMAT(' IS THIS A DEFAULT OPTION RUN (T/F)?')
      READ(NNCH,1004) DEFALT
C-2.6QF I/O REVIS NEXT 8 LINESIONS
      IF(DEFALT) IA2(1)=.TRUE.
      IF(DEFALT) IA2(2)=.TRUE.
      IF(DEFALT) IA2(6)=.TRUE.
      IF(DEFALT) IA2(9)=.TRUE.
      IF(DEFALT) WRITE(NNCH,1001)
1001  FORMAT(' DEFAULT OPTIONS IN EFFECT',/,
     +' NO DIAGNOSTICS',/,
     +' INPUT IS IN ENGINEERING UNITS',/,
     +' OUTPUT IS IN ENGINEERING UNITS',/,
     +' POWER HISTORY IS INPUT VERSUS BURNUP',/,
     +' PERCENT POWER CHANGES TIME NOT BURNUM',/,
     +' COOLANT HEAT TRANSFER COEFFICIENTS ARE CALCULATED INTERNALLY',/,
     +' CLAD SURFACE TEMPS ARE INPUT VERSUS NODE AND TIME',/,
     +' NO EDITED TABLES ARE GENERATED',/,
     +' STANDARD OUTPUT IS AT EACH CALCULATED TIME STEP',/,
     +' SWELLING IS TEMPERATURE DEPENDENT',/,
     +' CLAD OXIDATION MODEL FOR PWR IS BEING USED',/,
     +' TABULAR OUTPUT BEING PRODUCED')
      IF(DEFALT) GO TO 1008
      WRITE(NNCH,1002)
 1002 FORMAT(' ANSWER YES(T)/NO(F)')
C-2.6QF I/O REVISIONS NEXT 4 LINES.
      WRITE(NNCH,1013)
 1013 FORMAT(' NO GAS RELEASE:T/F')
      READ(NNCH,1004) IA2(14)
      WRITE(NNCH,1003)
 1003 FORMAT(' TIME IS INPUT IN DAYS:T/F')
      READ(NNCH,1004) IA2(11)
1004  FORMAT(L1)
      WRITE(NNCH,1005)
 1005 FORMAT(' STOP AFTER WRITING INPUT:T/F')
      READ(NNCH,1004)IA2(13)
```

```
      WRITE(NNCH,1015)
 1015 FORMAT(' NO RELOCATION ALLOWED:T/F')
      READ(NNCH,1004) IA2(16)
      WRITE(NNCH,1017)
 1017 FORMAT(' NO STANDARD PRINTOUT:T/F')
      READ(NNCH,1004)IA2(32)
      WRITE(NNCH,1018)
 1018 FORMAT(' OXIDE BASED ON:T-BWR/F-PWR')
      READ(NNCH,1004)IA2(10)
      WRITE(NNCH,1021)
 1021 FORMAT(' NO POWER TO MELT CALCULATION:T/F')
      READ(NNCH,1004)IA2(21)
      WRITE(NNCH,1020)
 1020 FORMAT(' NO AUXILIARY POWER CALCULATION:T/F')
      READ(NNCH,1004)IA2(22)
      WRITE(NNCH,1006)
 1006 FORMAT(' SHORT DIAG:T/F')
      READ(NNCH,1004) IA2(4)
      WRITE(NNCH,1007)
 1007 FORMAT(' LONG DIAG:T/F')
      READ(NNCH,1004) IA2(12)
      WRITE(NNCH,1101)
 1101 FORMAT('  INPUT IN ENGINEERING UNITS:T/F')
      READ(NNCH,1004) IA2(1)
      WRITE(NNCH,1102)
 1102 FORMAT('  OUTPUT IN ENGINEERING UNITS:T/F')
      READ(NNCH,1004) IA2(2)
      WRITE(NNCH,1103)
 1103 FORMAT(' POWER HISTORY IS VERSUS TIME(NOT BURNUP): T/F')
      READ(NNCH,1004) IA2(5)
      WRITE(NNCH,1104)
 1104 FORMAT(' PERCENT POWER CHANGES TIME NOT BURNUP:T/F')
      READ(NNCH,1004) IA2(6)
      WRITE(NNCH,1105)
 1105 FORMAT(' COOLANT HEAT TRANS COEF FOR CONV AND BOIL ARE INPUT:T/F')
      READ(NNCH,1004) IA2(7)
      WRITE(NNCH,1106)
 1106 FORMAT(' CLAD SURF TEMPS ARE INPUT VERSUS NODE AND TIME:T/F')
      READ(NNCH,1004) IA2(8)
C  VARIABLES THAT ARE NOT BEING INPUT BUT HAVE DEFAULT VALUES ARE:
      WRITE(NNCH,1107)
 1107 FORMAT(' CREATE TABLE 1,TEMPERATURE SUMMARY:T/F')
      READ(NNCH,1004) IA2(23)
      WRITE(NNCH,1108)
 1108 FORMAT(' CREATE TABLE 2,DETAILED TEMPERATURE DISTRIBUTION:T/F')
      READ(NNCH,1004) IA2(24)
      WRITE(NNCH,1109)
 1109 FORMAT(' CREATE TABLE 3,GAP CONDUCTANCE:T/F')
      READ(NNCH,1004) IA2(25)
      WRITE(NNCH,1110)
 1110 FORMAT(' CREATE TABLE 4,FISSION GAS RELEASE:T/F')
      READ(NNCH,1004) IA2(26)
      WRITE(NNCH,1111)
 1111 FORMAT(' CREATE TABLE 5,INTERNAL GAS PRESSURE:T/F')
      READ(NNCH,1004) IA2(27)
      WRITE(NNCH,1112)
 1112 FORMAT(' CREATE TABLE 6,FUEL DIMENSION CHANGES:T/F')
      READ(NNCH,1004) IA2(28)
      WRITE(NNCH,1113)
 1113 FORMAT(' CREATE TABLE 7,CLAD DIMENSION CHANGES:T/F')
      READ(NNCH,1004) IA2(29)
      WRITE(NNCH,1114)
```

```
 1114 FORMAT(' SHORTEN OUTPUT TO INCLUDE ONLY INPUT TIME STEPS:T/F')
      READ(NNCH,1004) IA2(17)
      WRITE(NNCH,1115)
 1115 FORMAT(' SWELLING IS TEMPERATURE DEPENDENT:T/F')
      READ(NNCH,1004) IA2(9)
      WRITE(NNCH,1116)
 1116 FORMAT(' CLAD OXIDATION MODEL:T=BWR/F=PWR')
      READ(NNCH,1004) IA2(10)
C  COXY  =.001
C  SYA   =137900000.
C  CFE   =-101.
C  CTANN =-101.
C SYAUI IS UNIRRADIATED YIELD STRENGTH AT ROOM TEMPERATURE
C  OVALTY=-101.
C  ECCENT=-101.
C-2.6QF I/O REV. NEXT LINE
C
C ******************************************************
C * THE FOLLOWING LINES HAVE BEEN COMMENTED OUT BECAUSE *
C * THEY FORM A REGION OF CODING WHICH IS UNREACHABLE   *
C ******************************************************
C
C      GOTO 1008
C1257  WRITE(NNCH,1009)
C1009  FORMAT(' RUN TO BE CONTINUED?-T/F')
C      READ(NNCH,1004) IA2(3)
C      WRITE(NNCH,1010)
C1010  FORMAT(' RESTART?-T/F')
C      READ(NNCH,1004) IA2(18)
1008  CONTINUE
      READ(MCH,1019) IDUM
      GO TO 1012
90    CONTINUE
 4101 READ(MCH,4081,END=999) XXX
      ICTR=ICTR+1
      IF(XXX(1) .EQ. XTXTX) GO TO 4101
      REWIND 50
      WRITE(50,4081) XXX
      REWIND 50
      READ(50,1011) (IA2(I),I=1,32)
1011  FORMAT(32L2)
1012  CONTINUE
      ENGIN=IA2(1)
      ENGOUT=IA2(2)
      TORBU=IA2(5)
      CTORBU=IA2(6)
      CHIN=IA2(7)
      TCOIN=IA2(8)
      OXSW=0.
      IF(IA2(10)) OXSW=1.
      CONT=IA2(3)
      NOGO=IA2(13)
      DAYS=IA2(11)
      NOGASR=IA2(14)
      NORELO=IA2(15)
      NOCREP=IA2(16)
      NOMELT=IA2(21)
      NOAUXP=IA2(22)
      TAB1=IA2(23)
      TAB2=IA2(24)
      TAB3=IA2(25)
      TAB4=IA2(26)
```

```
      TAB5=IA2(27)
      TAB6=IA2(28)
      TAB7=IA2(29)
      TAB8=IA2(30)
      TAB9=IA2(31)
      TAB0=IA2(32)
C TAB9 IS NOT BEING USED YET
      RSTRT=IA2(18)
      SPRNT=IA2(17)
      TDENS=IA2(9)
C*********************************************************************
C
C.. LIQUID BONDED FUEL OPTION
C
      NBOND=IA2(19)
      IF(NBOND) THEN
C
C
C  LEAD, BISMUTH, TIN EUTECTIC
C
      BONDCOND=12.333/.5778
      BONDEXP=0.
      ENDIF
      NPAD=IA2(20)
C*********************************************************************
C
C.. FOUT=SHORT FIXED FORMAT OUTPUT FOR EXTRACT
C.. OPTION TO WRITE FOUT IN BINARY FOR FASTER READING & WRITING
C
      IDD=0
      IF(IA2(4).OR.IA2(12)) IDD=1
      IF(IA2(12)) IDD=2
      IDDD=IDD
      PTIME=0.
      SPTIME=0.
      IF(IDD .GT. 0) GO TO 1022
 4102 READ(MCH,4081,END=999) XXX
      ICTR=ICTR+1
      IF(XXX(1) .EQ. XTXTX) GO TO 4102
      REWIND 50
      WRITE(50,4081) XXX
      REWIND 50
      READ(50,1019) IDUM
 1022 CONTINUE
C DUMMY FORMAT FOR SKIPPING A RECORD
 1019 FORMAT(55X,I1)
      IF(IDD.LE.0)GOTO 500
      IF(BTCH) GO TO 555
      WRITE(NNCH,256)
256   FORMAT(' INPUT BEGINNING AND ENDPOINT OF PRINT INTERVAL-2F10.3')
      READ(NNCH,257) PTIME,SPTIME
 4103 READ(MCH,4081,END=999) XXX
      ICTR=ICTR+1
      IF(XXX(1) .EQ. XTXTX) GO TO 4103
      REWIND 50
      WRITE(50,4081) XXX
      REWIND 50
      READ(50,558) BTCH
257   FORMAT(2F10.3)
      GO TO 556
555   CONTINUE
 4104 READ(MCH,4081,END=999) XXX
```

```
      ICTR=ICTR+1
      IF(XXX(1) .EQ. XTXTX) GO TO 4104
      REWIND 50
      WRITE(50,4081) XXX
      REWIND 50
      READ(50,255) PTIME,SPTIME
255   FORMAT(2F10.3)
556   CONTINUE
500   CONTINUE
      IF(IDD.GE.1)WRITE(NNCH,25)PTIME,SPTIME
25    FORMAT(1X,2F10.3)
C
C.. READ & WRITE TITLE OF INPUT FILE
557   CONTINUE
1     FORMAT(1X,20A4)
 4105 READ(MCH,4081,END=999) XXX
      ICTR=ICTR+1
      IF(XXX(1) .EQ. XTXTX) GO TO 4105
      REWIND 50
      WRITE(50,4081) XXX
      REWIND 50
      READ(50,101) TITLE
  101 FORMAT(10A8)
2     FORMAT(1X,20A4)
C THIS IS THE START OF THE INPUT ECHO
      CALL RDOUT2(JJJCH)
      WRITE(JJJCH,4001) TITLE,IVERS,IDAY,ITYM
      WRITE(JJJCH,4056)
      REWIND MCH
 5001 CONTINUE
      DO 5002 JCT=1,50
      READ(MCH,101,END=7) DUMMY
 5002 WRITE(JJJCH,4055) DUMMY
      CALL RDOUT1(NCH)
      WRITE(JJJCH,4001) TITLE,IVERS,IDAY,ITYM
      WRITE(JJJCH,4056)
      GO TO 5001
    7 REWIND MCH
      DO 8 I=1,ICTR
    8 READ(MCH,101) DUMMY
    9 CONTINUE
C
C.. READ NUMBER OF AXIAL NODES IN THIS DATA SET
 4106 READ(MCH,4081,END=999) XXX
      IF(XXX(1) .EQ. XTXTX) GO TO 4106
      REWIND 50
      WRITE(50,4081) XXX
      REWIND 50
      READ(50,12) NAX,JAS,JRINGS,JTCO,JVDFR
   12 FORMAT(20I4)
      IF(JRINGS.LE.0.OR.JRINGS.GT.20) JRINGS=10
      IF(JAS.LE.0) JAS=1
13    FORMAT(' NUMBER AXIAL NODES =',I3)
C
C.. READ UPPER LIMIT ON TIME STEP SIZE
 4107 READ(MCH,4081,END=999) XXX
      IF(XXX(1) .EQ. XTXTX) GO TO 4107
      REWIND 50
      WRITE(50,4081) XXX
      REWIND 50
      READ(50,113) DTLIM
  113 FORMAT(E13.5)
```

```
      IF(DTLIM.LE.0.)DTLIM=480.
      IF(IDD.GE.1)WRITE(NCH,1437) DTLIM
1437  FORMAT(' DTLIM=',E15.7)
C
C.. IF THIS IS A CONTINUATION RUN, SKIP FUEL PARAMETER READING
      IF(RSTRT)GOTO 20
C
C.. SET POINTER AT
C.. LINE FOLLOWING NEXT LINE WITH '****' AS LEFT-MOST FOUR CHARACTERS
  135 READ(MCH,4081,END=999) XXX
      IF(XXX(1) .EQ. XTXTX) GO TO 135
      REWIND 50
      WRITE(50,4081) XXX
      REWIND 50
      READ(50,114) IWORD
  114 FORMAT(20A4)
      IF(IWORD.NE.ITEST)GOTO 135
      IF(IDD.GE.2)WRITE(NCH,2) IWORD
C
C.. READ INPUT FUEL ROD PARAMETERS
3     FORMAT(1X,E13.5)
      IF(JSTK.LT.1) GO TO 5
      DO 35 KAB=1,2
   35 READ(KKKCH,REC=KAB) (AB(25*(KAB-1)+KKAB),KKAB=1,25)
C  35 READ(KKKCH'NREC) (AB(25*(KAB-1)+KKAB),KKAB=1,25)
    5 READ(MCH,4081,END=999) XXX
      IF(XXX(1) .EQ. XTXTX) GO TO 5
      REWIND 50
      WRITE(50,4081) XXX
      REWIND 50
      READ(50,103) IAB,IEN,JAB,(AB(JAB-1+KAB),KAB=1,IAB)
      IF(IEN) 5,5,6
    6 CONTINUE
      CALL RDOUT1(NCH)
      WRITE(JJJCH,4001) TITLE,IVERS,IDAY,ITYM
      WRITE(JJJCH,4041)
      IF(BTCH) WRITE(JJJCH,4021)
      IF(.NOT.BTCH) WRITE(JJJCH,4022)
      WRITE(JJJCH,4042) NAX
      IF(ENGIN) WRITE(JJJCH,4023)
      IF(.NOT.ENGIN) WRITE(JJJCH,4025)
      WRITE(JJJCH,4043) JRINGS
      IF(ENGOUT) WRITE(JJJCH,4024)
      IF(.NOT.ENGOUT) WRITE(JJJCH,4026)
C*********************************************************************
C
C  LIQUID BONDED CODE CHANGES
C
      IF(NBOND) WRITE(JJJCH,6666)
 6666 FORMAT(T5,' LIQUID BONDED FUEL')
      IF(.NOT.NBOND) WRITE(JJJCH,6667)
 6667 FORMAT(T5,' GAS BONDED FUEL')
      IF(.NOT.NBOND) THEN
      IF(NPAD) WRITE(JJJCH,6669)
 6669 FORMAT(T5,' PAD GAP CONDUCTANCE MODEL')
      IF(.NOT.NPAD) WRITE(JJJCH,6670)
 6670 FORMAT(T5,' ESCORE GAP CONDUCTANCE MODEL')
      ENDIF
C*********************************************************************
C
      WRITE(JJJCH,4044) JAS
      A1 = RCHAR(1)
```

```
      IF(DAYS) A1 = RCHAR(2)
      IF(TORBU) WRITE(JJJCH,4031)A1
      IF(.NOT.TORBU)WRITE(JJJCH,4030)A1
      IF(TCOIN) WRITE(JJJCH,4045) JTCO
      IF(CTORBU) WRITE(JJJCH,4032)
      IF(.NOT.CTORBU) WRITE(JJJCH,4033)
      IF(TAB8)WRITE(JJJCH,4082) JVDFR
      IF(RSTRT) WRITE(JJJCH,4027)
      IF(IDD-1)4810,4811,4812
 4812 WRITE(JJJCH,4029)
      GO TO 4813
 4811 WRITE(JJJCH,4028)
 4813 WRITE(JJJCH,4047) PTIME,SPTIME
 4810 CONTINUE
      IF(NOGO) WRITE(JJJCH,4034)
      IF(NOGASR)WRITE(JJJCH,4037)
      IF(NORELO)WRITE(JJJCH,4038)
      IF(NOCREP)WRITE(JJJCH,4036)
      IF(NOMELT)WRITE(JJJCH,4078)
      IF(NOAUXP)WRITE(JJJCH,4079)
      IF(CHIN) WRITE(JJJCH,4040)
      IF(TCOIN) WRITE(JJJCH,4039)
      IF(.NOT.TCOIN) WRITE(JJJCH,4054)
      WRITE(JJJCH,4046) DTLIM
      IF(SPRNT) WRITE(JJJCH,4065)
      IF(TDENS) WRITE(JJJCH,4067)
      IF(.NOT.TDENS) WRITE(JJJCH,4068)
      IF(OXSW.EQ.1.) WRITE(JJJCH,4076)
      IF(OXSW.EQ.0.) WRITE(JJJCH,4077)
      IF(TAB8)WRITE(JJJCH,4083)
      IF(.NOT.TAB8)WRITE(JJJCH,4084)
      IF(.NOT.(TAB1.OR.TAB2.OR.TAB3.OR.TAB4.OR.TAB5.OR.TAB6.OR
     +.TAB7.OR.TAB8.OR.TAB9.OR.TAB0)) GO TO 4815
      WRITE(JJJCH,4057)
      IF(TAB1) WRITE(JJJCH,4058)
      IF(TAB2) WRITE(JJJCH,4059)
      IF(TAB3) WRITE(JJJCH,4060)
      IF(TAB4) WRITE(JJJCH,4061)
      IF(TAB5) WRITE(JJJCH,4062)
      IF(TAB6) WRITE(JJJCH,4063)
      IF(TAB7) WRITE(JJJCH,4064)
 4815 CONTINUE
      WRITE(JJJCH,4002)
      IF(ENGOUT) GO TO 4801
      B1=F2
      B2=F7
      B3=F6
      B4=F4
      B5=F8
      B6=F9
      B7=F13
      B8=F4
      IF(ENGIN .AND. ENGOUT) GO TO 4807
      IF((.NOT. ENGIN) .AND. (.NOT. ENGOUT)) GO TO 4807
      G1=2.54
      G2=.0254
      G3=16.38706
      G4=.00689465
      G5=.0005677
      G6=6.89465
      GO TO 4803
 4801 B1=F1
```

```
      B2=F1
      B3=F5
      B4=F3
      B5=F10
      B6=F11
      B7=F12
      B8=F14
      IF(ENGIN .AND. ENGOUT) GO TO 4807
      IF((.NOT. ENGIN) .AND. (.NOT. ENGOUT)) GO TO 4807
      G1=.3937008
      G2=39.37008
      G3=.0610237
      G4=145.04
      G5=1761.493
      G6=0.14504
      GO TO 4803
 4807 G1=1.
      G2=1.
      G3=1.
      G4=1.
      G5=1.
      G6=1.0
 4803 CONTINUE
      IF(AB(16).EQ.1.) WRITE(JJJCH,4069) AB(16)
      IF(AB(16).EQ.2.) WRITE(JJJCH,4070) AB(16)
      IF(AB(16).EQ.3.) WRITE(JJJCH,4003) AB(16)
      IF(AB(16).EQ.4.) WRITE(JJJCH,4071) AB(16)
      IF((AB(16).NE.1.).AND.(AB(16).NE.2.).AND.(AB(16).NE.3.).AND.
     +(AB(16).NE.4)) GO TO 600
      GO TO 602
  600 WRITE(JJJCH,601)
  601 FORMAT(' *** FATAL ERROR -- SUBR. SFILE -- ILLEGAL CLAD TYPE ***')
      STOP
  602 CONTINUE
      WRITE(JJJCH,4015)
      XAB=G1*AB(3)
      WRITE(JJJCH,4005) B1,XAB
      WRITE(JJJCH,4016) AB(6)
      XAB=G1*AB(4)
      WRITE(JJJCH,4006) B1,XAB
      WRITE(JJJCH,4017) AB(7)
      XAB=G2*AB(2)
      WRITE(JJJCH,4007) B2,XAB
      WRITE(JJJCH,4018) AB(8)
      XAB=G2*AB(1)
      WRITE(JJJCH,4008) B2,XAB
      WRITE(JJJCH,4019) AB(9)
      XAB=G1*AB(11)
      WRITE(JJJCH,4009) B1,XAB
       WRITE(JJJCH,4020)
      XAB=G1*AB(12)
      WRITE(JJJCH,4010) B1,XAB
      WRITE(JJJCH,4048) AB(10)
      XAB=G3*AB(13)
      WRITE(JJJCH,4011) B3,XAB
      XAB=G3*AB(14)
      WRITE(JJJCH,4012) B3,XAB
      WRITE(JJJCH,4049) AB(17)
      XAB=G2*AB(15)
      WRITE(JJJCH,4013) B2,XAB
      WRITE(JJJCH,4050) AB(18)
      XAB=G4*AB(5)
```

```
      WRITE(JJJCH,4014) B4,XAB
      WRITE(JJJCH,4051) AB(19)
      WRITE(JJJCH,4072) AB(25)
      WRITE(JJJCH,4066) AB(20)
      XAB=G6*AB(26)
      WRITE(JJJCH,4073) B8,XAB
C*********************************************************************
C
C   LIQUID BOND CODE CHANGES
C   FOR PARTIAL FILL OF LIQUID METAL
C
      IF(NBOND) THEN
      WRITE(JJJCH,5073) AB(29)
 5073 FORMAT(10X,'LIQUID BOND FILL FRACTION',F10.4)
      FRACFIL=AB(29)
      ENDIF
C*********************************************************************
C
      IF(AB(16).EQ.4.) WRITE(JJJCH,4074) K0
      IF(AB(16).EQ.4.) WRITE(JJJCH,4075) GE
      FGRIN=AB(27)
      IF(FGRIN .LE. 0.) GO TO 4086
          WRITE(JJJCH,4080) FGRIN
4080      FORMAT(10X,'INPUT FISSION GAS RELEASE PERCENT',
     1          T50,F10.4)
          TAB4=.FALSE.
 4086 CONTINUE
      IF(.NOT. NOGASR) GO TO 4085
          FGRIN=-1.0
          TAB4=.FALSE.
 4085 CONTINUE
      XAB=G5*AB(21)
      IF(CHIN) WRITE(JJJCH,4052) B5,B6,B7,XAB
      XAB=G5*AB(22)
      IF(CHIN) WRITE(JJJCH,4053) B5,B6,B7,XAB
C THIS WRITE IS FOR NEXT PAGE(NODAL PARAMETERS)
      CALL RDOUT1(NCH)
      WRITE(JJJCH,4001)TITLE,IVERS,IDAY,ITYM
 4001 FORMAT(' ',///,' ',10A8,2X,'ESCORE VERS:',1X,A4,2X,'DATE:',
     +A10,'TIME:',A10,//)
 4002 FORMAT(///,5X,'WHOLE ROD FUEL FABRICATION DATA',/,5X,32('-'),//)
 4003 FORMAT(10X,'CLAD TYPE',10X,'ZIRCALOY-2',T50,F10.4)
 4005 FORMAT(10X,'CLAD OD,',A4,T50,F10.4)
 4006 FORMAT(10X,'CLAD ID,',A4,T50,F10.4)
 4007 FORMAT(10X,'CLAD LENGTH,',A4,T50,F10.4)
 4008 FORMAT(10X,'ACTIVE FUEL LENGTH,',A4,T50,F10.4)
 4009 FORMAT(10X,'TOTAL SPACER LENGTH,',A4,T50,F10.4)
 4010 FORMAT(10X,'SPACER OD,',A4,T50,F10.4)
 4011 FORMAT(10X,'SPRING VOLUME,',A4,T50,F10.4)
 4012 FORMAT(10X,'END CAP VOLUME,',A4,T50,F10.4)
 4013 FORMAT(10X,'CLAD SURFACE ROUGHNESS,MICRO',A4,T50,F10.4)
 4014 FORMAT(10X,'COLD ROD INTERNAL PRESSURE,',A4,T50,F10.4)
 4015 FORMAT('+',T80,'FILL GAS COMPOSITION,MOLE FRACTION')
 4016 FORMAT('+',T85,'HELIUM',T110,F10.5)
 4017 FORMAT('+',T85,'NITROGEN',T110,F10.5)
 4018 FORMAT('+',T85,'ARGON',T110,F10.5)
 4019 FORMAT('+',T85,'XENON',T110,F10.5)
 4020 FORMAT('+',T80,'HELIUM ABSORBTION COEFFICIENT,')
 4021 FORMAT(T5,' THIS IS A BATCH JOB')
 4022 FORMAT(T5,' THIS IS AN INTERACTIVE JOB')
 4023 FORMAT(T5,' ENGLISH UNITS ARE USED FOR INPUT')
 4024 FORMAT(T5,' ENGLISH UNITS ARE USED FOR OUTPUT')
```

```
 4025 FORMAT(T5,' STANDARD INTERNATIONAL UNITS ARE USED FOR INPUT')
 4026 FORMAT(T5,' STANDARD INTERNATIONAL UNITS ARE USED FOR OUTPUT')
 4027 FORMAT(T5,' A RESTART FILE WILL BE GENERATED')
 4028 FORMAT(T5,' A SHORT DIAGNOSTIC FILE IS CREATED')
 4029 FORMAT(T5,' A LONG DIAGNOSTIC FILE IS CREATED')
 4030 FORMAT(T5,' POWER HISTORY IS INPUT VERSUS BURNUP,TIME IS IN ',A4)
 4031 FORMAT(T5,' POWER HISTORY IS INPUT VERSUS TIME IN ',A4)
 4032 FORMAT(T5,' CONSTANT BURNUP CALCULATION DONE WITH',
     +' PERCENT POWER MULTIPLIER')
 4033 FORMAT(T5,' CONSTANT TIME CALCULATION DONE WITH',
     +' PERCENT POWER MULTIPLIER')
 4034 FORMAT(T5,' THIS RUN WILL TERMINATE AFTER PRINTING INPUT')
 4035 FORMAT(T5,' THIS RUN IS A RESTART')
 4036 FORMAT(T5,' CLAD CREEP IS SHUT OFF')
 4037 FORMAT(T5,' THERE IS NO GAS RELEASE ALLOWED')
 4038 FORMAT(T5,' THERE IS NO RELOCATION ALLOWED')
 4039 FORMAT(T5,' CLAD SURFACE TEMPERATURES ARE INPUT')
 4040 FORMAT(T5,' CONSTANT CORE HEAT TRANSFER COEFFICIENTS FOR ',
     +'CONVECTION AND BOILING ARE INPUT')
 4041 FORMAT(5X,'INITIAL PARAMETERS FOR THIS RUN',/,5X,31('*'),//)
 4042 FORMAT('+',T80,'NUMBER OF AXIAL NODES',T120,I2)
 4043 FORMAT('+',T80,'NUMBER OF FUEL RINGS',T120,I2)
 4044 FORMAT('+',T80,'NUMBER OF AXIAL POWER SHAPES',T120,I2)
 4045 FORMAT('+',T80,'NUMBER OF CLAD OD TEMPERATURE DIST.',T120,I2)
 4046 FORMAT('+',T80,'MAXIMUM TIME STEP',T114,F8.0)
 4047 FORMAT(T10,'THE DIAGNOSTICS START AT',F10.1,' HRS AND END AT',
     +F10.1,' HRS')
 4048 FORMAT('+',T85,'CM3 AT STP/GM UO2',T110,F10.5)
 4049 FORMAT('+',T80,'POWER MULTIPLIER,PERCENT',T110,F10.5)
 4050 FORMAT('+',T80,'MULTIPLIER ON RADIAL PEAK',T110,F10.5)
 4051 FORMAT('+',T80,'MULTIPLIER ON AUX. AXIAL SHAPE',T110,F10.5)
 4052 FORMAT(10X,'HT TRANS COEF,CONV,',3A4,T50,F10.0)
 4053 FORMAT(10X,'HT TRANS COEF,BOIL,',3A4,T50,F10.0)
 4054 FORMAT(T5,' CLAD SURFACE TEMPERATURES ARE CALCULATED')
 4055 FORMAT(1X,10A8)
 4056 FORMAT(' INPUT ECHO: A LISTING OF THE DATA RECORDS IN THIS RUN'
     +,/,' ',54('-'),//)
 4057 FORMAT(T6,'THE FOLLOWING TABLES ARE GENERATED:')
 4058 FORMAT(T10,'1 TEMPERATURE SUMMARY')
 4059 FORMAT(T10,'2 DETAILED TEMPERATURE DISTRIBUTION')
 4060 FORMAT(T10,'3 GAP CONDUCTANCE')
 4061 FORMAT(T10,'4 FISSION GAS RELEASE')
 4062 FORMAT(T10,'5 INTERNAL ROD PRESSURE')
 4063 FORMAT(T10,'6 FUEL DIMENSIONS')
 4064 FORMAT(T10,'7 CLAD DIMENSIONS')
 4065 FORMAT(T5,' OUTPUT IS SHORTENED TO INPUT TIME STEPS')
 4066 FORMAT('+',T80,'MULTIPLIER ON FLUX',T110,F10.5)
 4067 FORMAT(T5,' DENSIFICATION IS TEMPERATURE DEPENDENT')
 4068 FORMAT(T5,' DENSIFICATION IS TEMPERATURE INDEPENDENT')
 4069 FORMAT(10X,'CLAD TYPE',5X,'ZIRCALOY-4,TYPE 1',T50,F10.4)
 4070 FORMAT(10X,'CLAD TYPE',5X,'ZIRCALOY-4,TYPE 2',T50,F10.4)
 4071 FORMAT(10X,'CLAD TYPE',10X,'UNSPECIFIED',T50,F10.4)
 4072 FORMAT(10X,'CLAD TEXTURE ANGLE,RADIANS',T50,F10.4)
 4073 FORMAT(10X,'UNIRR CLAD YLD STRENGTH AT RT,',A4,T49,F11.4)
 4074 FORMAT(10X,'AXIAL CLAD GROWTH COEFFICIENT,A',T50,F10.4)
 4075 FORMAT(10X,'AXIAL CLAD GROWTH COEFFICIENT,N',T50,F10.4)
 4076 FORMAT('+',T80,'BWR CLAD OXIDATION MODEL USED')
 4077 FORMAT('+',T80,'PWR CLAD OXIDATION MODEL USED')
 4078  FORMAT(T5,' NO POWER-TO-MELT CALCS DONE')
 4079  FORMAT(T5,' NO AUX POWER OR MOLTEN FUEL CALCS DONE')
 4082 FORMAT('+',T80,'NUMBER OF VOID FRACTION DISTRIBUTIONS',T120,I2)
 4083 FORMAT(T6,'VOID FRACTION DISTRIBUTIONS ARE INPUT')
```

```
 4084 FORMAT(T6,'VOID FRACTIONS DEFAULT TO 0.0')
 4081 FORMAT(20A4)
      DO 40 KAB=1,2
   40 WRITE(KKKCH,REC=KAB) (AB(25*(KAB-1)+KKAB),KKAB=1,25)
C  40 WRITE(KKKCH'KAB) (AB(25*(KAB-1)+KKAB),KKAB=1,25)
  103 FORMAT(2I1,8X,I2,5E12.5)
      IF(IDD.GE.1)WRITE(NCH,1789)(AB(KAB),KAB=1,50)
 1789 FORMAT (10(1X,5E16.7,/))
      COXY=.001
      CFE=-101.
      CTANN=-101.
      APSI=AB(25)
      OVALTY=-101.
      ECCENT=-101.
      IF(ENGIN) GO TO 2000
      STHEGT=AB(1)
      SYAUI=AB(26)*1000000.
      CLADL=AB(2)
      RCOFAB=AB(3)/200.
      RCIFAB=AB(4)/200.
      PIFAB=AB(5)*1000000.
      SPL=AB(11)/100.
      SDD=AB(12)/100.
      SPV=AB(13)*1.E-6
      ECV=AB(14)*1.E-6
      CROUGH=AB(15)*1.E-6
C HCONV AND HBOIL HAVE UNITS OF BTU/HR/FT2/F
      HCONV=AB(21)*1761.493
      HBOIL=AB(22)*1761.493
      GO TO 2050
 2000 STHEGT=AB(1)*.0254
      SYAUI=AB(26)*6894649.75
      CLADL=AB(2)*.0254
      RCOFAB=AB(3)*.0127
      RCIFAB=AB(4)*.0127
      PIFAB=AB(5)/.14504E-3
      SPL=AB(11)*.0254
      SDD=AB(12)*.0254
      SPV=AB(13)*.0000163871
      ECV=AB(14)*.0000163871
      CROUGH=AB(15)/39370000.
      HCONV=AB(21)
      HBOIL=AB(22)
 2050 CONTINUE
      XGAS(1)=AB(6)
      XGAS(2)=AB(9)
      XGAS(3)=AB(7)
      XGAS(4)=AB(8)
      XGAS(5)=0.
      RELFAC=AB(28)
      IF( RELFAC.LE.0. ) RELFAC=1.0
      HEABS=AB(10)
      ZIRC=AB(16)
      INDEX = IFIX(ZIRC)
      GO TO (4820,4821,4822,4823), INDEX
 4820 GE=.794
      K0=3.E-20
      GO TO 4824
 4821 GE=1.
      K0=7.3E-25
      GO TO 4824
 4822 GE=.564
```

```
      K0=1.82E-15
      GO TO 4824
 4823 GE=AB(24)
      K0=AB(23)
 4824 CONTINUE
      PCTPWR=AB(17)
      RPFMUL=AB(18)
      AASMUL=AB(19)
      FLXMUL=AB(20)
      PY=3.141593
      PLNVL1=ECV-SPV-PY*SDD*SDD*SPL/4.
      PLVFAB=(CLADL-STHEGT)*PY*RCIFAB*RCIFAB+PLNVL1
20    CONTINUE
C-2.10QF SET XKFILL,AKAP
      RETURN
999   WRITE(NNCH,1436)
1436  FORMAT(' END OF FILE FIN ENCOUNTERED IN SFILE')
      STOP
      END
```

SUBROUTINE DTGAP SOURCE CODE LISTING

```
      SUBROUTINE DTGAP(TG,PC,TCI,TFNEXT,TFSS,DTFDPC,
     -C,GCPGF,ROUGH,PROF,AG,HG,DKGDTF,KG,KGG,RF,HL,T,
     +RHO,RHOF,POR,FDEP,DTIME,RCOLD,POR0,RELOC0,TFCL0,RCIFAB,
     +RFFAB,ENRICH,TCO,FCGAPD,
     +TGLOC,HGT,HGP,TOTGAP,RFCT,BUT,RELOC,RELOCM,RELOCR,
     +DRRMAX,RELCR0,NORELO,RELOC2,RELC20,IAX)
      REAL KG,KGAP,KGG
      DIMENSION C(1),KGG(1),T(1),RCOLD(1)
C
C  LIQUID BONDED CODE CHANGES ARE DELIMITED BY ********
C
C*********************************************************************
C
C
      COMMON /BOND/ NBOND,BONDCOND,VLBCOLD,BONDEXP,NPAD,XLLIQ,FRACFIL,
     +IWET(50)
      LOGICAL NBOND,NPAD
C*********************************************************************
C
      COMMON/CTF/ABTF,CCTF,LIMTF
      COMMON/PRNT/IDD
      COMMON/IFILE/ICH,JCH,KCH,LCH,MCH,NCH,NNCH
      COMMON/TEST/PROMPT,PORCOR,BOFRAC
      LOGICAL NORELO
      DATA ADIF,BU2,DKGDT,DTG,DTODTI,HEPER,QF,RELOCT,RUFF,TAVG,TFIN
     +  ,TFOUT,T100 /13*0./
      DATA NTRYTF /0/
C
C       CONVERT HL TO UNITS OF TWO PI
C
      QF=HL*FDEP/6.28319
C
      IF(IDD.GE.1) WRITE(NCH,25)
25    FORMAT(' ',' DTGAP')
      IF(IDD.GE.2) WRITE(NCH,26) TG,PC,TCI,TFNEXT,HL,QF,RF,ROUGH,PROF
C
      NTRYTF=1
100   TFIN=TFNEXT
C
C.. LIMIT TEMPERATURE SWINGS
      T100=1400.+FLOAT(NTRYTF-1)*200.
      IF(TFIN.GT.T100)TFIN=T100
      IF(TFIN.LT.10.)TFIN=10.
C
C.. COMPUTE AVERAGE GAP TEMPERATURE
      POR=POR0
      RHO=RHOF*(1.-POR)
      T(1)=TFIN
      TAVG=0.5*(TCI+T(1))
C
C
C
C     COMPUTE RELOCATION DUE TO NON-CONCENTRIC PELLET MODEL AND
C     THERMAL FEEDBACK CONTROL, WHICH ONLY AFFECT OPEN GAP CASE
      RELOCT=0.
      IF(NORELO) GO TO 104
      BU2=BUT*270./238.
      HEPER=C(1)*100.
      CALL RPERM(HL,BU2,RFFAB,RCIFAB,TG,FCGAPD,HEPER,RELOC,RELOC0,
     1  RELOCM,RELOCR,RELCR0,DRRMAX,RELOC2,RELC20,RELOCT,2)
  104 CONTINUE
C
```

```
      IF(IDD.GE.2)WRITE(NCH,26)RELOC,RELOC0,POR,POR0,TFCL0,T(1)
C.. COMPUTE GAP GAS CONDUCTIVITY
      KG=KGAP(TAVG,DKGDT,KGG)
      IF(IDD.GE.2) WRITE(NCH,107)TAVG,KG,DKGDT
107   FORMAT(' TAVG,KG,DKGDT=',3E15.7)
      DKGDTF=0.5*DKGDT
C
C
C.. COMPUTE EXTRAPOLATION LENGTH GCPGF
      GCPGF=0.
C
C.. COMPUTE GAP GAS CONDUCTIVITY CONTRIBUTION TO GAP CONDUCTANCE
      TGLOC=AMAX1(0.,TG-RELOCT)
      RUFF=ROUGH*PROF
      HGT=KG/(TGLOC+GCPGF+RUFF)
C     I/O ENHANCEMENTS ON NEXT 2 LINES
      TOTGAP=TGLOC+GCPGF+RUFF
      RFCT=RUFF+GCPGF
C
C.. COMPUTE CONTACT PRESSURE CONTRIBUTION TO GAP CONDUCTANCE
      HGP=8.*AG*PC
      IF( HGP.GT.14192.5 ) HGP=14192.5
C
C.. COMPUTE GAP CONDUCTANCE
      HG=HGT+HGP
C*********************************************************************
C
C  PAD GAP CONDUCTANCE
C
      IF(NPAD) THEN
      IF( HG.GE.17031.) HG=17031.
      ENDIF
C
C.. COMPUTE LIQUID BONDED GAP CONDUCTANCE
      IF(NBOND) THEN
        IF(IWET(IAX).EQ.1) THEN
          IF(TG.GT.0.) THEN
            HG=BONDCOND/TG
          ELSE
            HG=1.E8
          ENDIF
        ENDIF
      ENDIF
C*********************************************************************
C
C.. COMPUTE TEMPERATURE DROP ACROSS GAP
      DTG=QF/RF/HG
C
C.. COMPUTE FUEL SURFACE TEMPERATURE
      TFOUT=TCI+DTG
      IF(IDD.GE.2) WRITE(NCH,26) GCPGF,HGT,HGP,HG,DTG,TFOUT,DKGDTF
      IF(IDD.GE.2) WRITE(NCH,27) NTRYTF
26    FORMAT(' ',2(5E15.7,/))
27    FORMAT(' ',I2)
C
C.. TEST ABSOLUTE CONVERGENCE
      ADIF=ABS(TFOUT-TFIN)
      IF(ADIF.LT.ABTF)GOTO 900
C  CONVERGES
      NTRYTF=NTRYTF+1
      IF(NTRYTF.GT.LIMTF)GOTO 200
C  TOO MANY TRYS
```

```
C
C.. COMPUTE UP-DATED VALUE FOR TFIN
190   DTODTI=-DTG*DKGDTF/KG
      TFNEXT=(TFOUT-TFIN*DTODTI)/(1.-DTODTI)
      IF(IDD.GE.2) WRITE(NCH,26) DTODTI,TFNEXT
C
C.. TEST CAUCHY CONVERGENCE
191       ADIF=ABS(TFNEXT-TFIN)
      IF(ADIF.GT.CCTF)GOTO 100
C
C.. IF CRAWLING TOO SLOWLY
      WRITE(NNCH,905)NTRYTF
      WRITE(NCH,905)NTRYTF
905   FORMAT(' CAUCHY CONVG OF TFIN FAIL IN DTGAP ON NTRYTF',I5)
      STOP
C
C.. IF DIDN'T CONVERGE ON LIMIT TRYS
200   IF(NTRYTF.LE.2*LIMTF)GOTO 190
      WRITE(NCH,906)NTRYTF,TG,PC,TFIN,TFOUT
      WRITE(NNCH,906)NTRYTF,TG,PC,TFIN,TFOUT
906   FORMAT(' EXC LIMIT ON NTRYTF IN DTGAP:NTRYTF,TG,PC,TFIN,TFOUT',
     +/,I5,/,4E15.6)
      IF(NTRYTF.GT.5*LIMTF-2)IDD=2
      IF(NTRYTF.GT.5*LIMTF)STOP
      TFNEXT=.5*(TFOUT+TFIN)
      GOTO 191
900   TFSS=TFOUT
      IF(IDD.GE.1)WRITE(NCH,910) NTRYTF,TG,PC,TFIN,TFOUT
910   FORMAT(' DTGAP.FR: NTRYTF,TG,PC,TFIN,TFOUT=',I5,4E15.6)
C-2.5QF; ADD PROF TO NEXT LINE
      DTFDPC=QF*DKGDTF/(RF*HG*HG*(GCPGF+ROUGH*PROF))
      DTFDPC=-QF*AG/(RF*HG*HG*(1.+DTFDPC))
      IF(IDD.GE.1) WRITE(NCH,26) DTFDPC
      RETURN
      END
```

SUBROUTINE BEGIN SOURCE CODE LISTING

```
      SUBROUTINE BEGIN(MEMORY,NMEM,NMEMT,NAX,IDDD,NOGASR,NORELO,NOCREP,
     +NOMELT,NOAUXP,
     +PTIME,SPTIME,SENS,PFIRST,DSPTYM,
     +CONT,STEP1,SPTYM,FGPRO,FGREL,TF0,FOPEN,IFIRST,RSTRT,
     +JSTK,JCTR)
      DIMENSION MEMORY(1),TF0(1)
C
C  CODE CHANGES FOR LIQUID BONDED FUEL ARE DELIMITED BY ***********
C
C*********************************************************************
      COMMON /BOND/NBOND,BONDCOND,VLBCOLD,BONDEXP,NPAD,XLLIQ,FRACFIL,
     +IWET(50)
      LOGICAL NBOND,NPAD
C*********************************************************************
C
      COMMON TIME,TIME0,NITER,NITER0,RCO,RCI,TC,
     +GASPRO(20),GASRO0(20),
     -GASREL(20),TAUG(20),GASRET(20),GASRT0(20),
     +OXI,OXF,TRANSW,RF00(5)
      COMMON RELOC2,RELC20,RF01(9),IXXX,INDRPA,DCUM,TFAIL,PROBA,
     +PICLD,GRUG,GRGB,RFB,FROUGH,PFABO,PFABC,
     +RLTOD,AMP,DISH,ROUGH,PROF,ENRICH,QFBAR,PLPEAX,RELOC,TFCL0,
     -GASPLD(20),GASRLD(20),GRELLD(20),
     -RF0LD(20),GAMALD(20),RCOX,RCIX,TCX,RCX,
     +CLOSED,RCLAD,NRING,RFO(20),
     -GAMMA(20),GRELTT,GPRO,GREL,GPROTT,NNODE,PC,RF,RCOLD(20),
     -GTHTA,DVOVAB,DVVAB0,AEQ,BEQ,DE,ECZ,T(20),
     -DT(20),VFOLD,VFNEW,FOP,FCP,FOP0,RHONEW,AFF,
     +ACSWL0,DNSWL0,DLOPVL,GSWL0,EEQTHN,
     +EEQIRN,FCGAPD,VFRAC0,VFRAC,Y113(4),
     -DATDT(20),
     -FRCOLD(20),ARG,ICON2,PROB,C01PM,INDRP,
     -PCPREV,CLOS0,RFPREV,TGPREV,RCCOLD,RCHOT,NCRACK,
     -PHI,BUT,FLNCT,PFAB,NBEG,TCFAB,FNODHT,TCO,RHOT(20),
     -TG,SN,EC0,ACTC,TEMPC,DEEQTH,EEQTH,DEEQ,
     +EEQIR,EEQIR0,EEQ,ROUGH0,DEQIR,
     -EEQTH0,EEQIRR,EEQTHR,EEQR,EC0R,ECZR
      COMMON FLXR,SIGFX,RCOFAB,RCIFAB,FDEP,QI,HL,RHOL,RFFAB,
     -ESWAVG,TFCL,TCI,TF,AT,HG,ADEN,BDEN,ACCSWL,BURED,DENSWL,
     -SFPSWL,SEQ,STH,SZ,DECDT,MU,DTIME,P(20),
     +GRAIN,QL,TGPR,TGPR0,TME0,RELOC0,RELOCR,QS,FRELT,TM(20),
     -NRING0,NNODE0,ROLD(20),PM0(20),
     -CVAF,DVAF,OPVAF,VVAF,CRKVUP,DSHVUP,CTRVUP,OPVUP,CVAF0,DVAF0,
     -OPVAF0,VVAF0,CRKFIL,DSHFIL,OPFIL,CTRFIL,OPVOL,Y111(3),
     -ESW0(20),
     -RFTOT0(20),QM0(20),DVOVC(20),DVOVC0(20),
     -ESW(20),PM(20),ACC1,DELDEN,TSWL,
     +GFPSWL,RFINUP,LHOLE,RFIN01,FL,REP,KGG(5),Y110,PWRTM,
     -ACCVLC,ACCVL1,ACCVLH,ACCVL5,
     -RFTOT(20),QM(20),
     -GZ,FHOT(20),RFC,GAPVOL,GAPTEM,VOVTGP,
     -CRKVOL,CRKTMP,CVLVCT,V(20),FRATE,FREL,
     -NTRYPC,RFCOLD,P0(20),HL0,EELDP,GR,GCTHTA,
     -DSSDBU,ZZMAX,DONE,BU,FIRST,BUT0,FLNC0
      COMMON TADJ,FLNC,TPOW,LAST,
     -DBU,NSTART,GCZ,GCR,APV,RCOCLD,RCICLD,
     +DR(20),DKFDT(20),RM(20),D(20),KF(20),GCPGF,DKGDTF,KG,
     +NODELC,NODELH,RELOCM,AFTF(20),DRH(20),
     -PHI00,PHI10,PSI,PHI0C,PHI1C,PHID1C,
     +PCIN,TGOUT,TGIN,PSID,TGP,ZH,ZF,DRRMAX,RH,RC,WF,
     -FHOTX(20),PCOUT,TAVG,RELCLS,CLSPRV,RELCR0,IZ1,IZ2,IZ3
      COMMON TSWGR(20),FMIN(20),FDPC,RHOIN,RHOOUT,TWOSIG,FTYP,RFIN
```

```
     +,FPL,HDISH,RLAND,RBOT,VDISH,VCHAM,VHOLE,VTC,TCLNT,RABU,RABU0,
     +HL2,RR0(40),RR(40),WU0(40),WP0(40),H10(40),H20(40),BU0(40),
     -DUMMEM(31)
      COMMON/EDIT/IXCH(20),ENGOUT,TAB(10),SPRNT,DAYS
     +,ITC1,ITC2
      COMMON/BB/B(3),BA4,BA(5),BA10,BA1(8),IFMT(5),VF,VFUEL,VRAT(24)
      REAL KF,MU,NHE,KG,KGG,ICON2,NUC,MUC
      REAL LHOLE
      COMMON/CCOD/SY,APSI,BUEOL,SRO,ARG1,
     -CI2,TFLCON,ARECON,PLPERD,SIGD,RIDGE,FRELOC,TRELOC
      COMMON/PRNT/IDD
      COMMON/IFILE/ICH,JCH,KCH,LCH,MCH,NCH,NNCH
      COMMON/CXE/ABXE,CCXE,LIMXE,DXEIN,XEOUT0,
     -NTRYXE,DXODXI,XEIN,XENEXT
      COMMON/CDT/GRLIM,CRLIM,SWLIM,DTLIM,CRFACT
     -,RESET1
      COMMON/GASP/GPX(11),STHEGT,PLENHT,PIFAB,PO,GHTOT,GTOT,GXTOT
     -,PIOLD,DPOLD,PLVFAB,FXX,DELVV0,V0,PLNVL1
     +,EFFVOL,VOLCLD
      COMMON/CLAD/EC,NUC,MUC,FR,FZ,COXY,CWKF
     +,ZIRC
      COMMON/SWLDAT/A1,ADEN0,GACC,BBUB,BACC,GACC0,PNON,APV100,PACC
     +,ACC1A,ACC1B,TDENS
      COMMON/CFEAT/SYAUI,CFE,CTANN,OVALTY,ECCENT,CROUGH,OXSW
      COMMON/GAP/AG,PI,DP,XGAS(5),XMGAS(5),C(5),FGAP(25),
     +AGAP(5),RGAP(5),AAGAP(5),BBGAP(5),NNNCH
     -,PREVC(5)
      COMMON/CREP/AY1,AY2,AY3,AY4,AY5,AY6,AY7,AY8,
     +BE1,BE2,BE3,BE4,BE5,BE6,BE7,BE8
      LOGICAL TADJ,CLOSED,CLOS0,FIRST,LAST,SENS,NOGO,DONE,RELCLS,
     +CLSPRV,SAT,CONT,PFIRST,STEP1,RSTRT,RESET1,DAYS
     +,NOCREP,NORELO,NOMELT
      LOGICAL IFIRST,ENGIN,ENGOUT,TORBU,CTORBU,CHIN,TCOIN
      DIMENSION ZLGTH(24),QNOD(24),TSURF(24),TCOOL(24),FDEPC(24)
      DIMENSION AS(25,50),TCODA(24,25),Z(16),XT1(24),VFUEL(24),ZZ(16)
      DIMENSION VDFR(24,25),FUELOR(24),FUELIR(24),FUELDF(24),REPJ(24)
      CHARACTER*4 YVDFR
C     INTEGER YVDFR
      LOGICAL TAB,NOAUXP
      COMMON/TERM/NTERM,STERM,IWORD
      CHARACTER*4 NTERM,STERM,IWORD
C     INTEGER STERM
      CHARACTER*4 ITEST,ZWORD,YASN,YTCON
C     CHARACTER*5 AX1,A4,A12
      CHARACTER*5 AX1,A4,A12
C     INTEGER ZWORD,YASN,YTCON
      COMMON /ROD/ TITLE(10),IDAY,ITYM,IVERS
      CHARACTER*10 IDAY,ITYM
      CHARACTER*4 IVERS
      CHARACTER*8 TITLE
C     REAL IDAY,ITYM
      CHARACTER*4 B1,B2,B3
C     INTEGER B1,B2,B3
      CHARACTER*4 X1,X2,X3,X4,X5,X6,X7,X8,X9,X10,X11,X12,X13,X14,X15
     +  ,X16,X17,X18,X19,X20,X21,X22,X23,X24
C     INTEGER X1,X2,X3,X4,X5,X6,X7,X8,X9,X10,X11,X12,X13,X14,X15,X16
C    +  ,X17,X18,X19,X20,X21,X22,X23,X24
      CHARACTER*4 XXX(20)
C     DIMENSION XXX(20)
      CHARACTER*4 XTXTX
C     CHARACTER*5 RCHAR(6)
      CHARACTER*5 RCHAR(6)
```

```
C     DIMENSION RCHAR(6)
      DATA RCHAR /'W/CM ','DEG C','KW/FT','DEG F','DAYS ','HOURS'/
      DATA X2,X3,X8,X9,X10,X11,X12,X13,X14,X15/'C   ','F   ',' LBM',
     +'/FT2','/HR ',' KG/','M2/S','EC  ','PSIA',' MPA'/
      DATA X17,X18,X19,X20,X21,X22
     +/'IN  ','CM  ','KW/F','T   ',' W/C','M   '/
      DATA B1,B2/'IN3 ','CM3 '/
      DATA YVDFR/'---*'/
      DATA VDFR/600*0./
      DATA NCTR,ZCTR/0,0./
      DATA ZWORD,YASN,YTCON/'----','*-*-','-***'/
      DATA ITEST/'*---'/
      DATA XTXTX/'$$$$'/
      DATA AASMUL,APS1,APS2,APS3,AS,AX2,BUCOM,BUIN,BUINA,B4,CAP,CLADL
     +  ,CYCLE,DBURT,DCO,DELBU,DELBUA,DELBUR,DELTM,DELTMA,DENPOR,DH,DHZ
     +  ,DUM1,DUM2,FDEPC,FLUX,FLXMUL,FQRAT,FRZ,F1,HBOIL,HCHAM,HCONV
     +  ,HEABS,HLRA,PBARY,PBARZ,PCOOL,PCOOLZ,PCTPWR,PFLUX,PNC,QBAR,QNOD
     +  ,Q2,RABUT,RCHAM,RPFMUL,TCODA,TCOOL,TIMIN,TIMINA,TIMINB,TIMZ,TINY
     +  ,TINZ,TOTFN,TSURF,VF1,VTANN,VTCH,VTDSH,VTHOL,VTOP,VTOT,XNHEAB
     +  ,XT1,XZ15,YMASV,Z,ZBURT,ZDBRA,ZLGTH,ZMASV,ZZ,ZZ1,ZZ2,ZZ3
     +  /2095*0./
      DATA ICTR,ICYCLE,IFMT6,IFMT7,IFMT8,INUM,ITIN,IZ5,JAPS1,JAPS2
     +  ,JAPS3,JAPS4,JAS,JJCT,JJJCH,JNUM,JRINGS,JTCO,JZ1,JZ2,JZ3
     +  ,KKKCH,KREC,NREC /24*0/
      DATA CHIN,CTORBU,ENGIN,NOGO,SAT,TCOIN,TORBU /7*.FALSE./
C ASSIGN CHANNELS TO INTERMEDIATE STORAGE
      KKKCH = 51
      NNNCH = 52
C INPUT ECHO IS MOVED FROM CHANNEL JJJCH TO NCH
      JJJCH=NCH
C     OPEN(UNIT=51,FILE='FILEA',STATUS='NEW',ACCESS='DIRECT',
C    +     FORM='UNFORMATTED',RECL=25)
      OPEN(UNIT=51,STATUS='SCRATCH',ACCESS='DIRECT',RECL=400)
C     DEFINE FILE 51(1000,50,U,IASC51)
      CALL SFILE(IDD,IDDD,PTIME,SPTIME,NOGO,NOGASR,NOMELT,NOAUXP,
     +NORELO,NOCREP,CONT,NAX,DTLIM,STHEGT,PIFAB,FLXMUL,
     +PLVFAB,CROUGH,SYAUI,COXY,CFE,CTANN,CLADL,
     +APSI,OVALTY,ECCENT,IFIRST,RSTRT,RCOFAB,RCIFAB,
     +XGAS,HEABS,PCTPWR,RPFMUL,AASMUL,ENGIN,
     +JAS,JRINGS,TORBU,CTORBU,CHIN,TCOIN,ZIRC,KKKCH,JTCO,JSTK,
     +HBOIL,HCONV,PLNVL1,OXSW,JVDFR)
C - - INPUT IS BEGIN SAVED ON UNIT 51
      STEP1=.FALSE.
      PFIRST=.FALSE.
      RESET1=.FALSE.
      IF(RSTRT)GOTO 5000
      PFIRST=.TRUE.
      STEP1=.TRUE.
      AY8=AY1*(SYAUI*1.E-6)**AY6
      BE8=BE1*(SYAUI*1.E-6)**BE6*COS(APSI)**BE7
      TOTFN=0.
      PLENHT=0.
      PLPERD=0.
      PO=0.
      ICTR = 0
      JCTR=0
      VF=0.
      TIMIN=0.
      BUIN=0.
      VTHOL=0.
      ZZ3=0.
      VTANN=0.
```

```
      VTOP=0.
      VTCH=0.
      VTDSH=0.
      DBURT=0.
      TIMINA=0.
      BUINA=0.
      DO 40 I=1,24
   40 VFUEL(I)=0.
      DO 1000 IAX=1,NAX
      IF(ICTR-1)3001,3001,3011
 3001 CONTINUE
      JCTR=JCTR+1
C.. SET POINTER AT
C.. LINE FOLLOWING NEXT LINE WITH '*---' AS LEFT-MOST FOUR CHARACTERS
   14 READ(MCH,8056,END=999)XXX
      IF(XXX(1) .EQ. XTXTX) GO TO 14
      REWIND 50
      WRITE(50,8056) XXX
      REWIND 50
      READ(50,101) IWORD
  101 FORMAT(20A4)
1     FORMAT(1X,20A4)
      IF(IWORD.NE.ITEST)GOTO 14
      IF(IDD.GE.2) WRITE(NCH,2) IWORD
2     FORMAT(1X,A4)
C
C
C
 3011 CONTINUE
      CALL UNITS(IAX,NAX,PIFAB,CROUGH,SYAUI,STHEGT,FNODHT,TOTFN,
     +RCOFAB,RCIFAB,RFFAB,AMP,DISH,ROUGH0,ROUGH,GRAIN,
     +PFAB,ADEN,BDEN,ENRICH,FDEP,PLPERD,PLPEAX,
     +CWKF,PROF,QFBAR,RLTOD,FROUGH,PFABO,PFABC,
     +ENGIN,ENGOUT,ICTR,FDPC,RHOIN,RHOOUT,BUCOM,FOP,FTYP,
     +RFIN,FPL,HDISH,RLAND,RBOT,HCHAM,RCHAM,VTC,VDISH,VCHAM,
     +VHOLE,NNNCH,KKKCH,JSTK,JCTR,FL,REP)
C THE FOLLOWING CONTINUE MAY BE BETTER LATER IN THE PROGRAM
C
C
C.. CHECK INPUT DATA FOR BAD DATA
C
      TCO=0.
      CALL UNSAT(STHEGT,PIFAB,APSI,SY,FR,FZ,PO,RCOFAB,
     +RCIFAB,RFFAB,PFAB,ADEN,BDEN,GRAIN,FDEP,TCO,SAT,IAX,NAX)
      IF(.NOT.SAT) STOP
C
C.. ESTABLISH RING STRUCTURE
      NRING=JRINGS
      NNODE=NRING+1
      CALL RINGS ( NNODE,RFFAB,RCOLD,V,RFIN )
C
C.. INITIALIZATION
      DO 100 I=1,20
      GASPLD(I)=0.
      GASRLD(I)=0.
      GRELLD(I)=0.
      GASPRO(I)=0.
      GASREL(I)=0.
      GASRET(I)=0.
      RFO(I)=0.
      GAMALD(I)=0.
      ROLD(I)=0.
```

```
      ESW0(I)=0.
      RFTOT(I)=0.
      RFTOT0(I)=0.
      DVOVC(I)=0.
      DVOVC0(I)=0.
      QM0(I)=0.
      OXI=0.
      OXF=0.
      TRANSW=0.
      FRCOLD(I)=0.
      P0(I)=PFAB
      PM0(I)=PFAB
      ESW(I)=0.
      GASRO0(I)=0.
      TAUG(I)=0.
      FMIN(I)=0.
      RF0LD(I)=0.
100   GASRT0(I)=0.
      PWRTM=68897.64
      IF( NOMELT ) PWRTM=0.0
      TFAIL=1.E50
      PROBA=0.
      INDRPA=0
      DCUM=0.
      BURED=0.
C
C..  INITIALIZATION FOR RELOCATION MODEL
      FCGAPD=2.0*(RCIFAB-RFFAB)*100./2.54
      RELOC=0.
      RELOC2=0.
      RELC20=0.
      RELOC0=0.
      RELOCR=0.
      RELCR0=0.
      RELOCM=0.
      TFCL0=20.
      GPROTT=0.
      GRELTT=0.
      HL=0.
      MU=0.
      EEQTH=.1E-4
      EEQIR=.1E-4
C GIVE EEQIR AND EEQTH INITIAL VALUES FOR CREST.............
      EEQIRR=0.
      EEQTHR=0.
      EEQR=0.
      EC0R=0.
      ECZR=0.
      EEQIRN=0.
      EEQTHN=0.
      TME0=0.
      TGPR=RCIFAB-RFFAB
      TGPR0=TGPR
      DONE=.FALSE.
      TPOW=0.
      GR=0.
      GZ=0.
      APV=APV100*(1.-PFAB)
C.. SWELLING RATE OF 100  DENSE UO2 MODIFIED BY AS FAB POROSITY.
      EEQ=0.
C  EQUIVALENT STRAIN FOR CREEP CALC
      SEQ=0.
```

```
C  EQUIVALENT STRESS
      GTHTA=0.
C  CLAD GROWTH TANGENTIAL STRAIN
      EC0=0.
C  CLAD CREEP TANGENTIAL STRAIN
      ECZ=0.
C  CLAD CREEP AXIAL STRAIN
      DECDT=0.
      DEEQ=0.
      DEEQTH=0.
      DEQIR=0.
      EEQIR0=0.
      EEQTH0=0.
      EEQIRR=0.
      EEQTHR=0.
      IF(.NOT. NOCREP) GO TO 10
        EEQIR=0.
        EEQTH=0.
        DONE=.TRUE.
   10 CONTINUE
      NITER=0
      NITER0=0
C  TIME-STEP CUTTING ITERATION COUNTER
      FIRST=.TRUE.
C  FLAG TO SPECIFY FIRST CALL TO DELTIM
      LAST=.FALSE.
C  FLAG TO SPECIFY LAST TIME STEP IN POWER HISTORY
      TIME0=0.
C  TIME OF START OF TIME STEP
      TIME=0.
C  TIME TO END OF CURRENT TIME STEP
      RCO=RCOFAB
C  OUTER CLAD RADIUS
      RCI=RCIFAB
C  INNER CLAD RADIUS
      RF=RFFAB
C  FUEL SURFACE RADIUS
      PC=0.
C  CONTACT PRESSURE
      PCOUT=0.
      TGPREV=RCIFAB-RFFAB
C  PREVIOUS GAP
      PCPREV=0.
C  PREVIOUS CONTACT PRESSURE
      RCCOLD=0.
C  START WITH FULLY CRACKED FUEL
      RFPREV=RFFAB
C  EQUIVALENT FUEL SURFACE RADIUS
      RCLAD=0.5*(RCO+RCI)
C  NOMINAL CLAD RADIUS
      TCFAB=RCO-RCI
C  AS-FAB CLAD THICKNESS
      TC=RCO-RCI
C  CLAD THICKNESS
      NNODE0=2
C USED IN REAKEY,REBKEY
      NRING0=1
C USED IN REAKEY,REBKEY
      ROLD(1)=RFFAB
C USED IN REAKEY,REBKEY
      CLOSED=.FALSE.
C  FLAG TO SPECIFY GAP OPEN/CLOSED STATUS
```

```
      CLOS0=.FALSE.
C  FLAG TO SPECIFY PREVIOUS GAP STATUS
      FREL=0.
C  FRACTION GAS RELEASED
      TEMPC=TCO
      NBEG=0
      INDRP=0
      SN=0.0
      BUT=0.
      FLNCT=0.
      DBU=0.
      RCHOT=RFFAB
C     RELCLS IS TRUE IF THE GAP IS CLOSED OR ZERO
      RELCLS=.FALSE.
      CLSPRV=.FALSE.
C      TFB=TCO
C      T0B=TCO
C.. TENTATIVE STORAGE POSITIONS
C      T(19)=TFB
C      T(20)=T0B
      RFCOLD=RFFAB
      TFCL=TCO
      TF=TCO
      TF0(IAX)=300.
      ICON2=0.
      PROB=0.
      WF=1.E60
      C01PM=1.
C
C.. TEMPORARY VALUES FOR CHECKING ALIGNMENT OF BLANK COMMON
      ACCSWL=123.
      DTIME=234.
      DSSDBU=345.
      GCR=456.
      DKGDTF=567.
      RFC=0.
C.. AUXILIARY PARAMETERS FOR CHECKING ALIGNMENT OF BLANK COMMON
      IZ1=1111
      IZ2=2222
      IZ3=3333
C
      BUT0=0.
      FLNC0=0.
      BU=0.
      FLNC=0.
      VFUEL(IAX)=RHOIN*(FNODHT*RFFAB**2*3.141593-VDISH-VCHAM
     '           -VHOLE-VTC)*.01
C
C  CALCULATE OPEN POROSITY VOLUME THAT WILL DENSIFY OUT -- THIS
C  VOLUME WILL BE AVAILABLE FOR GAS RESIDENCE BUT NOT FOR
C  ACCOMMODATION
C
      DENPOR=ADEN*PFABO
      DLOPVL=DENPOR*VFUEL(IAX)/RHOIN*100.
      OPVOL=PFABO*(1.-ADEN)*VFUEL(IAX)/RHOIN*100.
      VTOP=VTOP+OPVOL+DLOPVL
      VF1=3.141593*FNODHT*RFFAB*RFFAB
      V0=V0+VF1
      CVAF=0.25
      DVAF=0.25
      VVAF=0.25
      OPVAF=0.25
```

```
      LHOLE=FNODHT*(FPL-2.*HDISH)/FPL
      RFIN01=RFIN
      VFOLD=VFUEL(IAX)*(1.+PFAB)
      FOP0=FOP
      VFRAC0=1.
      IF(NAX.GT.1)CALL PUT(MEMORY,NMEM,-4,IAX)
      ZLGTH(IAX)=FNODHT*39.37
      FDEPC(IAX)=FDPC
      VF=VF+VFUEL(IAX)
C VF IS A SUM OF (FUEL VOL * INITIAL DENSITY)(CUBIC METERS*PERCENT)
      VTHOL=VTHOL+VHOLE
      VTDSH=VTDSH+VDISH
      VTCH=VTCH+VCHAM
      VTANN=VTANN+FNODHT*3.14159*(RCIFAB**2-RFFAB**2)
C TOTAL VOID VOLUMES CALCULATED(VTOT,VTHOL,VTCH,VTANN,VTOP,PLVFAB)
C
C     SAVING SOME DATA FOR FLUX DEPRESSION RESONANCE ESCAPE
C     PROBABILITY CALCULATIONS BELOW IN VOIDP
      FUELOR(IAX)=RFFAB*100.
      FUELIR(IAX)=RFIN*100.
      FUELDF(IAX)=VFUEL(IAX)/VF1
      REPJ(IAX)=REP
C
1000  CONTINUE
      DO 52 I=1,NAX
   52 VRAT(I)=VFUEL(I)/VF
C*********************************************************************
C
C  CODE CHANGES FOR LIQUID BONDED FUEL
C
      IF(NBOND) THEN
      VLBCOLD=(VTANN+VTHOL+VTCH+CTOP+FTDSH)*FRACFIL
      VTHOL=VTHOL*(1.-FRACFIL)
      VTCH=VTCH*(1.-FRACFIL)
      VTANN=VTANN*(1.-FRACFIL)
      VTOP=VTOP*(1.-FRACFIL)
      VTDSH=VTDSH*(1.-FRACFIL)
      XLLIQ=FRACFIL*STHEGT
      XLNOD=STHEGT/NAX
      DO 6262 I=1,NAX
      IF(I*XLNOD.LE.XLLIQ) THEN
         IWET(I)=1
      ELSE
         IWET(I)=0
      ENDIF
 6262 CONTINUE
      ENDIF
C*********************************************************************
C
      VTOT=PLVFAB+VTHOL+VTDSH+VTCH+VTANN+VTOP
C CALCULATE INITIAL MOLES OF FILL GAS,HELIUM ABSORBTION,AND NEW FILL P
C GAS CONSTANT*T(68F)=8.292PA-M**3/GMOLE/K*293K=2429.556(PV=NRT)
      GHTOT=PIFAB*VTOT/2429.556
      DO 8401 I=1,5
      XMGAS(I)=XGAS(I)*GHTOT
 8401 CONTINUE
      PLENHT=CLADL-STHEGT
C HELIUM ABSORBTION TD UO2=10.96 GM/CC,T=273K,P=101351.35PA
      XNHEAB=490.7024*VF*HEABS
      XMGAS(1)=XMGAS(1)-XNHEAB
      IF(XMGAS(1).LT.0.)XMGAS(1)=0.
      GHTOT=XMGAS(1)+XMGAS(2)+XMGAS(3)+XMGAS(4)+XMGAS(5)
```

```
      GTOT=GHTOT
      DO 8402 I=1,5
      C(I)=XMGAS(I)/GHTOT
      PREVC(I)=C(I)
 8402 CONTINUE
C CALC NEW FILL PRESSURE
      PIFAB=2429.556*GHTOT/VTOT
      IF(ENGOUT) GO TO 6070
      B3=B2
      A4 = RCHAR(1)
      A12 = RCHAR(2)
      BA4=.01
      B4=1000000.
      X1=X2
      X4=X11
      X5=X12
      X6=X13
      X7=X15
      X16=X18
      X23=X21
      X24=X22
      GO TO 6071
 6070 B3=B1
      A4 = RCHAR(3)
      A12 =  RCHAR(4)
      BA4=.0003048
      B4=61023.744
      X1=X3
      X4=X8
      X5=X9
      X6=X10
      X7=X14
      X16=X17
      X23=X19
      X24=X20
 6071 CONTINUE
      IF(.NOT. DAYS) GO TO 6072
      AX1 = RCHAR(5)
        AX2=24.
      BA10=1./24.
        ASSIGN 8051 TO IFMT6
        ASSIGN 8052 TO IFMT7
        ASSIGN 8053 TO IFMT8
      GO TO 6073
 6072 CONTINUE
      AX1 = RCHAR(6)
        AX2=1.
      BA10=1.
        ASSIGN 8018 TO IFMT6
        ASSIGN 8025 TO IFMT7
        ASSIGN 8029 TO IFMT8
 6073 CONTINUE
      IOUNIT = IXCH(19)
      WRITE(IOUNIT,6081)TITLE,IVERS,IDAY,ITYM
      WRITE(IOUNIT,8055)A4,A12,A12,A12,A12,A12,A12,A12
      F1=B4*VTOT
      CALL RDOUT1(JJJCH)
      WRITE(JJJCH,6090) TITLE,IVERS,IDAY,ITYM
      WRITE(JJJCH,6082)
      WRITE(JJJCH,6083) B3,F1
      F1=B4*PLVFAB
      WRITE(JJJCH,6084) B3,F1
```

```
      F1=B4*VTANN
      WRITE(JJJCH,6085) B3,F1
      F1=B4*VTHOL
      WRITE(JJJCH,6086) B3,F1
      F1=B4*VTDSH
      WRITE(JJJCH,6087) B3,F1
      F1=B4*VTCH
      WRITE(JJJCH,6088) B3,F1
      F1=B4*VTOP
      WRITE(JJJCH,6089) B3,F1
C WRITE OUT NEW GAS PRESSURE AND COMPOSITION
      WRITE(JJJCH,8044)
      IF(ENGOUT)PNC=PIFAB*.00014504
      IF(.NOT.ENGOUT)PNC=PIFAB*1.E-6
      WRITE(JJJCH,8045)X7,PNC
      WRITE(JJJCH,8046)
      WRITE(JJJCH,8047) C(1)
      WRITE(JJJCH,8048) C(3)
      WRITE(JJJCH,8049) C(4)
      WRITE(JJJCH,8050) C(2)
 6081 FORMAT('1',///,' ',10A8,2X,'ESCORE VERS:',1X,A4,2X,'DATE',
     +A10,'TIME:',A10,//)
 6082 FORMAT(///,5X,'AS-FABRICATED OPEN VOID VOLUMES',/,5X,31('-'),//)
 6083 FORMAT(5X,'TOTAL ROD VOLUME,',A4,T40,F8.5)
 6084 FORMAT(5X,'PLENUM VOLUME,',A4,T40,F8.5)
 6085 FORMAT(5X,'ANNULUS VOLUME,',A4,T40,F8.5)
 6086 FORMAT(5X,'CENTRAL HOLE VOLUME,',A4,T40,F8.5)
 6087 FORMAT(5X,'DISH VOLUME,',A4,T40,F8.5)
 6088 FORMAT(5X,'CHAMFER VOLUME,',A4,T40,F8.5)
 6089 FORMAT(5X,'OPEN POROSITY VOLUME,',A4,T40,F8.5)
 6090 FORMAT(' ',///,' ',10A8,2X,'ESCORE VERS:',1X,A4,2X,'DATE:',
     +A10,'TIME:',A10,//)

****************** REST OF SUBROUTINE NOT MODIFIED ******************
```

REFERENCES

1 The University of Chicago Special Committee for the Integral Fast Reactor, Technical Subcommittee Review of Fuel Performance, Argonne National Laboratory-West, Argonne, IL (July 8, 1987).

2 Handbook of Tables for Applied Engineering Science, 2nd Edition, CRC Press, Cleveland, OH (1976).

3 J.R. Lamarsh, Introduction to Nuclear Engineering, Addison-Wesley Publishing, Reading, MA (1983).

4 Handbook of Thermodynamic and Transport Properties of Liquid Metals, Blackwell Scientific Publications, Boston, MA (1985).

5 Addison, C.C., The Chemistry of the Liquid Alkali Metals, Wiley-Interscience Publications, New York, NY (1984).

6 Hodge, R.I., Turner, R.B., Platten, J.L., "Corrosion by Liquid Metals," Proceedings of the Metallurgical Society of AIME, pp 283-303, Plenum Press, New York (1970).

7 T.M. Adams, Feasibility Study of Materials Compatibility for Liquid Metal Bonded Light Water Reactor Fuel Elements, Master's Thesis, University of Florida, Gainesville, FL (1993).

8 M. Dubecky, Liquid Metal Bonded Light Water Reactor Fuel Material Compatibility Study, Master's Thesis, University of Florida, Gainesville, FL, Work in Progress, (1994).

9 Fuel Design Manual, Technical Report WCAP-8476, Rev. 4, Westinghouse, Pittsburgh, PA (November 1981).

10 Barner, J.O., "Behavior of Sodium-Bonded (U, Pu)C Fuel Elements After Moderate Burnup," Proceedings of the Conference on Fast Reactor Fuel Element Technology, American Nuclear Society, Chicago, IL, pp 819-847 (1971)

11 J.A. Pearson, "Thermal Resistance of the Joint Between a Nuclear Fuel and its Canning Material," Nuclear Energy, pp 444-449 (December, 1962).

12 A.S. Bain, "UO_2/Sheath Heat Transfer During Irradiation," Nuclear Applications, vol. 3, pp 240-244 (April 1957).

13 H. Fenech and W.M. Rohsenow, "Predictions of Thermal Conductance of Metallic Surfaces in Contact," Journal of Heat Transfer, vol. 85, pp 15-24 (February 1963).

14 J.R. Weeks, "Lead, Bismuth, Tin and Their Alloys as Nuclear Coolants," Nuclear Engineering and Design, vol. 15 pp 363-372 (1971).

15 W.E. Berry, Corrosion in Nuclear Applications, John Wiley and Sons, Inc., New York (1971).

16 W.D. Manly, J.V. Caithcart, "Mass Transfer Properties of Various Metals and Alloys in Liquid Lead," Corrosion, Vol. 12, pp 46-52 (1956).

17 L.F. Epstein, "Static and Dynamic Corrosion and Mass Transfer in Liquid Metal Systems," Chemical Engineering Progress Symposium, vol. 53, pp 67-81 (1957).

18 O.F. Kammerer, J.R. Weeks, J. Sadofsky, W.E. Miller, D.H. Gurinsky, "Zirconium and Titanium Inhibit Corrosion and Mass Transfer of Steels by Liquid Heavy Metals," Transactions of the A.I.M.E., Vol 212, pp 20-25 (1958).

19 A.d.S. Brasunas, "Liquid Metal Corrosion," Corrosion, Vol. 9, pp 78-84, (1953).

20 J. Weeks, C. Klamut, "Reactions Between Steel Surfaces and Zirconium in Liquid Bismuth," Nuclear Science and Engineering, Vol. 8, pp 133-147 (1960).

21 H.H. Manko, Solders and Soldering, McGraw-Hill Book Co., New York, (1964).

22 J.H. Kittel, L.C. Walters, "Development and Performance of Metal Fuel Elements for Fast Breeder Reactors," ANS Trans., vol. 31, pp 117-179, (1979).

23 Edwards, A.L., TRUMP: A Computer Program for Transient and Steady-State Temperature Distributions in Multidimensional Systems, UCRL-14754, Rev. 3, Lawrence Livermore Laboratory, Livermore, CA (September 1, 1972).

24 ESCORE--The EPRI Steady-State Core Reload Evaluator Code: General Description, EPRI NP-5100, prepared by Combustion Engineering, Inc., Palo Alto, CA (February 1987).

25 Johansson, E.B., Potts, G.A., and Rand, R.A., GESTR: A Model for the Prediction of General Electric Boiling Water Reactor Fuel, Technical Report NEDO-23785, General Electric, San Jose, CA (March 1978).

26 Sundquist, B., LIFE-4 User's Manual, Technical Report WAES-TR-90-007, Westinghouse, Madison, PA (January 1990).

27 P.E. MacDonald, ed., MATPRO: A Handbook of Materials Properties for Use in the Analysis of Light Water Reactor Fuel Rod Behavior, ANCR-1263, NRC-5, Aerojet Nuclear Company, San Diego, CA (February 1976).

28 P.Bouffioux, H. Heckermann, N. Hoppe, and A. Strasser, LWR Fuel Rod Modeling Code Evaluation--COMETHE-IIId, Phase III Topical Report, Belgonucleaire, Brussels, Belgium (November 16, 1972)

29 QUATTRO PRO User's Guide, Borland International Inc., Scott's Valley, CA (1989).

30 G. Vesterlund and L.B. Corsetti, "Recent ABB Fuel Design and Performance," Proceedings of the 1994 International Topical Meeting on Light Water Reactor Fuel Performance, American Nuclear Society, West Palm Beach, FL, pp 62-70 (April 1994).

BIOGRAPHICAL SKETCH

The author was born on June 18, 1958, in Waynesburg, Pennsylvania. He completed public education at Ringgold High School in Monongahela, PA, in 1976. He attended the Pennsylvania State University where he graduated with a Bachelor of Science degree in engineering science in 1980. Upon completion of his Bachelor degree, he was employed at the General Electric Nuclear Energy Division in San Jose, California. While at General Electric, he completed the Edison Engineering Training Program and was admitted to the University of California at Berkeley where he received a Master of Science degree in mechanical engineering in 1983. Also in 1983, he joined Westinghouse Electric Advanced Energy Systems Division in Madison, Pennsylvania. In 1988, he was awarded the B.G. Lamme Scholarship from Westinghouse and entered the Nuclear Engineering Sciences Department at the University of Florida in Gainesville, Florida. He completed his Ph.D. degree in nuclear engineering at the University of Florida in 1994.

The author is married to Denise Iva Hart of Belle Vernon, Pennsylvania, and has two children; Laura Elizabeth Wright and Richard Frederick Wright, IV. He is an active ice hockey player and youth hockey coach.

I certify that I have read this study and that in my opinion it conforms to acceptable standards of scholarly presentation and is fully adequate, in scope and quality, as a dissertation for the degree of Doctor of Philosophy.

James S. Tulenko, Chairman
Professor of Nuclear Engineering Sciences

I certify that I have read this study and that in my opinion it conforms to acceptable standards of scholarly presentation and is fully adequate, in scope and quality, as a dissertation for the degree of Doctor of Philosophy.

Edward T. Dugan, Cochairman
Associate Professor of Nuclear Engineering Sciences

I certify that I have read this study and that in my opinion it conforms to acceptable standards of scholarly presentation and is fully adequate, in scope and quality, as a dissertation for the degree of Doctor of Philosophy.

G. Ronald Dalton
Professor of Nuclear Engineering Sciences

I certify that I have read this study and that in my opinion it conforms to acceptable standards of scholarly presentation and is fully adequate, in scope and quality, as a dissertation for the degree of Doctor of Philosophy.

David E. Hintenlang
Assistant Professor of Nuclear Engineering Sciences

I certify that I have read this study and that in my opinion it conforms to acceptable standards of scholarly presentation and is fully adequate, in scope and quality, as a dissertation for the degree of Doctor of Philosophy.

Glen J. Schoessow
Professor Emeritus of Nuclear
Engineering Sciences

I certify that I have read this study and that in my opinion it conforms to acceptable standards of scholarly presentation and is fully adequate, in scope and quality, as a dissertation for the degree of Doctor of Philosophy.

Richard G. Connell, Jr.
Associate Professor of Material Science
and Engineering

I certify that I have read this study and that in my opinion it conforms to acceptable standards of scholarly presentation and is fully adequate, in scope and quality, as a dissertation for the degree of Doctor of Philosophy.

F. Eugene Dunnam
Professor of Physics

This dissertation was submitted to the Graduate Faculty of the College of Engineering and to the Graduate School and was accepted as partial fulfillment of the requirements for the degree of Doctor of Philosophy

December 1994

Winfred M. Phillips
Dean, College of Engineering

Karen A. Holbrook
Dean, Graduate School